1-24-2018 2:15 PM

Metabolic and Expression Changes Associated with a Mouse Model of Intrauterine Growth Restriction (IUGR)

Bethany N. Radford
The University of Western Ontario

Supervisor
Han, Victor VKM.
The University of Western Ontario

Abstract

Intrauterine growth restriction (IUGR) is a pregnancy condition where fetal growth is suboptimal, resulting in an infant born small for gestational age ($<10^{th}$ percentile) and is associated with metabolic disorders such as type 2 diabetes in adulthood. This study aims to understand tissue-specific adaptations to fetal undernutrition which predispose the individual to metabolic disorders in adulthood. A model of growth restriction in mice was established using 70% of maternal *ad libitum* total food (g) (E6.5-birth). At weaning, male offspring received standard chow or a HFHS diet. Body weight and random blood glucose levels were measured at 6 months. To assess metabolism at 6 or 7 months, glucose tolerance, pyruvate challenge and hepatic portal vein insulin challenge tests were administered and serum peptide markers for obesity and diabetes were measured. Metabolic cages were also used at 2 and 7 months to measure activity, food intake and respiratory exchange ratios (RERs). Adult liver, adipose and skeletal muscle and fetal liver was collected for RNA sequencing. Maternal nutrient restricted (MNR) offspring were growth restricted with disproportionately smaller fetal livers. 19% of standard chow-fed MNR offspring became glucose intolerant. On an isocaloric high-fat high-sugar diet no differences in MNR growth or glucose metabolism were detected. However, RERs were reduced at all timepoints in MNR on a HFHS relative to MNR on standard chow. Differences in transcription of genes involved in hypoxia signalling were detected and HIF-2α and HIF-3α proteins were increased in fetal liver of MNR offspring. Genes differentially expressed in the fetus were not differentially expressed at 6 months. Gene expression of metabolically regulatory transcripts in liver, adipose and skeletal muscle did not differ in all MNR and glucose intolerant MNR relative to controls. This model results in a susceptible and non-susceptible population of maternal nutrient restricted offspring and supports the concept of hypoxia signalling contributing to fetal adaptations. Understanding adaptations in hepatic hypoxia signalling in response to fetal undernutrition and how they vary in susceptible and unsusceptible populations will provide insight into how fetal nutrition can influence adult metabolism.

Keywords

Co-Authorship Statement

All chapters in this thesis were written by me. Editing for chapter 2 was done by Dr. Victor Han. For chapter 3, Dr. Robert Gros and Dr. Victor Han provided revisions. Dr. Greg Gloor and Dr. Victor Han edited chapter 4, and Dr. Daniel Hardy and Dr. Victor Han revised chapter 5. I completed all revisions based on this feedback.

Chapter 3:

Metabolic cages were run by Dr. Robert Gros at Robarts Research Institute (London, Ontario). Additional animal work and data analysis included in this chapter were done by me.

Acknowledgments

First, I would like to thank my supervisor **Dr. Victor Han** for his guidance throughout my graduate career. His continued encouragement to participate in opportunities to develop professional skills beyond the laboratory has been greatly appreciated. I would also like thank my present and former advisory committee members: **Dr. Daniel Hardy**, **Dr. Melissa Mann**, **Dr. Greg Gloor**, and **Dr. Nathalie Berube** for their continued support and advice.

Technical and personal support throughout the project was provided by many. Advice on tissue-specific insulin challenge sensitivity tests was obtained from **Dr. Edith Arany**. Help with tissue collections was provided by **Steve Dixon**, **Heather Tarnowski-Garner**, **Dr. Rashid Mehmood**, and **Katarina Albrechtas**. I would like to thank **Karen Burrell** for her friendship and problem-solving abilities. An additional thank you is extended to other former and present members of the **Han Lab** and **Children Health Research Institute** including graduate students and administrative staff.

Finally, I would like to thank all of my family and friends for their support and encouragement, and for tolerating me when I disappear into the laboratory for extended periods of time. A special thank you to **Amanda** and **Seth Crook** for their encouragement and moral support. Lastly, I would like to thank my parents, **Roxanne Tivadar** and **Garry Radford**. I truly could not have done it without their help and am very grateful.

Table of Contents

List of Tables

List of Figures

List of Appendices

Abbreviations

α	Alpha
β	Beta
AUC	Area Under the Curve
Btg2	BTG Anti-Proliferation Factor 2
Ccng2	Cyclin G2
Cited2	Cbp/p300-Interacting Transactivator 2
CLAMS	Comprehensive Lab Animal Monitoring System
DE	Differentially Expressed
DNMT1	DNA Methyl Transferase 1
DOHaD	Developmental Origins of Health and Disease
DTT	Dithiothreitol
ELBW	Extremely Low Birth Weight
FDR	False Discovery Rate
FFA	Free Fatty Acids
FGR	Fetal Growth Restriction
FIH	Factor Inhibitor of Hypoxia
Fkbp5	FK506 Binding Protein 51
GIP	Glucose-Dependent Insulinotropic Peptide
GLP-1	Glucagon-Like Peptide-1
GSK-3β	Glycogen Synthase Kinase 3β
HFD	High-Fat Diet
HFHS	High-Fat High-Sugar diet
HIF	Hypoxia-Inducible Factor
HRE	Hypoxic Response Elements
HSF	Heath Shock Factor
HSP	Heat Shock Protein
IFBG	Impaired Fasting Blood Glucose
IP-GTT	Intraperitoneal Glucose Tolerance Testing
IUGR	Fetal Growth Restriction
KDM3a	Lysine Methyl Transferase 3a

LPS	Lipopolysaccaride
MNR	Maternal Nutrient Restriction
ODD	Oxygen Degradation Domain
PAI-1	Plasminogen Activator Inhibitor-1
PCA	Principle Component Analysis
PFKFB3	6-Phosphofructo-2-Kinase/Fructose-2,6-Biphosphatase 3
PHD	Prolyl Pydroxylase
PVDF	Polyvinylidene
rAAV	Recombinant Adeno-Associated Virus
RER	Respiratory Exchange Ratio
RT	Room Temperature
SDS	Sodium Dodecyl Sulfate
SGA	Small for Gestational Age
TAD	Transactivation Domain
VHL	von Hippel-Lindau

Chapter 1 : Introduction

1.1   Intrauterine Growth Restriction

Clinically intrauterine growth restriction (IUGR) or fetal growth restriction (FGR) is a pregnancy condition where the fetal growth rate is reduced, and the infant is born small for gestational age (<10th percentile). Causes can be maternal, fetal or placental. Maternal causes include smoking, infections and malnutrition (1). Alternatively, restriction to fetal growth can be caused by chromosomal abnormalities in the fetus or insufficient development of the placenta (1). Maternal malnutrition and placental insufficiency are the most common causes in developing and developed nations, respectively (2). IUGR can also be classified into early and late onset. Early-onset IUGR often results in a reduction in all organs proportional to body weight and is termed symmetric growth restriction (1). Conversely, late-onset IUGR can result in asymmetric growth restriction with preservation in brain and heart size at the expense of reductions of less essential organs such as the lungs, liver, and kidneys (1). Infants born from pregnancies complicated with IUGR are at increased risk for perinatal complications (3) and as adults are more likely to develop obesity, glucose intolerance and type II diabetes (4,5).

1.2   Developmental Origins of Health and Disease

Studies of populations that were exposed to the Dutch Famine *in utero* found increased occurrence of glucose intolerance and cardiovascular disease (6,7). Since these pivotal studies many other studies have demonstrated that pathological reduction in fetal growth can influence adult health. Such studies have led to the concept of 'Developmental Origins of Health and Disease' (DOHaD). In this concept, adversity during fetal development and early life can result in adaptations enhancing fetal survival. However, these adaptations may not be beneficial to the individual postnatally. For instance, fetal nutrient restriction may prime that individual to more efficiently store nutrients. If the infant is born into a nutrient-rich environment such as western society, fetal adaptations may increase their risk for metabolic disorders. This hypothesis is termed the 'Thrifty Phenotype Hypothesis'(8).

1.3   Models of Growth Restriction

Studies investigating the "Thrifty Phenotype Hypothesis" in human IUGR populations are complicated by many confounding variables and ethical limitations. Some of these variables can be controlled or adjusted for in the study design or analysis; including ethnicity, substance use and socioeconomic status. However, estimating length, extent and onset of fetal nutrient restriction can be more challenging. Additionally, adaptations are likely tissue-specific and obtaining fetal and adult samples of metabolically important tissues may not be feasible. Due to these challenges, animal models have been developed to understand mechanisms underlying IUGR and DOHaD.

To date, many animal models have been used with different species. Studies in larger mammals like pigs are informative due to similarities to humans in physiology, morphology and diet (9). However, relatively long lifespans limit outcomes studied to early life rather than adulthood. Additionally, these models are costly and will be challenging for genetic manipulation to prove the mechanistic importance of altered genes. Rodents such as mice are valuable in providing cost-efficient long-term studies, with similar genetics and metabolism to humans and the potential for downstream genetic manipulation.

IUGR models in rodents induce growth restriction by various strategies including intrauterine artery ligation, hypoxia, lipopolysaccharide (LPS) exposure and maternal nutrient restriction. Artery ligation results in decreased nutrient and oxygen delivery to the fetus and provides a model of placental insufficiency. However, it is limited to late-gestation surgeries and results in a higher fetal mortality than controls exposed to sham surgeries (10). Recently, a genetic knock out of a transcription factor important in trophoblast differentiation, AP-2y, has also been used to model placental insufficiency (11). Maternal exposure to low oxygen chambers results in reduced oxygen delivery to the pups similar to a pregnancy at high altitude and LPS-induced growth restriction can model IUGR from infections (12,13). Such models can be early to late onset and model a specific maternal condition. Maternal nutrient restriction (MNR) also allows a flexible onset with some models beginning nutrient restriction prior to conception and others in early to late gestation (14–16). Additionally, total calories, or specific micro or macro nutrients such as iron or protein can be restricted (15–17). Variations in maternal

nutrition can model maternal nutritional challenges experienced in humans such as iron deficiencies, inadequate access to protein, or total calorie malnourishment. Additionally, total calorie maternal nutrient restriction can be used to model the reduced nutrient delivery to the fetus in placental insufficiency. Each type of model is applicable to maternal conditions experienced in human pregnancies and are useful to understanding how certain adversities affect fetal and long-term health.

1.3.1 Fetal Adaptations to Growth Restriction

Growth restriction models exhibit reduced fetal and birth weight. Reductions in growth are symmetric or asymmetric depending on the type and time of insult (18–20). Growth restriction has also been associated with hypoglycemia, hypoinsulinemia and increased insulin sensitivity in the fetus or young offspring, suggesting an immediate impact on fetal glucose metabolism (15,21,22).

In humans and animal models, reduction in liver size relative to body weight or fractional growth rates suggests that the liver is sensitive to fetal nutrition (19,20,23). Reduced liver size from maternal nutrient restriction or maternal hypoxia is associated with reduced fetal glycogen deposits (24,25) and decreased hepatocyte numbers (26). Increased expression of genes in fatty acid oxidation, gluconeogenesis and insulin signalling in MNR fetal liver accompany phenotypic changes (27,28). Evidence of increased glucocorticoid signalling has also been detected but appears to be specific to the male fetus (29).

In addition to liver adaptations, mice born from nutrient restrictive pregnancies have smaller fat mass at birth (30). In total calorie restriction models cultured adipocytes from post-natal day 1 have increased hyperplasia, hypertrophy, and increased protein expression of lipogenic transcription factors (31). Increased proteins involved in glucocorticoid signalling that regulate the mobilization of energy stores are also increased in female, but not male, MNR offspring (29). Such adaptations could promote energy storage during postnatal development to accommodate for reduced fat stores.

Skeletal muscle is another metabolically important tissue that is developed into the postnatal period, and adaptations in growth restricted offspring include reduced muscle mass and fiber type switching. Often growth restricted fetus' have reduced oxidative type

I fibers which are more insulin sensitive (22,32). Some muscle groups like the soleus muscle have decreased cross-sectional area of type II fibers relative to controls (32). Although myofiber surface area is decreased, the number of myoblasts (progenitor cells that can differentiate and fuse to form myotubes) were similar to controls (32). Despite maintenance of proliferative capacity when cultured *in vitro*, myoblasts have reduced expression of a proliferation marker (Ki-67) *in vivo* (32). Regulation of *in vivo* myoblast proliferation and changes in fiber types are influences by protein uptake, blood flow and oxygenation which are reduced in muscles, such as the biceps femoris of growth restricted fetuses (33). This maintenance of capacity to proliferate could allow the fetus to adjust muscle mass if nutrient or oxygen levels are restored during development.

These tissue-specific fetal adaptations can promote immediate survival. Additionally, they could function to predict the postnatal environment in order to enhance survival of that offspring to a reproductive age. In the latter case, as described by the "predictive adaptive response hypothesis", these adaptations would be beneficial only if the postnatal environment is accurately predicted (34,35). For example, increased insulin sensitivity in peripheral tissues can accommodate for hypoinsulinemia due to nutritional scarcity. Similarly, reduction in energetically demanding skeletal muscle and an increased capacity for proliferation adipocyte proliferation, can promote energy conservation and storage. Conserving and storing energy are an advantage in a nutrient restrictive environment. However, if the environment proceeding the period of developmental placidity does not match that predicted, such as a nutrient abundant one, these changes can be maladaptive to long-term health.

1.3.2 Changes in Adult offspring in Response to Fetal Growth Restriction

Adaptations in animal models of growth restriction produce changes that influence adult metabolism. As adults, offspring are predisposed to glucose intolerance, insulin resistance, reduced energy requirement per body weight gain, reduced activity, increased appetite and/or increased preferences for fatty foods (16,30,36,37). Although model variations exist, male offspring tend to be more prone to changes in glucose metabolism and female offspring to adiposity (38,39).

Liver-specific changes are in both glucose and lipid metabolism. Increased transcription of genes involved in lipogenesis and decrease in proteins involved in cholesterol clearance are associated with steatosis in offspring from fetal undernutrition (20,40). Glycogen deposits are also increased in adult offspring from growth restricted pregnancies (41). In normal tissues, insulin receptor activation by binding of insulin results in increases IRS-2 and Akt phosphorylation, which increase glucose uptake and glycogen synthesis and prevent hepatic glucose output. However, in IUGR rats from placental insufficiency insulin stimulation does not result in increased phosphorylation of IRS-2 or AKT or suppression of hepatic glucose production (42). Although increased free fatty acids (FFAs) can contribute to hepatic insulin resistance, insulin resistance has been detected in the absence of dyslipidemia (42). These data suggest that fetal undernutrition results in offspring with insulin desensitization and an aberrant energy balance in the liver that favors storage of lipids and glycogen.

Adult offspring also have changes in adipocyte size, number and/or growth. Increased percent body fat has been observed with and without changes in body weight (20,43). Offspring from 50 % maternal nutrient restriction late in gestation have increased lipogenic gene expression and increased adipocyte size (44). Conversely, moderate maternal nutrient restriction throughout pregnancy is associated with an increased number but smaller adipocytes in female offspring (38). Decreased insulin sensitivity can also occur in adipose tissue when growth restriction extends into lactation, but impact males rather than females (39). Enhanced growth and inflammation in adipose tissue can also influence differences in body mass and insulin sensitivity (30). Such studies suggest that fetal adaptations to undernutrition can influence adult body mass composition, and glucose and lipid metabolism in a sex-specific and model-specific manner.

Changes in body composition are also associated with reduced lean mass. Similar to the growth restricted fetus, reduced muscle area and type I fiber number can persist into adulthood (45,46). Premature aging by telomere shortening and DNA damage has also been observed in the vastus lateralis muscle of aged prenatal protein restricted rats (47). Decreased p-AKT to AKT ratios in response to insulin have also been observed in adult male offspring from maternal protein restriction, suggesting impaired insulin sensitivity in skeletal muscle (39). Reduced mass, insulin sensitivity and aging in skeletal muscle

could contribute to aberrant glucose tolerance, reduced lean mass and insulin resistance in adult offspring, increasing risk metabolic disorders.

1.3.3 Growth Restriction and Postnatal Diets

Adaptations in growth restricted offspring can impact responses to stress. High caloric, high-fat (HFD) or high-fat high-sugar (HFHS) diets in animal models can mimic the 'western diet', a calorie dense diet that is high in saturated fat and refined sugars. Such diets, in combination with fetal changes to conserved energy due to fetal undernutrition, lead to further dysfunction in glucose and lipid metabolism and behavior. Growth restricted offspring are more susceptible to diet-induced obesity and adipose tissue inflammation (30). In part, due to increased lipogenesis in adipose tissue and decreased cholesterol clearance in the liver, which leads to ectopic lipid accumulation and increase serum lipids (31,48–50). Both ectopic lipids and serum FFAs are associated with decreased insulin sensitivity (51). Although sedentary behavior is observed in some models of IUGR, postnatal HFD diets can further reduce activity in offspring(16). These studies suggest that growth restricted offspring are maladapted to a nutrient abundant diet.

1.4   Hypoxia Signalling

One pathway activated in response to cellular stress such as low oxygen or nutrient over or under abundance, is hypoxia-inducible factor (HIF) signalling. In physiologically normal oxygen tension, oxygen is available for prolyl hydroxylases (PHDs) to hydroxylate the oxygen degradation domain (ODD) of the α subunit (HIF-1, 2 or 3 α) (52). Hydroxylation to the ODD of the α subunit allows recognition by the pVHL-containing ubiquitin ligase and degradation by the proteasome (53). In the absence of oxygen, the unhydroxylated α subunit can dimerize with HIF-1β. The HIF dimer can then translocate to the nucleus and transcriptionally regulate genes containing hypoxic response elements (HREs) (54) (**Figure 1.4.1**) . In addition to PHD hydroxylation, HIFα stability and transcriptional activity can be modulated by phosphorylation, hydroxylation, and ribosylation in the ODD, C-terminal and N-terminal transactivation domains (C-TAD, T-TAD) which are regulated by oxygen and nutrient availability (17,53,55). HRE-

containing genes are involved in pathways important in stress response as well as normal development including metabolism, angiogenesis, proliferation and apoptosis (54).
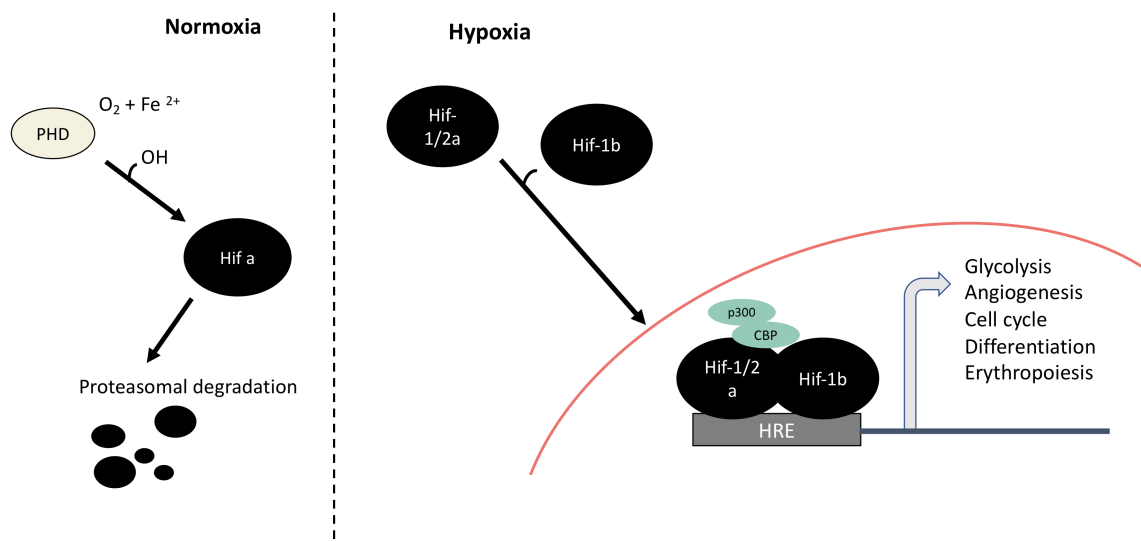
Figure 1.4.1 Regulation of HIF Alpha Subunits in Hypoxia and Normoxic Conditions.

Under normoxic conditions, the alpha subunit is hydroxylated by PHDs in the oxygen degradation domain, resulting in recognition and degradation by the proteasome. In hypoxia, oxygen is not available for hydroxylation and the alpha subunits are stabilized. Stable alpha subunits can dimerize with the beta subunit, translocate to the nucleus, and regulate expression of genes containing hypoxia response elements (HRE).

1.4.1 Hypoxia Signalling in Animal Models

Maternal hypoxia has been well documented to cause fetal growth restriction but recent evidence suggests that other models of growth restriction can lead to hypoxic signalling in placental or fetal tissues (56-58). Maternal nutrients and maternal protein restriction result in placental adaptations that could decrease oxygen delivery to fetal tissues and directly cause fetal hypoxia. In mice, the placenta can be divided into two functional zones, the junctional and labyrinth zone. The junctional zone is involved in endocrine signalling and energy storage and the labyrinth zone is the site of oxygen and nutrient exchange. In growth restricted models, the zone most often impacted is the junctional zone (59). Additionally, the placental weight relative to fetal weight ratio is increased and oxygen tension was not different in growth restricted placentas (56). Availability of

nutrients is known to modulate hypoxia signalling *in vitro*. In addition to oxygen, iron is required for PHD hydroxylation of the HIFα subunits. Pathways in nutrient sensing, such as GSK-3β, have also been implicated in regulation of α subunit stability or activity (53,57). Together these data suggest that fetal nutrition may mediate hypoxic signalling through redistribution of fetal circulation and nutrient signalling pathways and could potentiate fetal adaptations to growth restriction.

1.4.2 Hypoxia Signalling in Pregnancies Complicated with IUGR

Evidence of increased hypoxia-inducible signalling is present in placentas from IUGR with preeclampsia, however, induction of this pathway in pregnancies with IUGR only are inconsistent across studies (55,60). Similar to animal models of growth restriction, some placentas from intrauterine growth restriction exhibit no changes in HIF proteins (62). Whether hypoxia signalling may be induced in developing fetal tissues in human IUGR pregnancies is currently unknown. It is possible that HIFs are differentially regulating development or organ function, influencing perinatal and adult health.

1.5   Thesis Rationale

In this study we aimed to identify transcriptional changes that are associated with fetal adaptations and/or changes in adult glucose metabolism in offspring from maternal nutrient restriction (MNR) (70% *ad libitum* food) in mice, and how the postnatal diet may modulate these changes. To isolate fetal undernutrition to pregnancy, without having an impact on litter size or postnatal nutrition, maternal food restriction was applied post-implantation (E6.5) until birth and all litters were cross-fostered to *ad libitum fed* mothers. Unpublished work from our lab has shown that male, but not female, offspring develop glucose intolerance at 6 months of age. Despite detection of glucose intolerance, there was no difference in serum insulin which suggests peripheral insulin desensitization rather than insulin deficiency. Additionally, other models have shown males are vulnerable to changes in insulin sensitivity of peripheral tissues (39). Subsequently, male offspring were the focus in this study. The liver, adipose tissue and skeletal muscle are metabolically important peripheral tissues that have been impacted in other models of growth restriction (39,42) and could mediate long-term changes in glucose tolerance. To

this end, fetal and adult liver, as well as skeletal muscle and visceral adipose tissue in adults were assessed for changes in gene expression. This study is also unique because adult organs collected for gene expression analysis are from mice that underwent metabolic testing. Knowledge of the metabolic status for each mouse could aid in identifying relevant transcription changes to the biological outcome. While other models exist to study these tissues in nutrient restricted animals, most are in rats, guinea pigs and larger mammals (22,37,63). A mouse model will allow further studies to genetically manipulate identified genes and determine the role in fetal survival or offspring glucose metabolism. Understanding the mechanism underlying associations between fetal nutrition, growth restriction and adult metabolism will assist in identifying and treating IUGR most at risk for adult metabolic disorders.

1.6   Hypothesis and Objectives

Hypotheses: Changes in expression of genes regulating metabolism or tissue development in liver, adipose and/or skeletal muscle occur in response to fetal nutrient restriction and contribute to an altered adult glucose metabolism. We also hypothesized that a HFHS will amplify the changes in metabolism in maternal nutrient restricted (MNR) offspring.

<u>Objective 1</u>: Metabolically assess outcomes of maternal nutrient restriction in adult offspring.

> *Aim one: Characterize the impact of MNR on offspring adult glucose metabolism when maintained on a standard diet chow post-weaning.*

> *Aim two: Determine the effects of fetal undernutrition with a post-weaning high-fat high-sugar (HFHS) diet in adult offspring.*

<u>Objective 2</u>: Identify transcripts differentially expressed throughout the life of MNR offspring in metabolically important tissues.

> *Aim one: Determine whether differential expression of genes regulating metabolism or tissue development occurred in E18.5 liver in response to MNR.*

> *Aim two: Assess differential expression of genes regulating glucose metabolism in adult liver, skeletal muscle and adipose tissue.*

<u>Objective 3</u>: Evaluate protein levels of differentially expressed genes involved in hypoxia signalling in fetal liver.

1.7   References

1. Nardozza LMM, Araujo Júnior E, Barbosa MM, Caetano ACR, Lee DJR, Moron AF. Fetal growth restriction: current knowledge to the general Obs/Gyn. *Arch Gynecol Obstet*. 2012;286:1–13.

2. Han VKM, Seferovic MD, Albion CD, Gupta MB (2012) Intrauterine Growth Restriction: Intervention Strategies. In: Buonocore G., Bracci R., Weindling M. (eds) Neonatology. Springer, Milano, p. 89-93.

3. Garite TJ, Clark R, Thorp JA. Intrauterine growth restriction increases morbidity and mortality among premature neonates. *Am J Obstet Gynecol*. 2004;191:481–7.

4. Morrison KM, Ramsingh L, Gunn E, et al. Cardiometabolic Health in Adults Born Premature With Extremely Low Birth Weight. *Pediatrics*. 2016;138:e20160515.

5. Würtz P, Wang Q, Niironen M, et al. Metabolic signatures of birthweight in 18 288 adolescents and adults. *Int J Epidemiol*. 2016;45:1539–50.

6. Ravelli AC, van der Meulen JH, Michels RP, et al. Glucose tolerance in adults after prenatal exposure to famine. *Lancet*. 1998;351:173–7.

7. Roseboom TJ, van der Meulen JH, Ravelli AC, et al. Blood pressure in adults after prenatal exposure to famine. *J Hypertens*. 1999;17:325–30.

8. Hales CN, Barker DJ. Type 2 (non-insulin-dependent) diabetes mellitus: the thrifty phenotype hypothesis. *Diabetologia*. 1992;35:595–601.

9. Wang J, Cao M, Zhuo Y, et al. Catch-up growth following food restriction exacerbates adulthood glucose intolerance in pigs exposed to intrauterine undernutrition. *Nutrition*. 2016;32:1275–84.

10. Janot M, Cortes-Dubly M-L, Rodriguez S, Huynh-Do U. Bilateral uterine vessel ligation as a model of intrauterine growth restriction in mice. *Reprod Biol Endocrinol*. 2014;12:62.

11. Stojanovska V, Sharma N, Dijkstra DJ, et al. Placental insufficiency contributes to fatty acid metabolism alterations in aged female mouse offspring. *Am J Physiol Regul Integr Comp Physiol.* 2018; doi:10.1152/ajpregu.00420.2017.

12. Cahill LS, Hoggarth J, Lerch JP, Seed M, Macgowan CK, Sled JG. Fetal brain sparing in a mouse model of chronic maternal hypoxia. *J Cereb Blood Flow Metab.* 2017; doi: 10.1177/0271678X17750324.

13. Shalom-Paz E, Weill S, Ginzberg Y, et al. IUGR induced by maternal chronic inflammation: long-term effect on offspring's ovaries in rat model-a preliminary report. *J Endocrinol Invest.* 2017;40:1125–31.

14. Vomhof-DeKrey E, Darland D, Ghribi O, Bundy A, Roemmich J, Claycombe K. Maternal low protein diet leads to placental angiogenic compensation via dysregulated M1/M2 macrophages and TNFα expression in Sprague-Dawley rats. *J of Reprod Immunol.* 2016;118:9–17.

15. Desai M, Gayle D, Babu J, Ross MG. The timing of nutrient restriction during rat pregnancy/lactation alters metabolic syndrome phenotype. *Am J Obstet Gynecol.* 2007;196:555.e1-7.

16. Vickers MH, Breier BH, McCarthy D, Gluckman PD. Sedentary behavior during postnatal life is determined by the prenatal environment and exacerbated by postnatal hypercaloric nutrition. *Am J Physiol Regul Integr Comp Physiol.* 2003;285:R271-273.

17. Woodman AG, Care AS, Mansour Y, et al. Modest and Severe Maternal Iron Deficiency in Pregnancy are Associated with Fetal Anaemia and Organ-Specific Hypoxia in Rats. *Sci Rep.* 2017;7:46573.

18. Fung C, Brown A, Cox J, Callaway C, McKnight R, Lane R. Novel thromboxane A2 analog-induced IUGR mouse model. *J Dev Orig Health Dis.* 2011;2:291–301.

19. Nevin CL, Formosa E, Maki Y, Matushewski B, Regnault TRH, Richardson BS. Maternal Nutrient Restriction in Guinea Pigs as an Animal Model for Studying Growth Restricted Offspring with Post-Natal Catch-Up Growth. *Am J Physiol-Regul Integr Comp Physiol.* 1;314(5):R647-R654.

20. Liu X, Qi Y, Tian B, et al. Maternal protein restriction induces alterations in hepatic tumor necrosis factor-α/CYP7A1 signaling and disorders regulation of cholesterol metabolism in the adult rat offspring. *J Clin Biochem Nutr*. 2014;55:40–7.

21. Camacho LE, Chen X, Hay WW, Limesand SW. Enhanced insulin secretion and insulin sensitivity in young lambs with placental insufficiency-induced intrauterine growth restriction. *Am J of Physiol-Regul Integr Comp Physiol.* 2017;313:R101–9.

22. Yates DT, Cadaret CN, Beede KA, et al. Intrauterine growth-restricted sheep fetuses exhibit smaller hindlimb muscle fibers and lower proportions of insulin-sensitive Type I fibers near term. *Am J of Physiol-Regul Integr Comp Physiol*. 2016;310:R1020-1029.

23. Man J, Hutchinson JC, Ashworth M, Jeffrey I, Heazell AE, Sebire NJ. Organ weights and ratios for postmortem identification of fetal growth restriction: utility and confounding factors. *Ultrasound Obstet Gynecol*. 2016;48:585–90.

24. Parimi PS, Croniger CM, Leahy P, Hanson RW, Kalhan SC. Effect of reduced maternal inspired oxygen on hepatic glucose metabolism in the rat fetus. *Pediatr Res*. 2003;53:325–32.

25. Hsu SD, Cardell RR, Drake RL. Maternal malnutrition does not affect fetal hepatic glycogen synthase ontogeny. *Dig Dis Sci.* 1993;38:1500–4.

26. Ferenc K, Pietrzak P, Wierzbicka M, et al. Alterations in the liver of intrauterine growth retarded piglets may predispose to development of insulin resistance and obesity in later life. *J Physiol Pharmacol*. 2018;69.

27. Limones M, Sevillano J, Sánchez-Alonso MG, Herrera E, Ramos-Álvarez MDP. Metabolic alterations associated with maternal undernutrition during the first half of gestation lead to a diabetogenic state in the rat. *Eur J Nutr*. 2018; doi: 10.1007/s00394-018-1805-z.

28. Thorn SR, Regnault TRH, Brown LD, et al. Intrauterine Growth Restriction Increases Fetal Hepatic Gluconeogenic Capacity and Reduces Messenger Ribonucleic Acid

Translation Initiation and Nutrient Sensing in Fetal Liver and Skeletal Muscle. *Endocrinology*. 2009;150:3021–30.

29. Guo C, Li C, Myatt L, Nathanielsz PW, Sun K. Sexually dimorphic effects of maternal nutrient reduction on expression of genes regulating cortisol metabolism in fetal baboon adipose and liver tissues. *Diabetes*. 2013;62:1175–85.

30. Xie L, Zhang K, Rasmussen D, et al. Effects of prenatal low protein and postnatal high fat diets on visceral adipose tissue macrophage phenotypes and IL-6 expression in Sprague Dawley rat offspring. *PLOS ONE*. 2017;12:e0169581.

31. Yee JK, Lee W-NP, Ross MG, et al. Peroxisome proliferator-activated receptor gamma modulation and lipogenic response in adipocytes of small-for-gestational age offspring. *Nutr Metab (Lond)*. 2012;9:62.

32. Soto SM, Blake AC, Wesolowski SR, et al. Myoblast replication is reduced in the IUGR fetus despite maintained proliferative capacity in vitro. *J Endocrinol*. 2017;232:475–91.

33. Rozance PJ, Zastoupil L, Wesolowski SR, et al. Skeletal muscle protein accretion rates and hindlimb growth are reduced in late gestation intrauterine growth-restricted fetal sheep. *J Physiol (Lond)*. 2018;596:67–82.

34. Gluckman PD, Hanson MA, Beedle AS, Spencer HG. Predictive adaptive responses in perspective. *Trends Endocrinol Metab.* 2008;19:109–10; author reply 112.

35. Gluckman PD, Hanson MA, Spencer HG. Predictive adaptive responses and human evolution. *Trends Ecol Evol (Amst)*. 2005;20:527–33.

36. Lira LA, Almeida LCA, da Silva AAM, et al. Perinatal undernutrition increases meal size and neuronal activation of the nucleus of the solitary tract in response to feeding stimulation in adult rats. *Int J of Dev Neurosci.* 2014;38:23–9.

37. Kind KL, Clifton PM, Grant PA, et al. Effect of maternal feed restriction during pregnancy on glucose tolerance in the adult guinea pig. *Am J Physiol Regul Integr Comp Physiol.* 2003;284:R140-152.

38. Joaquim AO, Coelho CP, Motta PD, et al. Maternal food restriction in rats of the F0 generation increases retroperitoneal fat, the number and size of adipocytes and induces periventricular astrogliosis in female F1 and male F2 generations. *Reprod Fertil Dev.* 2017;29:1340–8.

39. Chamson-Reig A, Thyssen SM, Hill DJ, Arany E. Exposure of the Pregnant Rat to Low Protein Diet Causes Impaired Glucose Homeostasis in the Young Adult Offspring by Different Mechanisms in Males and Females. *Exp Biol Med.* 2009;234:1425–36.

40. Wolfe D, Gong M, Han G, Magee TR, Ross MG, Desai M. Nutrient sensor-mediated programmed nonalcoholic fatty liver disease in low birthweight offspring. *Am J Obstet Gynecol.* 2012;207:308.e1-6.

41. Gosby AK, Maloney CA, Phuyal JL, Denyer GS, Bryson JM, Caterson ID. Maternal Protein Restriction Increases Hepatic Glycogen Storage in Young Rats. *Pediat Res.* 2003;54:413–8.

42. Vuguin P, Raab E, Liu B, Barzilai N, Simmons R. Hepatic insulin resistance precedes the development of diabetes in a model of intrauterine growth retardation. *Diabetes.* 2004;53:2617–22.

43. Crossland RF, Balasa A, Ramakrishnan R, Mahadevan SK, Fiorotto ML, Veyver IBV den. Chronic Maternal Low-Protein Diet in Mice Affects Anxiety, Night-Time Energy Expenditure and Sleep Patterns, but Not Circadian Rhythm in Male Offspring. *PLOS ONE.* 2017;12:e0170127.

44. Isganaitis E, Jimenez-Chillaron J, Woo M, et al. Accelerated postnatal growth increases lipogenic gene expression and adipocyte size in low-birth weight mice. *Diabetes.* 2009;58:1192–200.

45. Confortim HD, Jerônimo LC, Centenaro LA, et al. Effects of aging and maternal protein restriction on the muscle fibers morphology and neuromuscular junctions of rats after nutritional recovery. *Micron.* 2015;71:7–13.

46. Cabeço LC, Budri PE, Baroni M, et al. Maternal protein restriction induce skeletal muscle changes without altering the MRFs MyoD and myogenin expression in offspring. *J Mol Histol.* 2012;43:461–71.

47. Tarry-Adkins JL, Fernandez-Twinn DS, Chen JH, et al. Poor maternal nutrition and accelerated postnatal growth induces an accelerated aging phenotype and oxidative stress in skeletal muscle of male rats. *Dis Model Mech*. 2016;9:1221–9.

48. Zinkhan EK, Chin JR, Zalla JM, et al. Combination of intrauterine growth restriction and a high-fat diet impairs cholesterol elimination in rats. *Pediatr Res*. 2014;76:432–40.

49. Yan H, Zheng P, Yu B, et al. Postnatal high-fat diet enhances ectopic fat deposition in pigs with intrauterine growth retardation. *Eur J Nutr*. 2017;56:483–90.

50. Zinkhan EK, Zalla JM, Carpenter JR, et al. Intrauterine growth restriction combined with a maternal high-fat diet increases hepatic cholesterol and low-density lipoprotein receptor activity in rats. *Physiol Rep*. 2016;4.

51. Moro C, Bajpeyi S, Smith SR. Determinants of intramyocellular triglyceride turnover: implications for insulin sensitivity. *Am J Physiol Endocrinol Metab*. 2008;294:E203-213.

52. Bruick RK, McKnight SL. A Conserved Family of Prolyl-4-Hydroxylases That Modify HIF. *Science*. 2001;294:1337–40.

53. Brahimi-Horn C, Mazure N, Pouysségur J. Signalling via the hypoxia-inducible factor-1α requires multiple posttranslational modifications. *Cell Signal*. 2005;17:1–9.

54. Slemc L, Kunej T. Transcription factor HIF1A: downstream targets, associated pathways, polymorphic hypoxia response element (HRE) sites, and initiative for standardization of reporting in scientific literature. *Tumour Biol J Int Soc Oncodevelopmental Biol Med.* 2016;37:14851–61.

55. Mennerich D, Dimova EY, Kietzmann T. Direct phosphorylation events involved in HIF-α regulation: the role of GSK-3β. *Hypoxia (Auckl)*. 2014;2:35–45.

56. Elias AA, Maki Y, Matushewski B, Nygard K, Regnault TRH, Richardson BS. Maternal nutrient restriction in guinea pigs leads to fetal growth restriction with evidence for chronic hypoxia. *Pediatr Res.* 2017;82:141–7.

57. Cahill LS, Rennie MY, Hoggarth J, et al. Feto- and utero-placental vascular adaptations to chronic maternal hypoxia in the mouse. *J Physiol (Lond)*. 2018;596:3285–97.

58. Robb KP, Cotechini T, Allaire C, Sperou A, Graham CH. Inflammation-induced fetal growth restriction in rats is associated with increased placental HIF-1α accumulation. *PLoS ONE.* 2017;12:e0175805.

59. Gonzalez PN, Gasperowicz M, Barbeito-Andrés J, Klenin N, Cross JC, Hallgrímsson B. Chronic Protein Restriction in Mice Impacts Placental Function and Maternal Body Weight before Fetal Growth. *PLOS ONE*. 2016;11:e0152227.

60. Rabinovitch RC, Samborska B, Faubert B, et al. AMPK Maintains Cellular Metabolic Homeostasis through Regulation of Mitochondrial Reactive Oxygen Species. *Cell Rep*. 2017;21:1–9.

61. Dai S-Y, Kanenishi K, Ueno M, Sakamoto H, Hata T. Hypoxia-inducible factor-2alpha is involved in enhanced apoptosis in the placenta from pregnancies with fetal growth restriction. *Pathol Int*. 2004;54:843–9.

62. Rajakumar A, Jeyabalan A, Markovic N, Ness R, Gilmour C, Conrad KP. Placental HIF-1 alpha, HIF-2 alpha, membrane and soluble VEGF receptor-1 proteins are not increased in normotensive pregnancies complicated by late-onset intrauterine growth restriction. *Am J Physiol Regul Integr Comp Physiol*. 2007;293:R766-774.

63. Nowacka-Woszuk J, Szczerbal I, Malinowska AM, Chmurzynska A. Transgenerational effects of prenatal restricted diet on gene expression and histone modifications in the rat. *PLoS ONE*. 2018;13:e0193464.

Chapter 2 : Offspring from Maternal Nutrient Restriction in Mice Show Variations in Adult Glucose Metabolism Similar to Human Fetal Growth Restriction

2.1   Introduction

Fetal growth restriction (FGR) or intrauterine growth restriction (IUGR) is a pregnancy condition where the fetus fails to achieve optimal growth expected for gestational age resulting in a small for gestational age (SGA) newborn with birth weight of <10th percentile. The most common causes include maternal malnutrition in developing countries and placental insufficiency in developed countries (1). Irrespective of the cause, poor macro- and micro-nutrient and substrate concentrations in the fetus are a common pathophysiological finding. Growth restricted infants are at increased risk for morbidity and mortality in the perinatal period (2). As adults IUGR populations are also at increased risk for chronic diseases including cardiovascular diseases (3), metabolic disorders such as type 2 diabetes and glucose intolerance (3), and obesity and abnormal lipid metabolism (4).

Associations between poor fetal growth and adult health and disease have led to the concept of Developmental Origins of Health and Disease (DOHaD). The theory of DOHaD proposes that environmental exposures, such as nutrient restriction, during development can result in metabolic adaptations that enhance the survival of the fetus but increase the risk for metabolic disorders as children and adults (5). The concept underlying the association between poor fetal nutrition and predisposition to adult diseases is termed the "thrifty phenotype hypothesis"(5).

Fetal growth restriction has been studied using maternal nutrient restriction in animals such as rats (6–8) and guinea pigs (9), or larger mammals like pigs (10,11). These models providing a short lifespan or similar morphology and diet to humans, respectively, and insight into long and short-term changes in IUGR offspring. Genetic manipulation in offspring to identify genes and epigenetic changes moderating impacts of fetal nutrition are limited. Such limitations can be addressed by using maternal nutrient restriction in mice.

Models of growth restriction in rodents by manipulating maternal nutrition provide insight into certain types of fetal undernutrition in humans, either due to the onset of placental insufficiency or food availability. For example, nutrient restriction prior to and

throughout pregnancy in rodents (9,12) model mothers that experience extended nutritional deficits. However, these models would not mimic fetal undernutrition due to placental insufficiency. Conversely, nutrient restriction beginning later in gestation may imitate insufficient placental development (6). Nutrient restriction just after implantation in the mouse at E6.5 has not been studied and would be more similar to early- to mid-gestation-onset placental insufficiency.

Evidence suggests that metabolic adaptions to fetal undernutrition are tissue-specific and serum peptides for obesity and diabetes can aid in identification of impacted tissues. Incretin hormones, glucagon-like peptide-1 (GLP-1) and glucose-dependent insulinotropic peptide (GIP), are released by the gut upon ingestion of food and stimulate release of insulin (13,14). Insulin and glucagon are pancreatic hormones that regulate tissue glucose uptake and energy utilization. In addition to hormone release, c-peptide, the cleaved portion of proinsulin, can indicate changes in insulin maturation (15). Leptin, resistin (16) and plasminogen activator inhibitor (PAI-1) (17) are secreted primarily from adipose tissue in mice. Leptin and ghrelin, which is released from the gut, regulate appetite (18,19). Changes in these markers in addition to other metabolic tests can provide insight into tissues with metabolic adaptations.

The objective of this study was to establish a moderate total calorie nutrient restriction in mice to mimic human FGR populations and examine the long-term metabolic complications. We hypothesized that a 30% reduction in maternal food consumption by weight during early and late pregnancy would result in reduced fetal and newborn weight and tissue-specific alterations in adult glucose metabolism similar to humans.

2.2   Methods

2.2.1 Animals

The animal experiments were conducted as approved by the Council on Animal Care at the University of Western Ontario. All mice received free access to water in a standard 12 h light/dark cycle. Eight-week-old virgin female CD-1 mice, obtained from Charles River Laboratories (Montreal, PQ, Canada), were mated. The presence of mucous plugs indicated E0.5. After mating mice were housed individually. To avoid reduction in the

number of conceptuses of each litter, mated females received *ad libitum* food until after embryo implantation at about E5. At E6.5, the mice were randomly assigned into two groups, the control group was fed *ad libitum* and the maternal nutrient restriction (MNR) group was fed 70% average *ad libitum* total calorie intake (both groups receiving #F0173, Bio-Serv, Flemington, NJ). At E18.5, 3 control and 3 MNR pregnant females were euthanized by CO_2 narcosis. No differences between the number of males and females were observed between MNR and control litters (**Supplementary Table 2.2.1**). Litter size ranged from 6 to 22 pups. To control for variations in litter size only litters with 11-15 pups were analyzed in fetal (Control litters = 3, MNR litters = 3) and long-term studies (Control litters = 5, MNR litters =10). Because many studies suggest that male offspring are more sensitive to maternal undernutrition (20–22) and that post-reproductive changes complicate long term studies in females (23), only males were examines in this study. PCR of the SRY gene, which is located on the y chromosome and is important in sex determination in mice, (forward primer - TGGACTGGTGACAARGCTA, reverse primer - TGGAAGTACAGGTGTGCACTCT) was used in fetal studies to include males only (Control N=21, MNR=15). Right liver lobes were snap frozen in liquid nitrogen.

For postnatal studies, pups' paws were tattooed at birth to track weights for each pup with the Armis Microtatoo kit (Braintree Scientific, Inc., Braintree, MA). To assess impacts of reduced nutrition during fetal development without the influence of nutrition during lactation, all litters were cross-fostered to females that were fed *ad libitum* throughout pregnancy and the litters were culled or fostered to 13 pups each. Since MNR resulted in similar male-to-female ratios to control litters, the sex of pups was selected randomly (**Supplementary Table 2.2.1**). *Ad libitum* standard chow (Teklad LM-485 Mouse/Rat Serializable Diet, Mississauga, ON, Canada) was used for the remainder of the study in both MNR and control offspring .

At weaning (P21) only male offspring were kept for further study (Control litters N=5, MNR litters N=10) and were housed with 3 to 5 siblings per cage (**Figure 2.2.1**) Weight was measured once a month. With the exception of littermates used for the intrahepatic portal vein insulin challenge, offspring at 1 month (control N=12, MNR N=19, 1-2 pups

per litter) and 6 months (control N=30, MNR N=52, all remaining pups) were euthanized with CO_2 narcosis. Weight was measured and serum was collected *via* intracardiac puncture. Individual liver lobes, perigonadal adipose tissue, and quadriceps femoris were collected, snap frozen in liquid nitrogen, and stored at -80°C until analysis. Seven-month old animals used for the intrahepatic portal vein insulin challenge (N=8 per group) and were euthanized after tissue collections.

2.2.2 Glucose Tolerance and Hepatic Glucose Production

Glucose tolerance was assessed in 36 MNR (10 litters) and 25 controls (5 litters, 3-8 pups/litter) one week prior to tissue collections or pyruvate challenge test at 6 months by intraperitoneal glucose tolerance testing (IP-GTT). Briefly, fasted mice (4 h) (at 8 00 am) were injected with glucose 2 g/kg body weight and blood glucose was measured via tail vein every 30 minutes for 2 h using a Freestyle Lite Glucometer (Abbott, Alameda, CA). At 6 months, hepatic glucose output was measured with a pyruvate challenge test (5 pups per group, 1 pup/litter). Pyruvate was injected (IP) into mice fasted for 4 h (at 8 00 am) at 2 g/kg body weight and blood glucose was measured via tail vein every 30 min for 2 h.

2.2.3 Random Blood Glucose

From 1 to 6 months, monthly random blood glucose (non-fasted) was measured. Blood samples were collected at 10:30 am via tail vein prick and measured using a Freestyle Lite Glucometer (Abbott, Alameda, CA).

2.2.4 Intrahepatic Portal Vein Insulin Challenge Test

Seven months-old mice were fasted for 4 hours and anaesthetized with isoflurane. Insulin stock was diluted 100X into sterile saline (Humalin R, Eli Lilly Canada Inc., Toronto, ON Canada, 100U/mL). Using a mid-line incision, intestines were moved to expose the hepatic portal vein and 2 U/kg of insulin (Control and MNR N=5, 1 pup/litter) or saline (Control and MNR N=3, 1 pup/litter) was injected. After 1 minute and 15 seconds, a piece of right medial liver lobe, a quadriceps femoris muscle and perigonadal fat were frozen in liquid nitrogen. Samples were store in -80°C until western blot analysis (24).

2.2.5 Protein Isolation

Fifty mg of frozen liver and muscle and 100 mg of adipose tissue were pulverized (Medium Bessman Tissue Pulverizer, Spectrum Laboratories, Rancho Dominguez, CA) and then homogenized for 30 seconds with the Brinkmann Homogenizer Polytron® 3000 in 1x Cell Lysis Buffer (9803S, Cell Signaling Technology® Inc., Danvers, MA) and protease inhibitor cocktail 1, 2, and 3 (P1860, P5726, and P0044, Sigma-Aldrich, St. Louis, MO, USA). The homogenate was then sonicated (F550 Sonic Dismemberator, Fisher Scientific, Markham, ON Canada) and rocked for 40 minutes at 4°C. Samples were spun at 12,000 x g for 10 minutes at 4°C. Supernatants were collected, with care not to collect the lipid layer, and stored at -20°C until analysis. Protein quantification was done with the Bio-Rad Protein Assay according to the manufacturer's protocol using BSA standards (Cat #500-0006, Bio-Rad Laboratories Inc., Des Plaines, IL).

2.2.6 Western Blotting

Protein samples were boiled in sodium dodecyl sulfate (SDS) sample loading buffer with 0.1M dithiothreitol (DTT) at 75 °C for 5 min then incubated on ice for 5 minutes. 10 μg of protein was loaded and run on a 10% SDS polyacrylamide gel. Proteins were transferred to a polyvinylidene difluoride (PVDF) membrane using the Trans-Blot® Turbo™ Transfer System and Trans-Blot® Turbo™ RTA Midi Transfer Kit (170-4273, Bio-Rad Laboratories Inc., Des Plaines, IL) according to the manufacturer's protocol.

Once the transfer was completed, membranes were dipped in methanol and blocked with 5% milk in TBST (TBS + 1 % tween). Blocking buffer was rinsed from the membrane for 5 min (3x) with TBST at room temperature (RT). Primary antibody for p-AKT (#4000, rabbit mAB, Cell Signaling Technology® Inc.) was diluted 1:1000 into 5% BSA in TBST and incubated with blots shaking at overnight at 4°C. Membranes were rinsed with TBST 3 x (5 min.) at RT and then incubated with secondary rabbit IgG (#170-6515, Bio-Rad Laboratories Inc., Des Plaines, IL) diluted 1:10,000 in 5% milk in TBST for 1 hour at RT. After rinsing the secondary antibody, Clarity™ Western ECL Substrate (170-5061, Bio-Rad Laboratories Inc., Des Plaines, IL) and a VersaDoc Imaging System (Bio-Rad Laboratories Inc., Des Plaines, IL), was used to capture an image of the gel. Membranes were then rinsed and stripped with 0.5M NaOH, rinsed in TBS (3 x 5 min at

RT) and reprobed with AKT (#9272, Bio-Rad Laboratories Inc., Des Plaines, IL), according to the protocol above.

Quantification of blots was done using Imagelab software® version 5.1 BETA (Bio-Rad Laboratories Inc., Des Plaines, IL) and quantities were compared using p-AKT to total AKT ratios.

2.2.7 Serum Peptide Markers for Obesity and Diabetes

Blood samples collected by intracardiac puncture at 1 (Control N=7, MNR N=18, 4 control and 10 MNR litters, 1-2 pups/litter) and 6 months (5 control and 10 MNR litters, 3-7 pups/litter, MNR N=52, control N= 30) in non-fasted mice (8 30 - 9 30 h) were used in this multiplex assay. At the time of collection, protease inhibitors, 10mM DPP-IV (EMD Millipore, DPP4-010) and 1.3% aprotinin inhibitor (EMD Millipore, 616399) in 0.9% sterile saline, were added to the blood samples (10uL/mL). Samples were allowed to clot for 45 minutes and spun at twice at 12 000 x g for 10 minutes to obtain serum. All serum samples were stored at -80°C. Ghrelin, leptin, insulin, glucagon, PAI-1, GLP, GIP and resistin were assayed on the Bio-rad Multiplex at Lawson's Multiplex Facility, London, ON, using the Bio-Plex Pro Mouse Diabetes Assay (171F7001M, Bio-Rad Laboratories Inc., Des Plaines, IL). Serum C-peptide was also quantified according to the manufacturer's protocol (Mouse C-Peptide ELISA, 80-CPTMA-E1, Alpco, Salem, NH).

2.2.8 Lipid Quantification in Serum and Liver

An aliquot of non-fasted serum as described above was used to for cholesterol (Cholesterol Quantification Kit MAK043, Sigma-Aldrich®, St. Louis, MO) and triglyceride quantification (Triglyceride Quantification Assay Kit ab65336, Abcam®, Cambridge MA). Liver cholesterol was also isolated from non-fasted liver tissue and quantified according the manufacturer's protocol. Measurements were taken from 5 control and 10 MNR litters, 3-6 pups/litter.

2.2.9 Statistical Analysis

Data are presented as mean ± SEM or as whisker plots (median and data range in quartiles). For glucose tolerance testing, pyruvate challenge tests and random blood glucose measurements a repeated measures ANOVA and Bonferroni post hoc correction

was used. For all other analyses, a Mann-Whitney test was used to compare means where samples sizes were > 8, and an unpaired *t*-test with ≤ 8 samples. Means are considered significantly different if $p < 0.05$. All statistics and graphs were produced in Prism software (Graphpad®, version 5.2), or the R console (version 3.3.2) with ggplot2 (version 2.2.1) and sciplot (version 1.1-0) software packages.
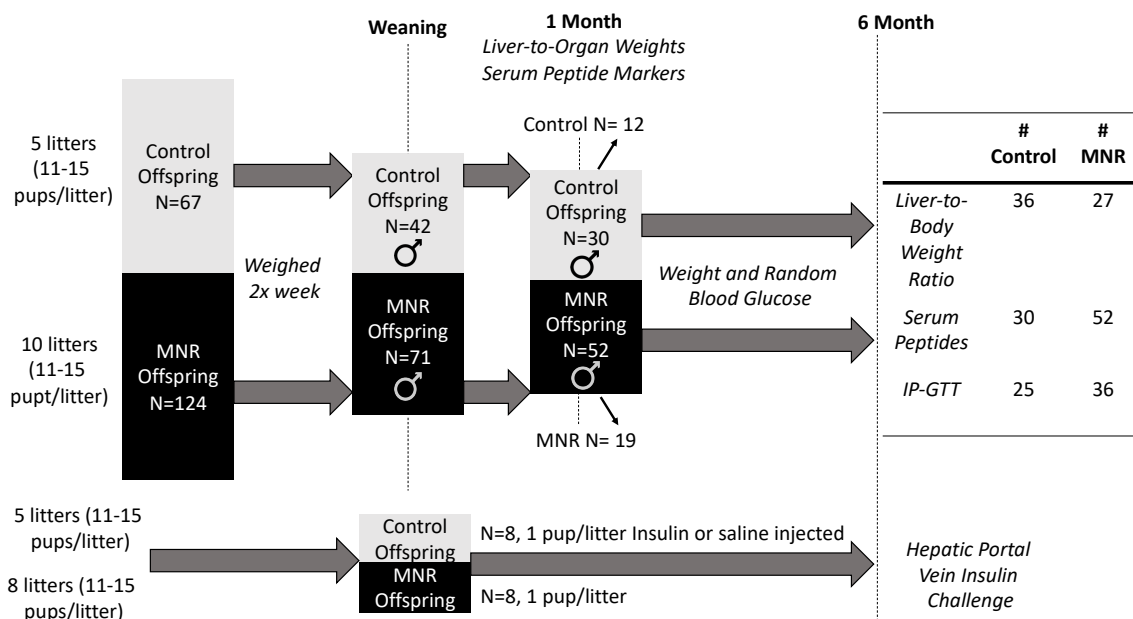
Figure 2.2.1 Litter and Pup Sample Size for Postnatal Studies.

2.3   Results

Maternal total-calorie nutrient restriction (MNR) resulted in a 13% reduction ($p = 0.001$) in fetal weight at E18.5 in males (**Figure 2.3.1A**), and 14% reduction ($p = 1.5 \times 10^{-8}$) in birth weight of males (**Figure 2.3.1B**), relative to controls. E18.5 weight did not vary significantly with position relative to blood supply ($p = 0.4$) (**Supplementary Figure S2.3.1**). Body weights are not significantly different in MNR offspring between day 3 of life and 6 months (**Figure 2.3.1C**), except at 1 month ($p = 0.006$) when controls (23.5 ± 0.4 g) were heavier than MNR (22.3 ± 0.3 g). This protocol demonstrated a reproducible fetal growth restriction from moderate maternal nutrient restriction.

In addition to body weight, organ weights were measured at each dissection. Fetal liver-to-body weight ratio was 1.4-fold reduced in MNR offspring (0.05 ± 0.003) relative to controls (0.07 ± 0.002, $p < 0.0001$), indicating a disproportionate effect of maternal nutrition on the liver (**Figure 2.3.2A**). All other organs were proportionally reduced with body weight. At one-month liver weight relative to body weight was similar in MNR offspring (0.053 ± 0.005) ($p = 0.09$) (**Figure 2.3.2B**) but decreased again by 6 months (0.039 ± 0.004) ($p = 0.03$) compared to controls (0.057 ± 0.008 and 0.042 ± 0.006, at 1 and 6 months respectively). The disproportionate impact on the liver growth suggests the effects of fetal nutrition extend into adulthood (**Figure 2.3.2C**).

Whole body glucose metabolism and hepatic glucose output was assessed with IP-GTT and pyruvate challenge tests, respectively. Reduced AUC in 6-month-old MNR offspring (1553 +/- 57) relative to controls (1323 +/- 68, $p = 0.045$) demonstrated impaired glucose tolerance (**Figure 2.3.3A and B**). Fasting blood glucose at the time of GTT did not differ in MNR offspring ($p = 0.3$) (**Figure 2.3.3A**). Blood glucose at all time points and the AUC for pyruvate challenge testing (**Supplementary Figure S2.3.2**) indicated similar hepatic glucose output in MNR offspring relative to controls. Therefore, moderate differences in glucose metabolism were detected in the MNR offspring.

Random blood glucose was measured once a month until 6 months of age. MNR offspring had similar blood glucose to controls each month ($p = 0.4$) and the AUC did not differ ($p = 0.3$) (**Figure 2.3.4**).

Serum peptide markers for diabetes and obesity were also assayed at one and six months of age. At one month, PAI-1 was 1.9-fold higher in MNR offspring relative to controls ($p = 0.04$) (**Figure 2.3.5A *i***). PAI-1 remained higher in six-month MNR offspring (1.5-fold) ($p = 0.04$) (**Figure 2.3.5B *i***). Increased resistin was also detected at 6 months in MNR offspring (189.8 + 9.8 ng/mL) relative to controls (171.2 + 14.5 ng/mL, $p = 0.04$) (**Figure 2.3.5B *v***). C-peptide, insulin-to-glucagon ratio, GIP, GLP, ghrelin and leptin did not differ based on maternal nutrition at one and six months (**Figure 2.3.5**).

In addition to peptide markers, lipids were measured in serum and the right lateral liver lobe at 6 months. No differences were observed between control and nutrient restricted offspring in serum triglycerides ($p = 0.6$) (**Figure 2.3.6 A*i***) or total cholesterol ($p = 0.7$) (**Figure 2.3.6 A*ii***). Additionally, control and MNR offspring had a similar liver cholesterol ($p = 0.07$) (**Figure 2.3.6 B**).

A hepatic portal vein insulin challenge was used to examine tissue-specific insulin sensitivity. Relative to controls, the p-AKT to AKT ratio was increased 2.5-fold in the liver of MNR offspring in response to the insulin injection ($p = 0.004$) (**Figure 2.3.7A**). Although not significant, insulin stimulated phosphorylation of AKT in adipose tissue (**Figure 2.3.7B**) and skeletal muscle (**Figure 2.3.7C**) was not significantly different in the nutrient restricted offspring, respectively ($p = 0.08$ and 0.05 respectively).

While changes in glucose metabolism occurred to some extent in all MNR offspring, there was a variation in the degree of response to fetal nutrient restriction on adult glucose metabolism. At 6 months, 19% of the offspring were less tolerant to glucose (**Figure 2.3.8A**) and had a higher AUC than any controls (**Figure 2.3.8B**). The remaining MNR have AUCs that were similar to those of controls.

Serum peptide analysis in the less tolerant mice showed increased insulin ($p = 0.006$), leptin ($p = 0.001$) (**Figure 2.3.9G**), and resistin ($p = 0.005$) (**Figure 2.3.9F**) levels, with no changes in other assayed peptide markers (**Figure 2.3.9**).
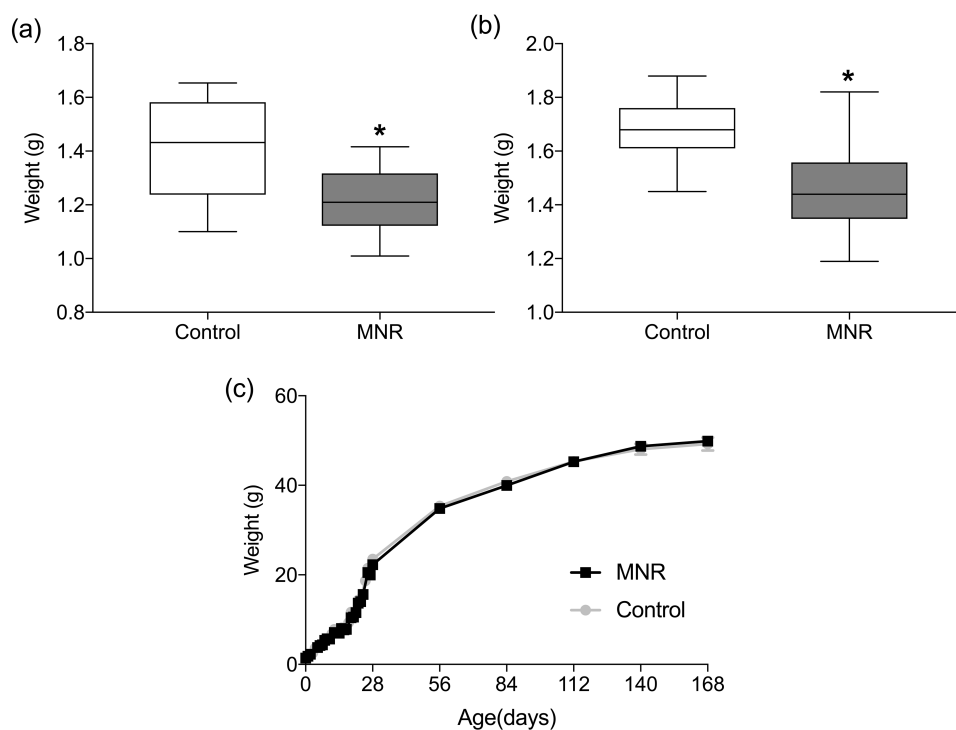
Figure 2.3.1 Body weights of MNR and Control offspring from E18.5 until 6 months.

At E18.5, fetal weights of MNR (N=15) were 13% smaller than controls (N=20) (p = 0.001) (3 Control and 3 MNR litters, 3-8 pups per litter) (*a*). Birth weight of MNR offspring remained 14% smaller (p = 1.5 x 10^{-8}) (Control N=39 from 5 litters, MNR N=58 from 10 litters, 4-9 pups/litter) (*b*). Except at 1 month when controls were heavier than MNR (p = 0.005), no differences were observed in weight from day 3 to 6 months. From birth-1-month, Control N= 37 and MNR N= 52 from 5 control and 10 MNR litters (3-11 pups/litter). From 2 months-6 months, Control N= 27 and MNR N=36 from 5 control and 10 MNR litters (3-9 pups/litter) (*c*). Growth curve data is plotted as the mean + SEM. Asterisk represents significance (p < 0.05) with a Mann-Whitney test.
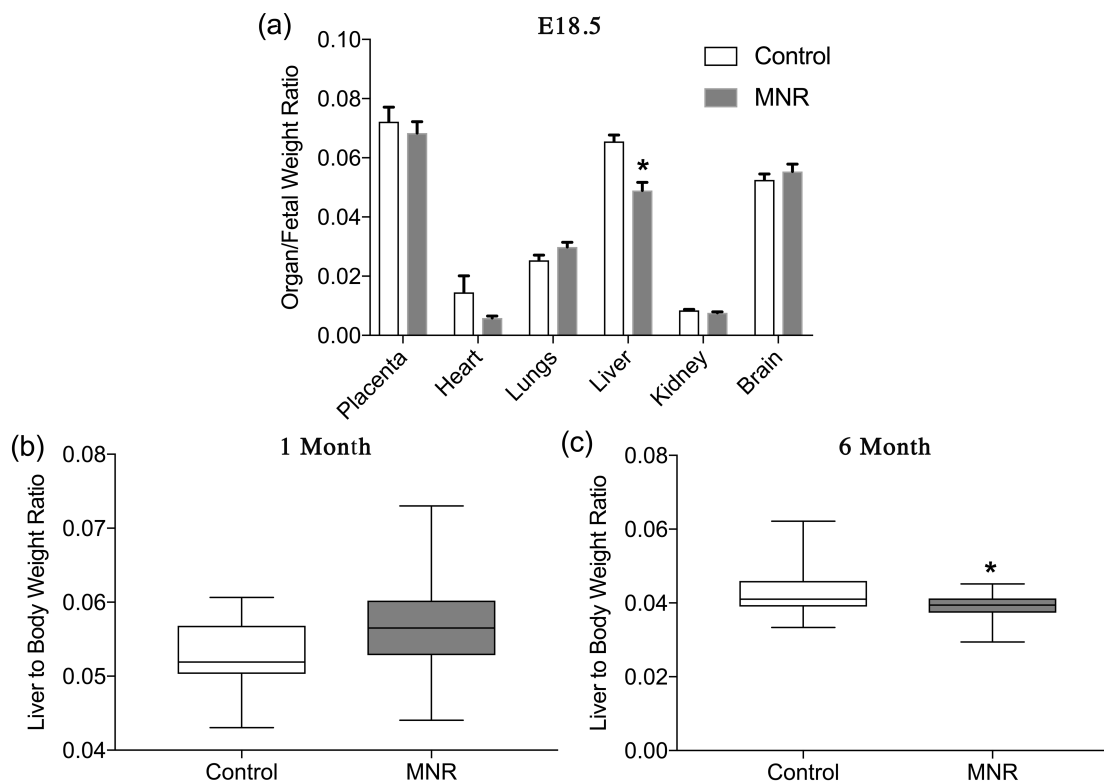
Figure 2.3.2 Organ weights of male offspring at E18.5, 1 month and 6 months.
(*a*) At E18.5, liver weight was reduced in MNR offspring relative to their body weight (*p* < 0.0001) (Control N=20 and MNR N=15, 3 litters/group, 3-8 pups/litter). (*b*) Relative to body weight the liver of MNR offspring was similar to controls at 1 month (*p* = 0.09) (control N=12 from 5 litters, MNR N=19, 9 litters, 1-3 pups/litter) and significantly lower at 6 months (*p* = 0.03) (control N= 24, MNR N=30, 5 control and 10 MNR Litters, 3-8 pups/litter). (*c*). Fetal data are mean + SEM (*a*). Asterisk represents a *p* < 0.05 with a Mann-Whitney test.
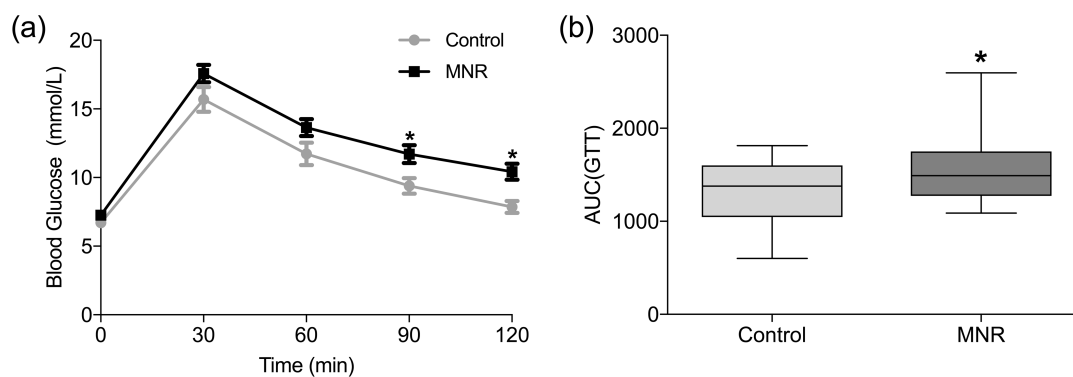
Figure 2.3.3 IP-GTT of male offspring at 6 months.

Blood glucose at 90 and 120 minutes were significantly higher in MNR offspring (N=36, 10 litters) relative to controls (N= 25, 5 litters, 3-8 pups/litter) (*a*). The AUC was also significantly higher ($p = 0.045$) (*b*). Glucose tolerance data (*a*) are mean + SEM. Asterisk represents a $p < 0.05$ with a Bonferroni post hoc (*a*) or Mann-Whitney test (*b*).
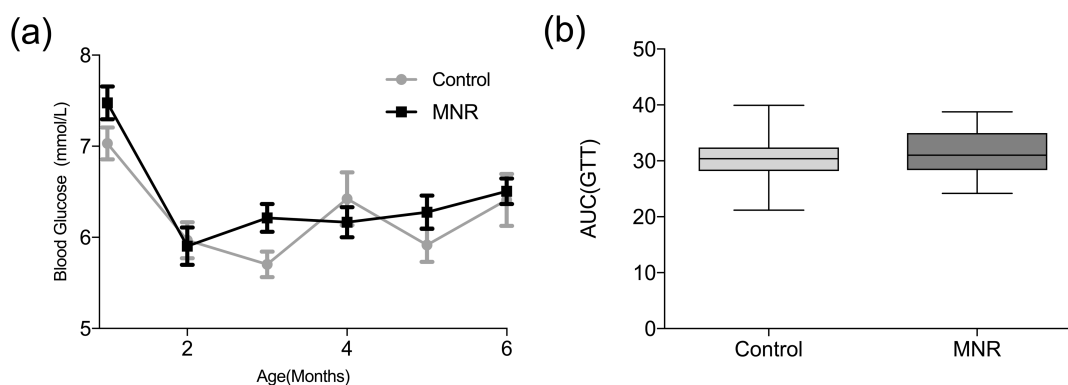
Figure 2.3.4 Random blood glucose in male MNR and control offspring from 1 to 6 months of age.

(A) Random blood glucose did not significantly differ at age. (B) AUC from random blood glucose was similar between MNR and control indicating normoglycemia in MNR offspring. At 1 month Control N= 33, MNR N= 51 (5 control and 10 MNR litters, 3-11 pups/litter); from 2 months-6 months Control N= 26, MNR N=36 (5 control and 10 MNR litters, 3-9 pups/litter). Data are mean + SEM (*a*) or whisker plots (*b*). Asterisk represents a $p < 0.05$ with a repeated measures ANOVA(*a*) or Mann-Whitney test(*b*).
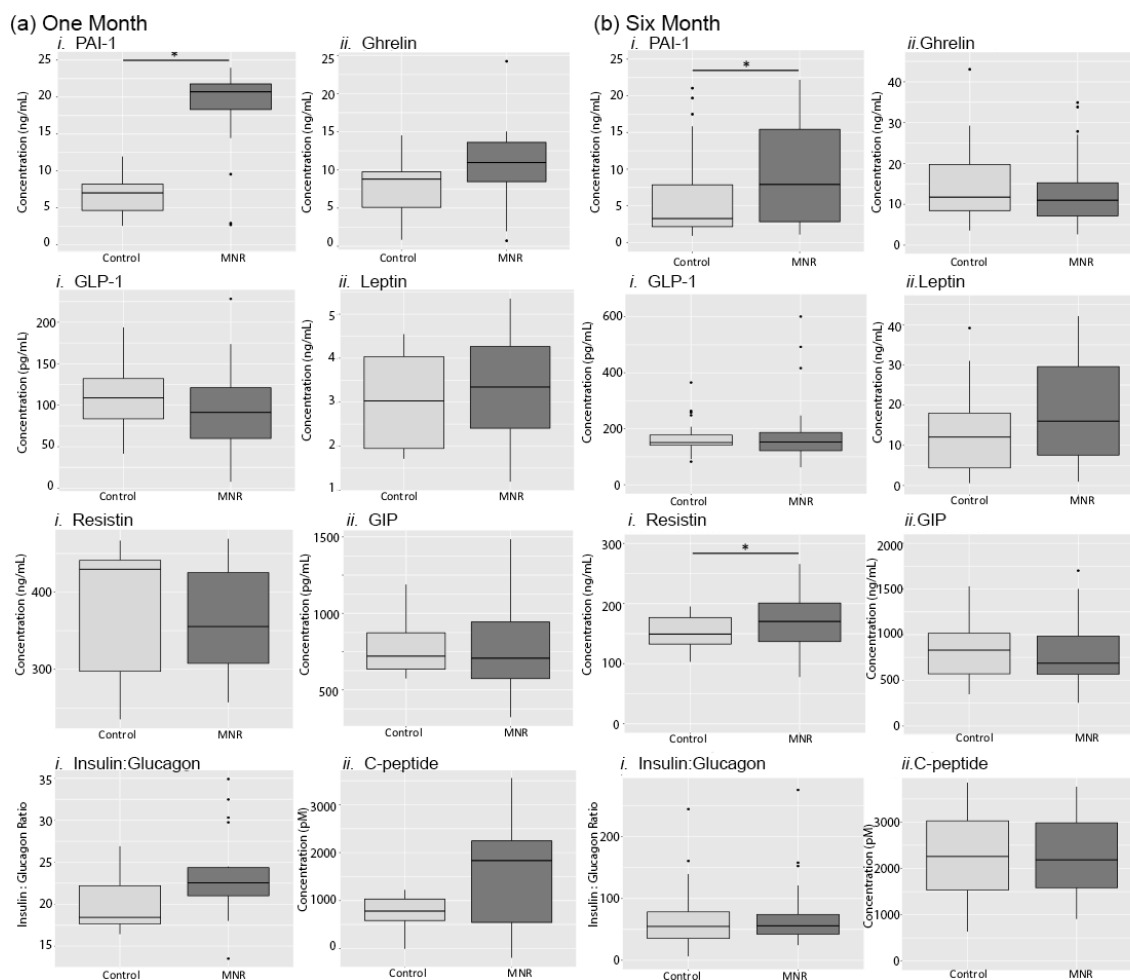
Figure 2.3.5 Serum peptide markers for obesity and diabetes.

Peptides were measured at (*a*) 1 month (Control N=7, MNR N=18, 4 control and 10 MNR litters, 1-2 pups/litter), and (*b*) 6 months of age (5 control and 10 MNR litters, 3-7 pups/litter, MNR N=52, control N= 30). PAI-1 was increased in MNR offspring at 1 month (*p* = 0.04) and 6 months (*p* = 0.04), (i) and resistin at 6 months (*p* = 0.04) (v). Ghrelin (*ii*), GLP-1 (*iii*), leptin (*iv*), GIP (*vi*), insulin to glucagon ratios (*vii*), and C-peptide (viii) levels were similar between control and MNR offspring. Data are presented as the median and quartiles in whisker plots. Asterisk indicates a *p* < 0.05 with a Mann-Whitney test.
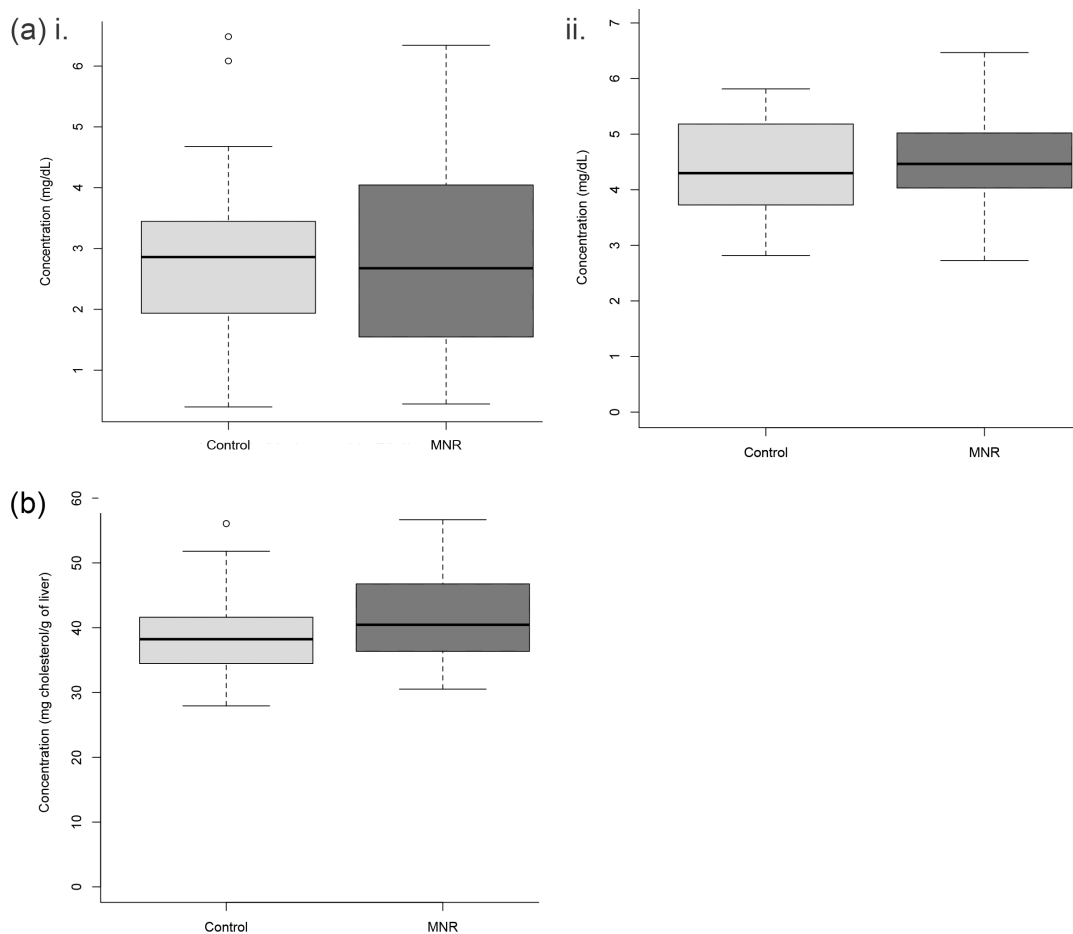
Figure 2.3.6 Serum and liver lipids in male MNR (N=36) and control (N=27) offspring at 6 months of age.

A. Serum triglyceride ($p = 0.6$) (i) and total cholesterol (ii) ($p = 0.7$) were not significantly different between MNR and control offspring. B. Liver total cholesterol was also similar between MNR and control offspring ($p = 0.07$). 5 control and 10 MNR litters, 3-6 pups/litter. Data are mean + SEM (a). Asterisk represents a $p < 0.05$ with a Mann-Whitney test.

(a) Liver
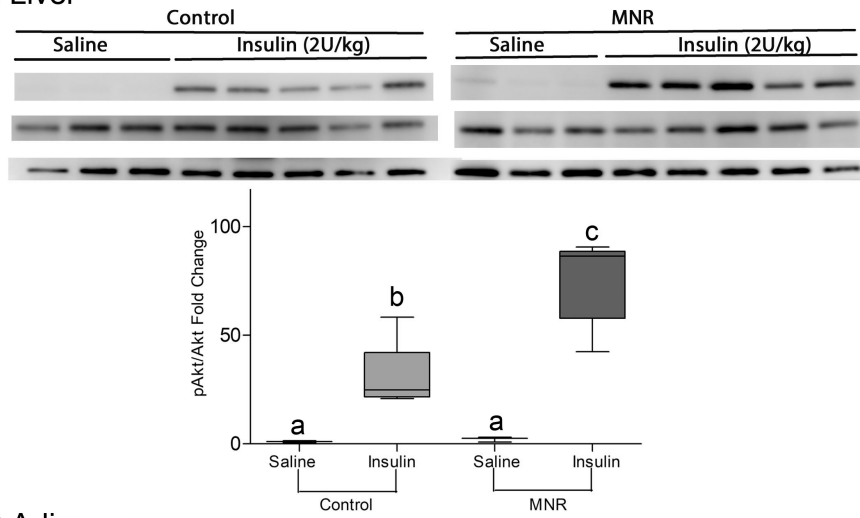
(b) Adipose
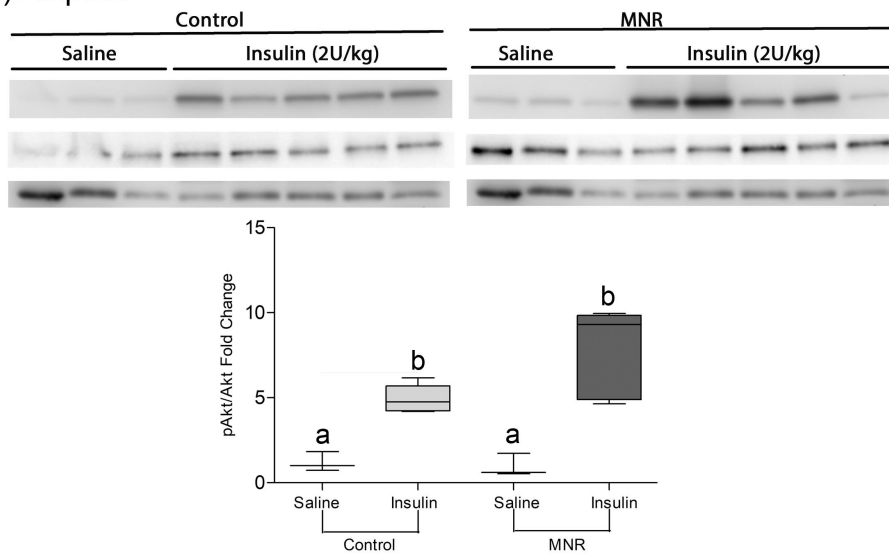
(c) Muscle
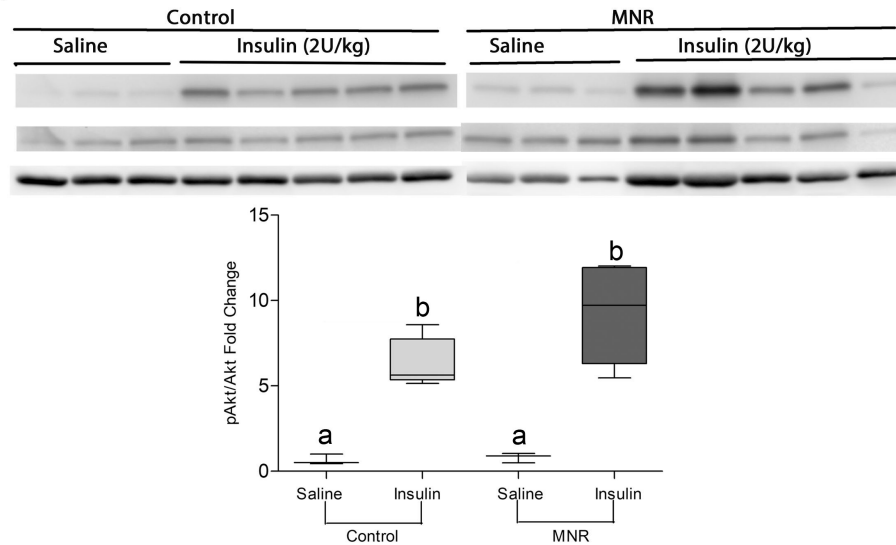
Figure 2.3.7 Insulin signalling as determined by phosphorylation of AKT in response to an insulin bolus in male MNR and control offspring at 7 months of age. p-Akt relative to AKT after an insulin dose was increased in MNR offspring relative to controls in the right medial liver lobe ($p = 0.004$) (*a*). p-AKT to AKT ratios were relatively increased in MNR adipose tissue and (*b*) skeletal muscle of insulin injected mice, but this change was not significant ($p = 0.08$ and 0.05, respectively) (*c*). Saline injected N=3 and insulin injected N=5 for both maternal nutrition groups (5 control and 8 MNR litters, 1 pup/litter). Western blots were done in quadruplicates. A representative blot and quantification of the replicates are shown with whisker plots. Means with different letters are significantly different ($p < 0.05$, unpaired *t*-test).

(a)

(b)

(c)
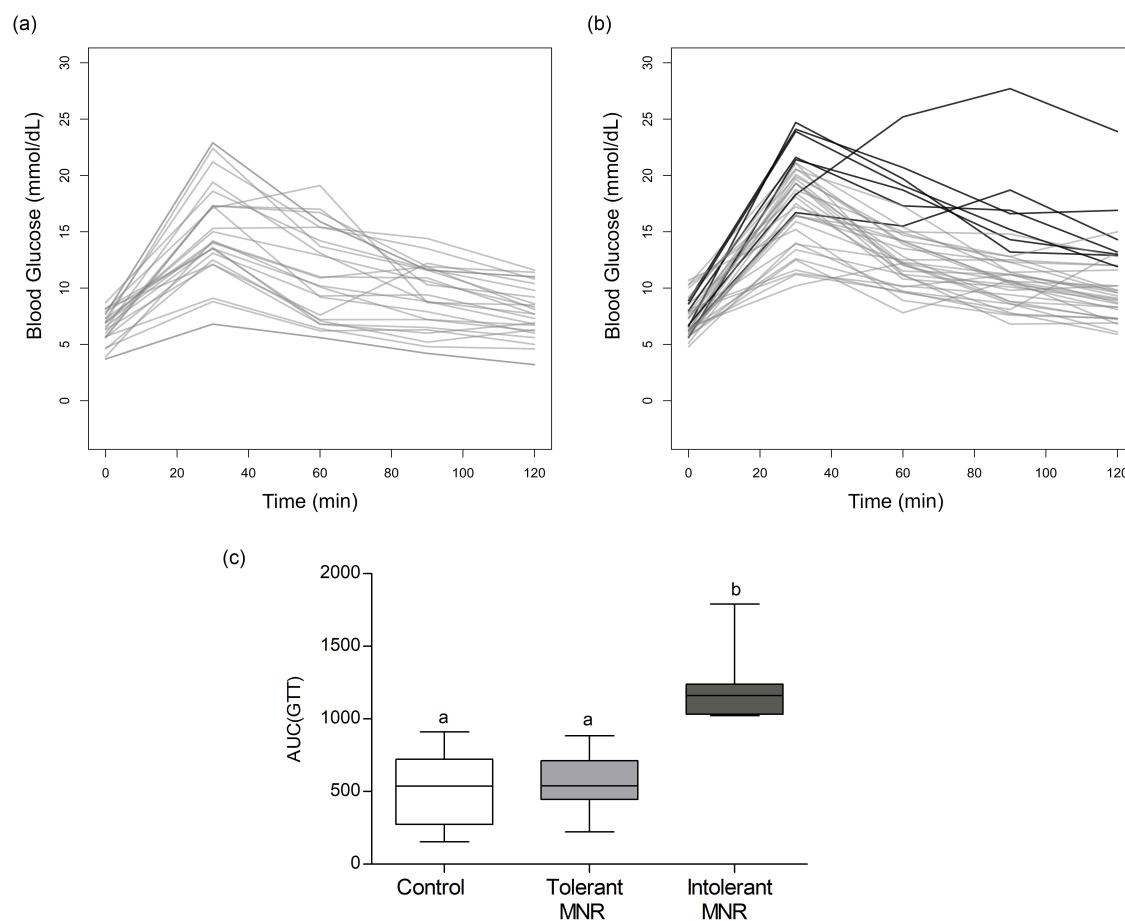
Figure 2.3.8 Glucose tolerance tests for all MNR and control offspring at 6 months.
(*a*) Individual glucose tolerance tests for controls demonstrate the range of responses. (*b*)
7 MNR (black) had an AUC under the curve greater than other MNR or controls (grey)
(*c*) which are referred to as intolerant MNR (5 control and 10 MNR litters, 3-8
pups/litter).

(a) PAI-1

(b) Ghrelin

(c) GLP-1

(d) Resistin

(e) Leptin

(f) GIP

(g) Insulin-to-Glucagon ratio
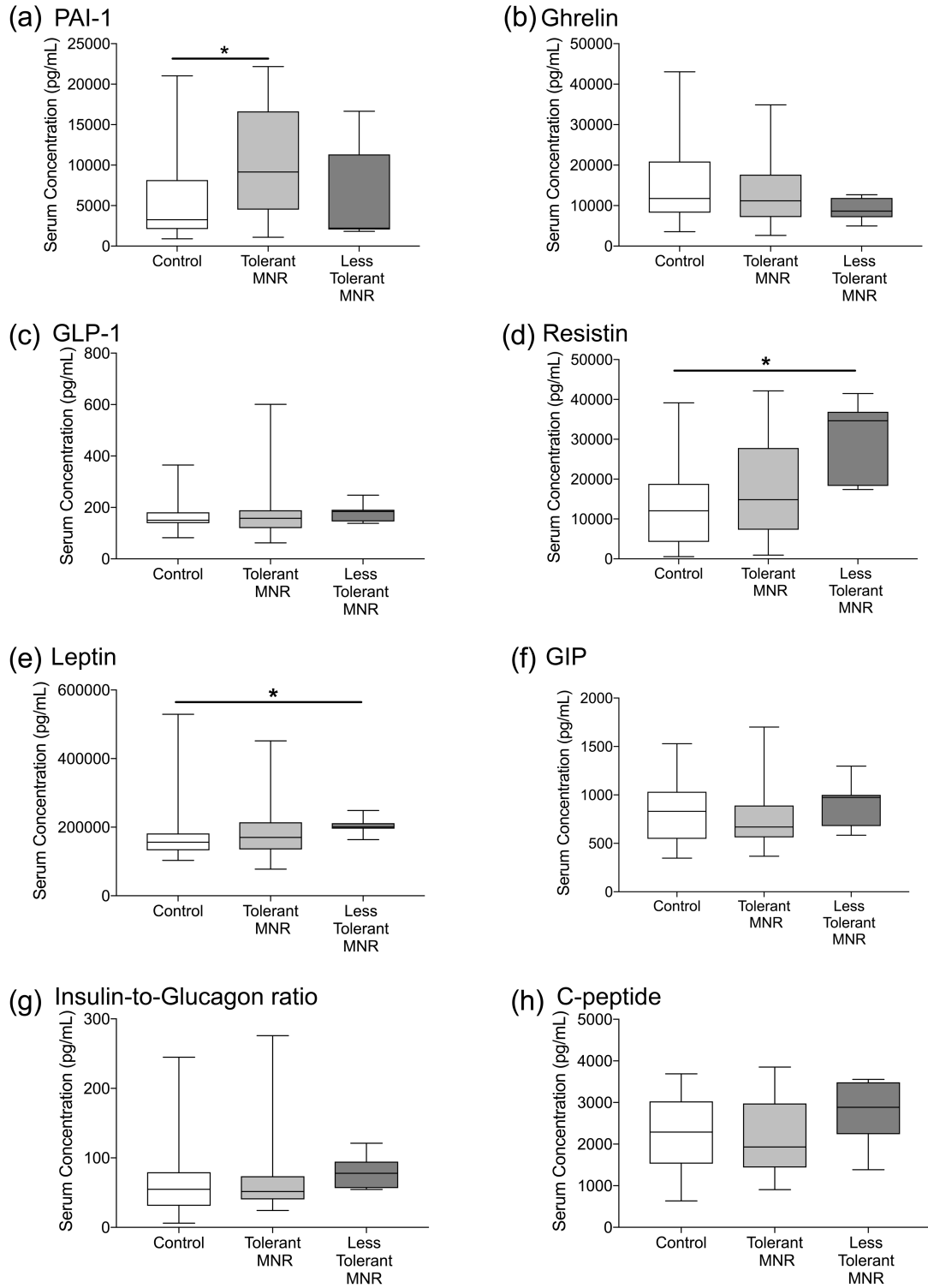
(h) C-peptide

Figure 2.3.9 Serum peptide markers for obesity and diabetes in male MNR and control offspring at 6 months old according to glucose tolerance.

Resistin ($p = 0.005$) (*d*) and leptin ($p = 0.001$) (*e*) were significantly increased in MNR offspring that are glucose intolerant. PAI-1 (*a*), Ghrelin (*b*), GLP-1(*c*), GIP(*f*), insulin:glucagon (*g*) and c-peptide (*h*) were not significantly different in intolerant MNR. Control N=30 (5 litters, 3-8 pups/litter), tolerant MNR N=43 (10 litters, 3-8 pups/litter) and intolerant MNR N=7 (5 litters, 1-2 pups/litter). Asterisk represents a $p < 0.05$ with a Mann-Whitney test.

2.4   Discussion

In humans, FGR can be symmetric or asymmetric. Symmetric FGR, meaning all organs are reduced proportionately to body weight, is often associated with an insult of early-onset (25). Conversely, asymmetric FGR is more common in late-onset growth restriction, and is where less essential organs are reduced but vital organs such as the brain and the heart are spared (25). Similar to humans, maternal undernutrition in mice resulted in an asymmetric growth restriction and had the most significant impact on the liver (26). The thymus and spleen are also smaller relative to body weight in SGA autopsies (26) but were not measured in this study. Although reduced again at 6 months, one-month relative liver weights were similar to controls which might indicate differences in growth rate of the liver in MNR offspring. MNR in guinea pigs do not result in reduced liver-to-fetal weight ratios but fractional growth rates are increased near term (9). These data suggest that liver growth may be more sensitive than other organs to fetal undernutrition.

The variation in response to fetal nutrient restriction in our model was similar to the variations observed in the human FGR populations. Some individuals with extremely low birth weights (ELBW) although having 3 times greater risk will not develop glucose intolerance and type 2 diabetes(3). In adults, genetic variation and differential expression contribute to obesity and metabolic disorder resistant and/or susceptible populations of non-human primate (27) and rodent models (28,29) in response to nutritional stress, such as a high fat diet. Offspring in models exposed to a maternal high fat diet or nutrient restriction have metabolic (7,30), gut microbe (31) and epigenomic changes (32), but to our knowledge none of these models focus on changes specific to susceptible and resistant populations in these offspring. Having glucose tolerant and intolerant offspring resulting from MNR allow future studies to examine adaptations in glucose metabolism within the MNR populations and in all offspring exposed to nutrient restriction *in utero*.

In this study, normal glucose tolerance observed in 81% of the offspring might have been due to increased insulin sensitivity as adults despite having smaller livers. Increased insulin sensitivity is present at birth and persists a few weeks postnatally in lambs exposed to hypoxia-induced placental insufficiency (33). To our knowledge, evidence of

insulin desensitization (6,7) has been observed rather than persistence of the increased sensitivity into adulthood. Intolerant MNR offspring, which had relatively higher insulin-to-glucagon ratios, could have insulin resistance that was not detectable during insulin sensitivity test due to the limited sample size. Studies comparing liver responses in intolerant and tolerant MNR mice may provide insight into why some offspring are able to adapt to the postnatal parameters assessed in this study.

Despite having similar body weight at 6 months, PAI-1 and resistin levels were increased in MNR offspring. Both are produced primarily in adipose tissue in mice (16,17) and are associated with obesity and low-grade chronic inflammation (16,17,34). Individuals born SGA with the highest body mass index (BMI) have reduced insulin sensitivity (35). However, total fat pads are increased in female adult rats that experienced 50% nutrient restriction throughout gestation with similar adult body weights to controls (36). ELBW babies have also have similar BMI with increased body fat mass (3). Subsequently, increased markers for obesity and meta-inflammation may indicate reduced lean mass in male offspring in response to fetal undernutrition even with similar adult body weights. MNR offspring with glucose intolerance had higher serum resistin, and it cannot be excluded that increased fat mass may contribute to the development of glucose intolerance.

Leptin was also increased in intolerant offspring. Serum leptin is correlated with body fat mass in humans (37) and mice(38), supporting the notion of differences in body composition. This marker could also indicate a decreased appetite in less tolerant MNR offspring. Alternatively, leptin resistance occurs in diet-induced obesity (39) and increased leptin in offspring with impaired glucose homeostasis may be a sign of leptin resistance. Leptin may also play a role in regulation of energy expenditure (39) and behavior changes, such as food preference and total activity. These behaviors are also altered in adulthood following IUGR or undernourishment during development (40,41). Increased serum leptin levels suggest that behaviors or body mass composition may be altered in susceptible MNR offspring and require further investigation.

Moderate nutrient restriction throughout gestation resulted in changes to the liver and adipose tissue including decreased fetal liver weight and increased adult insulin sensitivity in the liver. Serum markers for body mass composition and meta-inflammation were also increased. The liver is important in regulation of lipid and glucose metabolism and a key tissue in the development of type 2 diabetes. While it is possible that some adaptations occur in all offspring exposed to MNR, additional physiological and biochemical changes in the liver or other organs may be specific to those that develop glucose intolerance. This model provides an opportunity to investigate the tissue-specific molecular mechanism underlying changes between control and MNR as well as susceptible and resistance offspring. The variation in MNR offspring represents the diversity in human FGR populations and their susceptibilities towards type 2 diabetes (3,4).

2.5   References

1. Han VKM, Seferovic MD, Albion CD, Gupta MB (2012) Intrauterine Growth Restriction: Intervention Strategies. In: Buonocore G., Bracci R., Weindling M. (eds) Neonatology. Springer, Milano, p. 89-93.

2. Garite TJ, Clark R, Thorp JA. Intrauterine growth restriction increases morbidity and mortality among premature neonates. *Am J Obstet Gynecol*. 2004;191:481–7.

3. Morrison KM, Ramsingh L, Gunn E, et al. Cardiometabolic Health in Adults Born Premature With Extremely Low Birth Weight. *Pediatrics*. 2016;138:e20160515.

4. Würtz P, Wang Q, Niironen M, et al. Metabolic signatures of birthweight in 18 288 adolescents and adults. *Int J Epidemiol*. 2016;45:1539–50.

5. Hales C, Barker D. Type 2 (non-insulin-dependent) diabetes mellitus: the thrifty phenotype hypothesis. *Diabetologia*. 1992;35:595~601.

6. Oliveira D, Cezar J, Gomes RM, et al. Protein Restriction During the Last Third of Pregnancy Malprograms the Neuroendocrine Axes to Induce Metabolic Syndrome in Adult Male Rat Offspring. *Endocrinology*. 2016;157:1799–812.

7. Xiao D, Kou H, Zhang L, Guo Y, Wang H. Prenatal Food Restriction with Postweaning High-fat Diet Alters Glucose Metabolic Function in Adult Rat Offspring. *Arch Med Res*. 2017;48:35–45.

8. Lee S, You Y-A, Kwon EJ, Jung S-C, Jo I, Kim YJ. Maternal Food Restriction during Pregnancy and Lactation Adversely Affect Hepatic Growth and Lipid Metabolism in Three-Week-Old Rat Offspring. *Int J Mol Sci*. 2018;314:R647-R654.

9. Nevin CL, Formosa E, Maki Y, Matushewski B, Regnault TRH, Richardson BS. Maternal Nutrient Restriction in Guinea Pigs as an Animal Model for Studying Growth Restricted Offspring with Post-Natal Catch-Up Growth. *Am J Physiol-Regul Integr Comp Physiol* 2018;314: R647-R654. doi: 10.1152/ajpregu.00317.2017.

10. Wang J, Cao M, Zhuo Y, et al. Catch-up growth following food restriction exacerbates adulthood glucose intolerance in pigs exposed to intrauterine undernutrition. *Nutrition*. 2016;32:1275–84.

11. Liu Y, Ma C, Li H, Li L, Gao F, Ao C. Effects of intrauterine growth restriction during late pregnancy on the cell apoptosis and related gene expression in ovine fetal liver. *Theriogenology* 2017;90:204–9.

12. Vomhof-DeKrey E, Darland D, Ghribi O, Bundy A, Roemmich J, Claycombe K. Maternal low protein diet leads to placental angiogenic compensation via dysregulated M1/M2 macrophages and TNFα expression in Sprague-Dawley rats. *J Reprod Immunol*. 2016;118:9–17.

13. Palha AM, Pereira SS, Costa MM, et al. Differential GIP/GLP-1 intestinal cell distribution in diabetics' yields distinctive rearrangements depending on Roux-en-Y biliopancreatic limb length. *J Cell Biochem*. 2018;119:7506-7515.

14. Nauck MA, Meier JJ. Incretin hormones: Their role in health and disease. *Diabetes Obes Metab*. 2018;20 Suppl 1:5–21.

15. Leighton E, Sainsbury CA, Jones GC. A Practical Review of C-Peptide Testing in Diabetes. *Diabetes Ther*. 2017;8:475–87.

16. Qatanani M, Szwergold NR, Greaves DR, Ahima RS, Lazar MA. Macrophage-derived human resistin exacerbates adipose tissue inflammation and insulin resistance in mice. *J Clin Invest*. 2009;119:531–9.

17. Kaji H. Adipose Tissue-Derived Plasminogen Activator Inhibitor-1 Function and Regulation. *Compr Physiol*. 2016;6:1873–96.

18. Bewick GA, Kent A, Campbell D, et al. Mice With Hyperghrelinemia Are Hyperphagic and Glucose Intolerant and Have Reduced Leptin Sensitivity. *Diabetes*. 2009;58:840–6.

19. Kalra SP, Ueno N, Kalra PS. Stimulation of Appetite by Ghrelin Is Regulated by Leptin Restraint: Peripheral and Central Sites of Action. *J Nutr*. 2005;135:1331–5.

20. Lecoutre S, Marousez L, Drougard A, et al. Maternal undernutrition programs the apelinergic system of adipose tissue in adult male rat offspring. *J Dev Orig Health Dis*. 2017;8:3–7.

21. Simchen MJ, Weisz B, Zilberberg E, et al. Male disadvantage for neonatal complications of term infants, especially in small-for-gestational age neonates. *J Matern Fetal Neonatal Med*. 2014;27:839–43.

22. Delahaye F, Wijetunga NA, Heo HJ, et al. Sexual dimorphism in epigenomic responses of stem cells to extreme fetal growth. *Nat Commun*. 2014;5:5187.

23. Pae M, Baek Y, Lee S, Wu D. Loss of ovarian function in association with a high-fat diet promotes insulin resistance and disturbs adipose tissue immune homeostasis. *J Nutr Biochem*. 2018;57:93–102.

24. Chamson-Reig A, Thyssen SM, Hill DJ, Arany E. Exposure of the Pregnant Rat to Low Protein Diet Causes Impaired Glucose Homeostasis in the Young Adult Offspring by Different Mechanisms in Males and Females. *Exp Biol Med*. 2009;234:1425–36.

25. Nardozza LMM, Araujo Júnior E, Barbosa MM, Caetano ACR, Lee DJR, Moron AF. Fetal growth restriction: current knowledge to the general Obs/Gyn. *Arch Gynecol Obstet*. 2012;286:1–13.

26. Man J, Hutchinson JC, Ashworth M, Jeffrey I, Heazell AE, Sebire NJ. Organ weights and ratios for postmortem identification of fetal growth restriction: utility and confounding factors. *Ultrasound Obstet Gynecol Off J Int Soc Ultrasound Obstet Gynecol*. 2016;48:585–90.

27. Harris RA, Alcott CE, Sullivan EL, et al. Genomic Variants Associated with Resistance to High Fat Diet Induced Obesity in a Primate Model. *Sci Rep*. 2016;6:36123.

28. Weingarten A, Turchetti L, Krohn K, et al. Novel genes on rat chromosome 10 are linked to body fat mass, preadipocyte number and adipocyte size. *Int J Obes*. 2016;40:1832–40.

29. Chen K, Jih A, Osborn O, et al. Distinct gene signatures predict insulin resistance in young mice with high fat diet-induced obesity. *Physiol Genomics*. 2018;50:144–57.

30. Zhu W-F, Zhu J-F, Liang L, Shen Z, Wang Y-M. Maternal undernutrition leads to elevated hepatic triglycerides in male rat offspring due to increased expression of lipoprotein lipase. *Mol Med Rep*. 2016;13:4487–93.

31. Ma J, Prince AL, Bader D, et al. High-fat maternal diet during pregnancy persistently alters the offspring microbiome in a primate model. *Nat Commun*. 2014;5:3889.

32. Heo HJ, Tozour JN, Delahaye F, et al. Advanced aging phenotype is revealed by epigenetic modifications in rat liver after in utero malnutrition. *Aging Cell*. 2016;15:964–72.

33. Camacho LE, Chen X, Hay WW, Limesand SW. Enhanced insulin secretion and insulin sensitivity in young lambs with placental insufficiency-induced intrauterine growth restriction. *Am J Physiol-Regul Integr Comp Physiol*. 2017;313:R101–9.

34. Kim S-H, Park H-S, Hong MJ, et al. Tongqiaohuoxue decoction ameliorates obesity-induced inflammation and the prothrombotic state by regulating adiponectin and plasminogen activator inhibitor-1. *J Ethnopharmacol*. 2016;192:201–9.

35. Veening MA, Weissenbruch V, M M, Waal D de, A H. Glucose Tolerance, Insulin Sensitivity, and Insulin Secretion in Children Born Small for Gestational Age. *J Clin Endocrinol Metab* 2002;87:4657–61.

36. de Souza AP, Pedroso AP, Watanabe RLH, et al. Gender-specific effects of intrauterine growth restriction on the adipose tissue of adult rats: a proteomic approach. *Proteome Sci*. 2015;13:32. DOI: 10.1186/s12953-015-0088-z.

37. Soininen S, Sidoroff V, Lindi V, et al. Body fat mass, lean body mass and associated biomarkers as determinants of bone mineral density in children 6–8years of age – The Physical Activity and Nutrition in Children (PANIC) study. *Bone*. 2018;108:106–14.

38. Xiao X, Sun Q, Kim Y, et al. Exposure to permethrin promotes high fat diet-induced weight gain and insulin resistance in male C57BL/6J mice. *Food Chem Toxicol*. 2018;111:405–16.

39. Meakin PJ, Jalicy SM, Montagut G, et al. Bace1-dependent amyloid processing regulates hypothalamic leptin sensitivity in obese mice. *Sci Rep*. 2018;8:55.

40. Silveira PP, Pokhvisneva I, Gaudreau H, et al. Fetal growth interacts with multilocus genetic score reflecting dopamine signaling capacity to predict spontaneous sugar intake in children. *Appetite*. 2018;120:596–601.

41. Lira LA, Almeida LCA, da Silva AAM, et al. Perinatal undernutrition increases meal size and neuronal activation of the nucleus of the solitary tract in response to feeding stimulation in adult rats. *Int J Dev Neurosci*. 2014;38:23–9.

Chapter 3 : High-Fat High-Sugar Diet Impairs Offspring Glucose Tolerance Independent of Poor Maternal Nutrition in Mice

3.1   Introduction

Intrauterine growth restriction (IUGR) is a pregnancy condition where fetal growth is suboptimal, resulting in an infant born small for gestation age (<10th percentile). These infants have increased risk for perinatal morbidity and mortality (1), and as adults are more likely to develop obesity and type II diabetes (2,3). Common causes of IUGR include maternal malnutrition and placental insufficiency, both resulting in fetal nutrient restriction (4). It is thought that the fetus may adapt metabolically to enhance survival in a nutrient restrictive environment, but these adaptations may persist to adulthood where nutrients are abundant and increase the risk for metabolic diseases. This concept is termed the "thrifty hypothesis" (5).

Modulation of the post-weaning diet may mediate these long-term effects. Studies have shown that 'catch-up' growth is associated maladaptive effects on glucose metabolism, and that dietary prevention of 'catch-up' growth is metabolically protective (6). A post-weaning nutrient-rich diet provides a larger mismatch between fetal and post-natal environments that will increase 'catch-up' growth, worsening glucose intolerance and obesity (7).

In humans and animals, a high caloric diet is associated with insulin resistance and type II diabetes (7,8). Different types of high caloric diets have been studied including high fat, fructose, sucrose, or to a lesser extent combination diets (9,10). While controversy exists on which type of diet is most harmful, excess calories seem to be important in metabolic disease promotion (8, 11). Regardless of the challenge, it is thought that fetal and adult diets can potentially interact and impact long term health. The data described in this report indicate a post-weaning high-fat high-sugar (HFHS) diet can disrupt adult glucose metabolism and overcome differences in offspring exposed to maternal undernutrition.

3.2   Methods

3.2.1 Animals

All animal handling was completed within the University of Western Animal Ethics Guidelines (2017-033). Maternal nutrient restriction was used as described by Radford and Han, *2018* (12). Briefly, virgin 8-week-old female CD-1 mice were mated and

vaginal plugs indicated E0.5. At E6.5 pregnant mice were randomly assigned to *ad libitum*-fed controls or maternal nutrient restriction (MNR) (70% of *ad libitum* total calories)(#F0173, Bio-Serv, Flemington, NJ) until E18.5. Litters with 11-15 pups were cross-fostered to *ad libitum*-fed mothers. Fostered litters were culled or fostered to 13 pups. At weaning, female offspring were euthanized and male offspring were randomly assigned to standard chow (Standard) or a high-fat high-sugar diet (HFHS) (Harlan TD.88137) (**Table 3.2.1**). The four groups studied were Control:Standard, Control:HFHS, MNR:Standard and MNR:HFHS (**Figure 3.2.1**).

Weights were measured once a month from 1 to 6 months. Monthly non-fasted blood glucose was also measured (1030 h) using a tail vein puncture and the Freestyle Lite Glucometer (Abbott Laboratories, USA) (Control:Standard N= 25, MNR:Standard N=36, Control:HFHS N=33 and MNR HFHS N=52) (**Figure 3.2.1).**

Table 3.2.1 Composition of Post-Weaning Diets.

Diet	Protein (% calories)	Carbohydrates (% calories)	Fat (% calories)	Fat composition (% of diet)	Sucrose (% by weight)
Standard Chow (Teklad LM-485)	25	17	58	0.8 saturated 1.3 monounsaturated 2.9 polyunsaturated - cholesterol	30
HFHS-diet (Harlan TD.88137)	15	43	42	13 saturated 6 monounsaturated 1 polyunsaturated 0.2 cholesterol	12

3.2.2 Metabolic caging

At 2 (N=4 per group) and 7-months (N=5 per group), metabolic analysis was assessed using the Comprehensive Lab Animal Monitoring System (CLAMS) with the Oxymax software (Columbus Instruments, Columbus, OH, USA) at the Robarts Research Institute (**Figure 3.2.1**). Mice were individually caged and acclimated for 16 hours. During the acclimation and measurement periods, cages were maintained at 24 ± 1 °C and mice

received free access to food and water. Measurements of respiratory exchange ratio (RER), food consumption, heat, and total activity were obtained every 10 minutes for 24h (12-h light/12-h dark), as previously described (13). Briefly, VO_2 and VCO_2 measurements were normalized to body weight (mL/kg/h) and used to calculate RER (VCO_2/VO_2). The use of pure carbohydrates as a metabolic substrate would result in a RER of 1 and exclusive fat oxidation would be 0.7. Heat produced was also calculated with VO_2 and RER [VO_2 x (3.816 +1.232 x RER)]. To assess activity, infrared beam breaks were monitored. Total activity is the sum of ambulatory activity or consecutive breaks along the x and y axis, and stereotypy activity which is beam breaks that do not meet ambulatory threshold.

3.2.3 Glucose Tolerance and Pyruvate Challenge Tests

For 6-month intraperitoneal glucose tolerance tests (IP-GTT), mice fasted for 4h (starting at 8 00 h) were injected intraperitoneally with glucose (2 g/kg). Blood glucose was measured at 0, 30, 60, 90 and 120 minutes via tail vein (Control:Standard N= 25, MNR: Standard N=36, Control:HFHS N=39, Control:HFHS N=63) (**Figure 3.2.1).** After one week of recovery, pyruvate challenge was completed with the same protocol as IP-GTT but pyruvate was injected at a dose of 2 g/kg (N=5 per group) (**Figure 3.2.1).**

3.2.4 Statistical Analysis

All statistical and graphical analysis were completed in Graphpad Prism (version 5.2 and 8). Mean body weights between groups were compared with a Mann-Whitney test. A two-way repeated measures ANOVA with a Bonferroni post-hoc was used to compare means from random blood glucose, glucose tolerance and pyruvate challenge tests. All data collected from metabolic caging was analyzed with a two-way ANOVA and a Bonferroni post-hoc test.
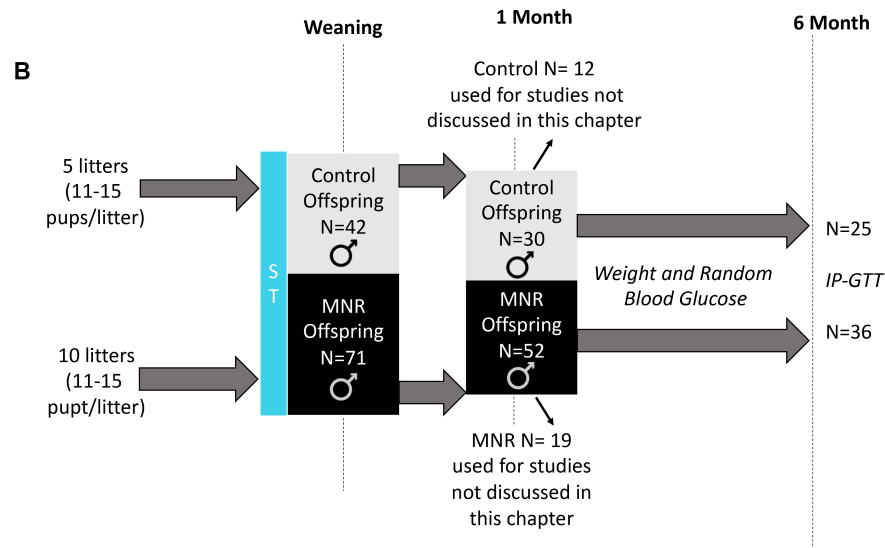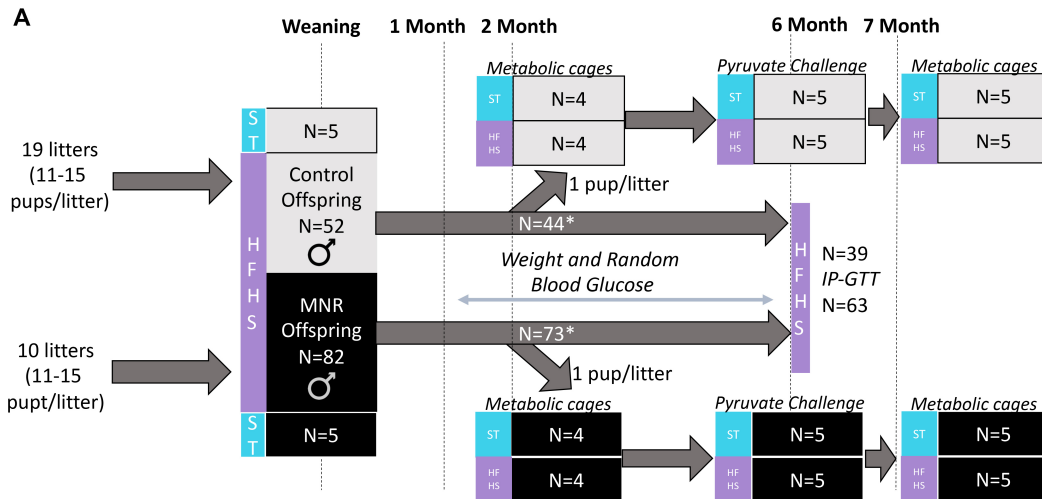
Figure 3.2.1 Litter and Sample Size Summary for MNR Offspring on a Post-Weaning Standard Chow or HFHS diet.

A cohort of male offspring on a post-weaning high-fat high-sugar (HFHS) from 19 MNR and 10 control litters was assessed for body weight, random blood glucose and glucose tolerance (**A**). Five offspring from separate litters were placed on a standard chow diet at weaning and compared to a littermate on a HFHS diet in metabolic cages (2 and 7 months) and with a pyruvate challenge test (6 months) (**B**). A second cohort was produced with 5 control and 10 MNR litters to measure body weight, random blood glucose and glucose tolerance. Tissues from 1 and 6 months were also collected for studies not describes in this chapter. Note: the number of pups on the HFHS diet declined between 2 and 7 months due to mortality or ulcerative dermatitis.

3.3   Results

Birth and weaning weights of MNR offspring prior to exposure to a post-weaning HFHS diet were discussed in chapter 2. Weights of MNR and controls were similar from 1 to 6 months on a HFHS diet. Weight from 1 to 6 months was significantly higher in HFHS-fed offspring relative to those on standard chow (1 month Control:Standard and MNR:HFHS $p = 0.03$, and all other $p < 0.0001$) (**Figure 3.3.1A**).

Random blood glucose measurements from 1 to 6 months did not differ significantly between maternal nutrition groups in HFHS-fed offspring. However, blood glucose levels were significantly increased from 1 to 5 months in HFHS-fed mice compared to standard chow-fed offspring (**Figure 3.3.1B**). These findings suggest that post-weaning diet, but not maternal nutrition, had an impact on growth and random blood glucose in the offspring.

Glucose tolerance and hepatic glucose output were assessed with IP-GTT and pyruvate challenge tests, respectively. No differences in glucose tolerance were detected in between maternal nutrient groups within the same diet (**Figure 3.3.1C**). All HFHS-fed offspring had higher a blood glucose relative to those fed standard show in response to a glucose bolus at all time points (**Figure 3.3.1C**). AUCs for Control:HFHS (1001 ± 54.52) and MNR:HFHS (1126 ± 36.02) offspring during 6 month IP-GTT was higher than controls (538 ± 51.06) and MNR (692.2 ± 55.75) on standard chow fed offspring ($p < 0.0001$) (**Figure 3.3.1D**). Hepatic glucose output during a pyruvate challenge test did not differ significantly between maternal nutrition status with similar post-weaning diets from 0-120 minutes (**Figure 3.3.1E**). Similar AUCs were also measured for control (811 ± 208.6) and MNR (762.4 ± 227.9) on HFHS ($p = 0.88$) (**Figure 3.3.1F**). These data suggest that a HFHS diet decreased glucose tolerance and caused a relative increase in hepatic glucose output in response to pyruvate (**Figure 3.3.1**); regardless of prenatal condition.

Metabolic cages were used to compare post-weaning diets (HFHS and standard chow) or maternal nutrition (MNR and control). At 2 (**Figure 3.2.2A**) and 7 months (**Figure**

3.2.2B), a post-weaning HFHS diet significantly decreased RERs (2 month: light-cycle p = 0.01, dark-cycle p = 0.002; 7 month: light-cycle p = 0.0001, dark-cycle p = 0.0001), and increased heat produced (2 month: light-cycle p = 0.0001, dark-cycle p = 0.003; 7 month: light-cycle p = 0.005). Maternal nutrient restriction significantly decreased 2-month food intake during the day (p = 0.007) and activity at night (p = 0.01) (**Figure 3.2.2A**). Seven-month-old MNR offspring also had reduced RER during light-cycle (p = 0.04). There was no significant interaction between post-weaning diets and maternal nutrition in any parameters measured.

Post hoc tests of metabolic parameters were used to compare MNR and control offspring on a HFHS diet. At 2 months, no differences in respiratory exchange ratios (RERs) or heat production were detected between Control:HFHS and MNR:HFHS(**Figure 3.3.2A i and ii**). Food consumption during the day was decreased in MNR:HFHS (6210 ± 572.5 kCal) relative to Control:HFHS (9866 ± 545.1) (p = 0.004) (**Figure 3.3.2A iii**). No other parameters measured were significantly different between control and MNR on standard chow (**Figure 3.3.2A**) or on either diet at 7 months (**Figure 3.3.2B**).

In addition to changes from maternal diet, effects of post-weaning diets in offspring with similar maternal nutrition was assessed. At 2 months, MNR offspring RERs were significantly lower on a HFHS (day= 0.8525 ± 0.01702, night= 0.8975 ± 0.019) relative standard chow (day= 0.94 ± 0.014 , night = 0.9900 ± 0.0041) during the day (p < 0.05) and night (p < 0.01) (**Figure 3.3.2A i**) and maintained to 7 months (daytime HFHS= 0.8460 ± 0.018 and standard chow= 0.9500 ± 0.0084, nighttime HFHS= 0.8800 ± 0.018 and standard chow= 0.9840 ± 0.014) (p < 0.01 and 0.001, respectively) (**Figure 3.3.2B i**). Decreased RERs in Control:HFHS relative to Control:Standard were only evident at 7 months during both light and dark-cycles (p < 0.05 and 0.01 respectively). (**Figure 3.3.2 A i**). In 2-month-old control:HFHS diet had increased heat production (daytime= 0.5925 ± 0.026, nighttime = 0.6240 ± 0.0433) relative to controls on a standard chow diet during the light and dark-cycle (daytime = 0.4800 ± 0.01080, nighttime = 0.5120 ± 0.01655, p < 0.01) (**Figure 3.3.2A ii**), which was maintain at 7 months during the light-cycle (p <

0.05). Heat produced was increased in 2-month old MNR:HFHS ($0.5550 \pm 0.0.01848$) compared to MNR:Standard (0.4700 ± 0.02449) during the day ($p < 0.01$), but was not maintained at night or 7 months. No other significant differences were detected between maternal nutrition on a similar post-weaning diet.
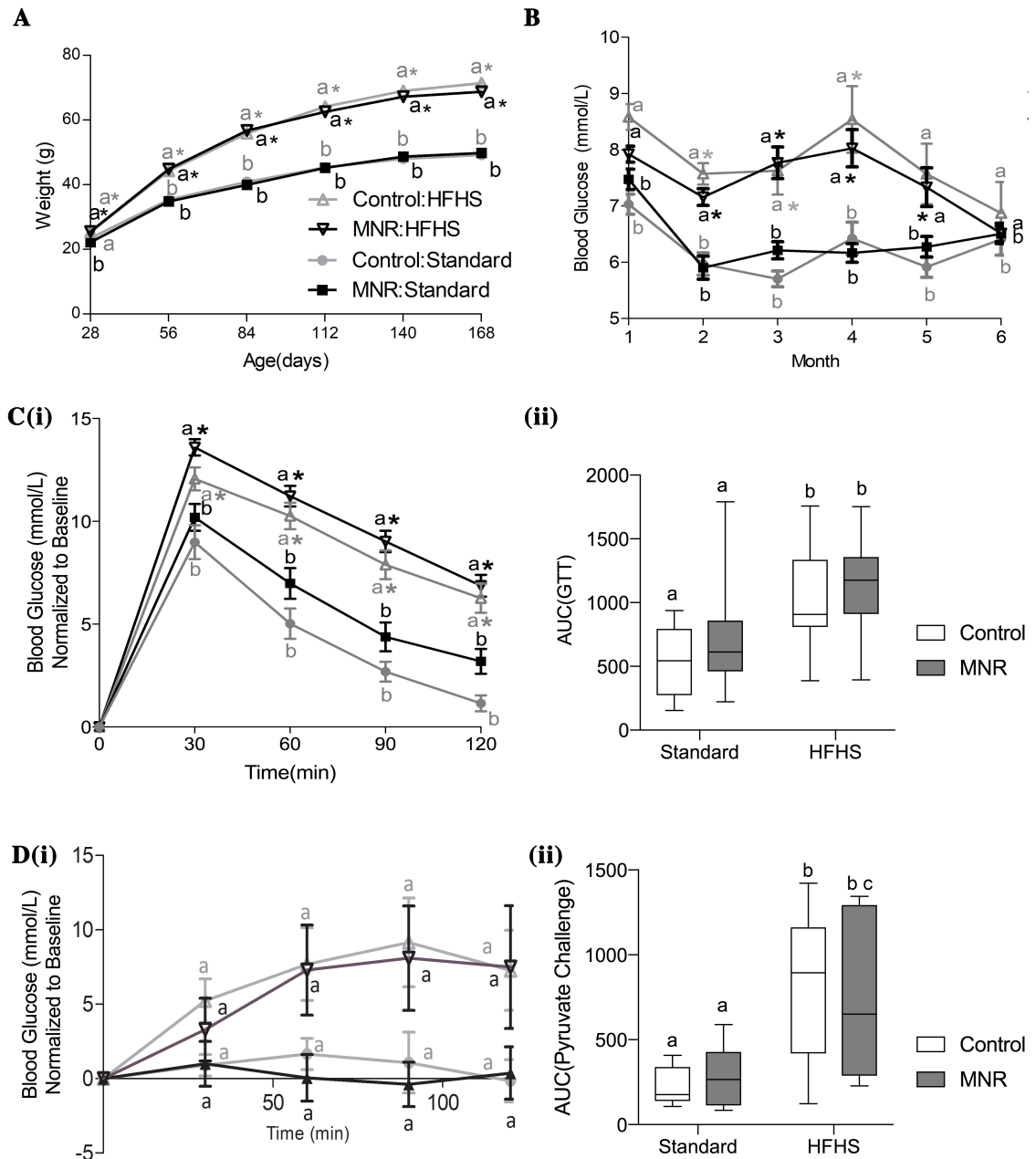
Figure 3.3.1 Weight and blood glucose regulation in MNR and control offspring.

A. Body weight was measured from 1 to 6 months. At one month, MNR were significantly smaller than controls on a standard chow diet ($p = 0.006$). No other differences were detected between maternal nutrition, but all offspring on a HFHS diet had significantly higher body weight relative to offspring fed standard chow ($p < 0.05$). **B.** MNR had similar random blood glucose to control offspring on similar post-natal diets. HFHS-fed offspring had significantly higher random blood glucose from 2 to 4 months relative the same maternal diet group fed standard chow. MNR on a HFHS diet also had higher blood glucose at 5 months compared to MNR on standard chow. (Control:Standard N=25, MNR:Standard N=36, Control:HFHS N=33, MNR:HFHS N= 52). **C.** Glucose tolerance did not differ between control and MNR on similar diets and normalized blood glucose at all timepoints were higher on the HFHS diet-fed offspring compared to standard chow fed offspring from similar maternal diets. (Control:Standard N=25 , MNR:Standard N=36, Control:HFHS N=39, MNR:HFHS N= 63) **D.** Pyruvate challenge tests showed hepatic glucose output did not differ between control and MNR on similar diets, or between diets from the same maternal nutrition at all timepoints (N=5 per group, 1 pup/litter in each group). Data are expressed as mean ± SEM. Man Whitney tests (A, Cii and Dii) or a two-way repeated measures ANOVA with a Bonferroni post-hoc was used (B, Ci and Di). Different letters represent significant differences between maternal nutrition and asterisks represent significant differences between diets within the same maternal nutrient group.

Sample numbers per month are as followed for A:

Month	Control:Standard	MNR:Standard	Control:HFHS	MNR:HFHS
1	37	52	52	82
2	28	37	44	68
3	28	37	43	73
4	28	37	43	71
5	28	37	42	66
6	28	37	39	64

A. 2 Months

i) RER
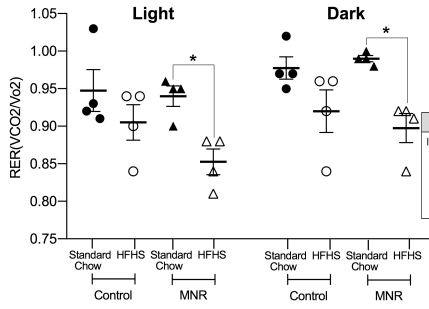
ii) Heat Produced
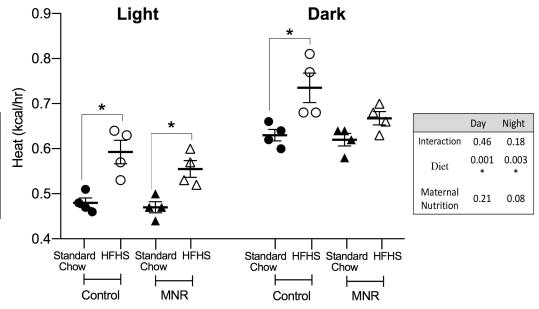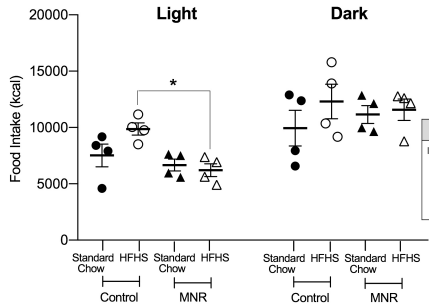
iii) Food Consumed
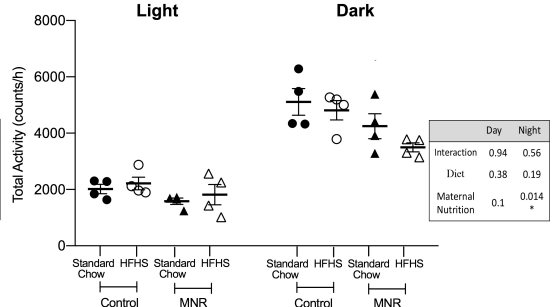
iv) Total Activity

B. 7 Months

i)RER
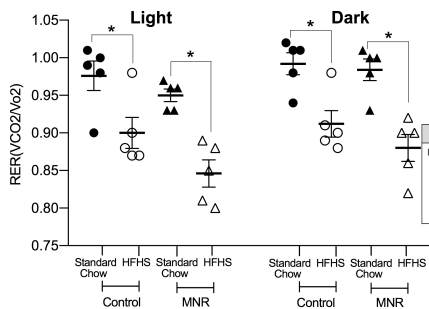
ii) Heat Produced
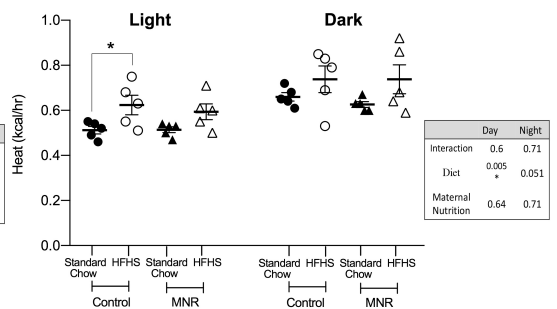
iii) Food Consumed
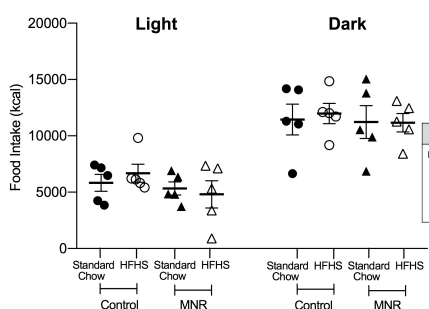
iv) Total Activity
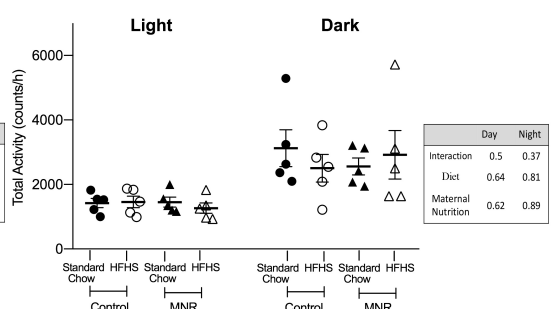
Figure 3.3.2 Metabolic caging data from 2 (A) and 7 (B) month-old offspring during the day (light cycle) and night (dark-cycle).

At two months, RER (**A i)** was significantly lower in MNR fed HFHS diets than MNR fed on standard chow at both light cycles ($p = 0.002$ and 0.03, respectively). Controls on a HFHS produced more heat than controls on standard chow during the day at 2 months ($p = 0.01$) (**A ii**). Control:HFHS consumed more food than MNR:HFHS ($p = 0.004$)(**A iii**) and total activity was decreased in MNR relative to controls on a HFHS diet ($p = 0.03$) (**A iv**). In 7-month-old offspring RERs were reduced in MNR fed HFHS diets compared to MNR fed on standard chow at both light cycles (**B i**, $p = 0.01$ and 0.02, respectively). No other differences were detected at 7 months. Data are presented as the mean ± SEM). A two-way ANOVA was used to compare post-weaning and maternal diet or interactions between these parameters and the p-values are shown in the chart beside each graph. Bonferroni multiple comparisons were used for any changes detected and significant differences ($p < 0.05$) are represented by an asterisk. 2 month N=4 and 7 month N= 5 per group (1 mouse per litter).

3.4   Discussion

The concept of a 'second hit' such as a dietary challenge or sedentary life style is essential to the "Thrifty Phenotype Hypothesis", where the fetus is primed to conserved nutrients but experiences a nutrient abundant post-natal environment. A HFHS diet was used in this study to mimic the western diet and investigate the role of a 'second hit' in the adult males. The MNR males were expected to have reduced glucose tolerance and insulin sensitivity compared to controls. However, MNR offspring showed no differences in glucose tolerance, hepatic glucose output, random and fasting blood glucose, RER, food consumption or activity compared to controls on a HFHS diet.

Moderate nutrient restriction during pregnancy resulted in similar body weights in adulthood compared to controls on standard chow or HFD. Rat offspring from 50% maternal nutrient restriction late in gestation that were a fed standard chow (14) or a HFD (14,15) after weaning have also resulted in similar adult body weights to offspring from control pregnancies on the same postnatal diet. Increased growth of fat mass and phenotypic switching of pro-inflammatory macrophages (16) have been observed without changes in body weight and could impact the tissue function in MNR offspring. Conversely, mice with low maternal protein or calorie restriction throughout pregnancy became more obese than offspring from control pregnancies (17,18). This variation might be due to timing of catch-up growth, with catch-up growth prior to day 3 which was previously observed in this model (12) or after weaning (19) having a protective effect against diet-induced obesity. Additionally, although diet composition varied, daily calorie consumption was similar in all experimental groups, except at 2 months when MNR:HFHS ate less than Control:HFHS. If higher calories were consumed differences between MNR and control might have been observed.

Maternal diet during pregnancy had no impact on non-fasting random blood glucose, glucose challenge or pyruvate challenge in our mouse offspring on a HFHS post-weaning diet. Rat offspring from low maternal protein throughout pregnancy and lactation or intrauterine artery ligation weaned into a HFD resulted in no significant differences in glucose tolerance (17,20), fasting and non-fasting blood glucose (20). Islet aging was

similar from a maternal HFD and maternal low protein, suggesting that both environmental exposures may converge on similar mechanisms (20). A similar mechanism underlying HFD exposure and reduced maternal nutrition could explain why there were no significant interactions in metabolic assessments and similar blood glucose regulation in MNR and control offspring fed a HFD. Conversely, evidence of maternal undernutrition with (15) and without (14) a high a caloric post- weaning diet causing decreased insulin sensitivity (14,15,21) or alterations in expression of hepatic genes important in gluconeogenesis (22) have been observed. The age of 'catch-up' growth and total calories consumed may have minimized differences between control and MNR offspring on HFHS.

MNR on a HFHS diet showed decreased RERs at all ages and time points relative to MNR on standard chow, but this decrease was only significant in controls at 7 months. Pure carbohydrates as an energy source would result in a RER of 1 and oxidation of only fats would be 0.7. Reduced RERs imply decreased carbohydrate and increased use of fat as a metabolic substrate. Some studies indicate that nutrition during weaning or gestation impact RER only when stimulated with metabolic regulatory peptides such as adiponectin or leptin (21,23), which have not been assessed in this study. Stimulation by adiponectin or leptin may have been required to detect significant differences between maternal nutrition on the same diet or at other ages and time points.

A calorie dense post-weaning diet did not significantly impact activity levels of offspring at 2 or 7-months old. Activity was also similar between control and MNR groups within the same post-weaning diet. Consistent with our results, no changes in energy expenditure from a calorie dense or standard chow diet were also observed in rat offspring from early gestation maternal nutrient restriction compared to controls (21).

Both suboptimal nutrition during early development and a high caloric adult diet have been associated with increased appetite, changes in food preference and sedentary behavior (14,18,21,23,24). Conversely, restriction of nutrients during lactation by increasing litter size (23), adjusting maternal diet (18) or preconception maternal diet (24)

could have a greater impact on such behaviours compared to maternal nutrition alone. In fact 50% maternal nutrient restriction minimized sedentary behaviour induced by a HFD (14). In addition to minimal impact from maternal nutrition, diet did not lead to significant changes in food intake or activity. Rat offspring from maternal nutrient restriction resulted in increased caloric intake and reduced activity (21), suggesting that total calories rather than dietary composition could influence total activity. While the amount of food consumed did not differ in MNR offspring, preference for dietary intake of high fat or high sugar diets was not measured and cannot be eliminated in this study. Because maternal nutrient restriction was limited to pregnancy and offspring did not consume excess calories on the HFHS diet, changes to activity and food consumption were not observed in MNR offspring relative to controls.

Moderate maternal nutrient restriction during gestation in mice did not result in differences in metabolic parameters measured in this study in response to a post-weaning isocaloric HFHS diet. The timing of the 'second hit' as well as the total calories consumed may have contributed to minimal interaction with maternal diet. However, MNR on standard chow started out with increased insulin sensitivity (12) and have similar abilities to regulate blood glucose on the high fat diet. A use of fat as a metabolic substrate was also more evident in MNR offspring at all time points, indicating that they may have been more impacted than controls. This study demonstrates differences due to maternal nutrition and the interaction with diet composition without excess calories and sedentary activity. Additionally, it underlines the importance of dietary composition in adult life.

3.5   References

1. Garite TJ, Clark R, Thorp JA. Intrauterine growth restriction increases morbidity and mortality among premature neonates. *Am. J. Obstet. Gynecol.* 2004;191(2):481–487.

2. Huang Y-T, Lin H-Y, Wang C-H, Su B-H, Lin C-C. Association of preterm birth and small for gestational age with metabolic outcomes in children and adolescents: A population-based cohort study from Taiwan. *Pediatr. Neonatol.* 2017;

3. Morrison KM, Ramsingh L, Gunn E, et al. Cardiometabolic Health in Adults Born Premature With Extremely Low Birth Weight. *Pediatrics.* 2016;138(4):e20160515.

4. Han VKM, Seferovic MD, Albion CD, Gupta MB (2012) Intrauterine Growth Restriction: Intervention Strategies. In: Buonocore G., Bracci R., Weindling M. (eds) Neonatology. Springer, Milano, p. 89-93.

5. Hales CN, Barker DJP. Type 2 (non-insulin-dependent) diabetes mellitus: the thrifty phenotype hypothesis. *Int. J. Epidemiol.* 2013;42(5):1215–1222.

6. Jimenez-Chillaron JC, Hernandez-Valencia M, Lightner A, et al. Reductions in caloric intake and early postnatal growth prevent glucose intolerance and obesity associated with low birthweight. *Diabetologia.* 2006;49(8):1974–1984.

7. Xiao D, Kou H, Zhang L, Guo Y, Wang H. Prenatal Food Restriction with Postweaning High-fat Diet Alters Glucose Metabolic Function in Adult Rat Offspring. *Arch. Med. Res.* 2017;48(1):35–45.

8. Donin AS, Nightingale CM, Owen CG, et al. Dietary energy intake is associated with type 2 diabetes risk markers in children. *Diabetes Care.* 2014;37(1):116–123.

9. Softic S, Gupta MK, Wang G-X, et al. Divergent effects of glucose and fructose on hepatic lipogenesis and insulin signaling. *J. Clin. Invest.* 2017;127(11):4059–4074.

10. Kendig MD, Fu MX, Rehn S, et al. Metabolic and cognitive improvement from switching to saccharin or water following chronic consumption by female rats of 10% sucrose solution. *Physiol. Behav.* 2018;188:162–172.

11. Veum VL, Laupsa-Borge J, Eng Ø, et al. Visceral adiposity and metabolic syndrome after very high-fat and low-fat isocaloric diets: a randomized controlled trial. *Am. J. Clin. Nutr.* 2017;105(1):85–99.

12. Radford BN, Han VKM. Offspring from maternal nutrient restriction in mice show variations in adult glucose metabolism similar to human fetal growth 3 restriction. *J. Dev. Orig. Health Dis.* 2018; DOI: 10.1017/S2040174418000983.

13. Guzman MS, De Jaeger X, Drangova M, et al. Mice with selective elimination of striatal acetylcholine release are lean, show altered energy homeostasis and changed sleep/wake cycle. *J. Neurochem.* 2013;124(5):658–669.

14. Cunha F da S, Molle RD, Portella AK, et al. Both Food Restriction and High-Fat Diet during Gestation Induce Low Birth Weight and Altered Physical Activity in Adult Rat Offspring: The "Similarities in the Inequalities" Model. *PLOS ONE.* 2015;10(3):e0118586.

15. He Z, Lv F, Ding Y, et al. Insulin-like Growth Factor 1 Mediates Adrenal Development Dysfunction in Offspring Rats Induced by Prenatal Food Restriction. *Arch. Med. Res.* 2017;48(6):488–497.

16. Xie L, Zhang K, Rasmussen D, et al. Effects of prenatal low protein and postnatal high fat diets on visceral adipose tissue macrophage phenotypes and IL-6 expression in Sprague Dawley rat offspring. *PLOS ONE.* 2017;12(1):e0169581.

17. Arentson-Lantz EJ, Zou M, Teegarden D, Buhman KK, Donkin SS. Maternal high fructose and low protein consumption during pregnancy and lactation share some but not all effects on early-life growth and metabolic programming of rat offspring. *Nutr. Res*. 2016;36(9):937–946.

18. Palou M, Priego T, Sánchez J, et al. Moderate Caloric Restriction in Lactating Rats Protects Offspring against Obesity and Insulin Resistance in Later Life. *Endocrinology*. 2010;151(3):1030–1041.

19. Bieswal F, Ahn M-T, Reusens B, et al. The Importance of Catch-up Growth after Early Malnutrition for the Programming of Obesity in Male Rat. *Obesity*. 2006;14(8):1330–1343.

20. Delghingaro-Augusto V, Madad L, Chandra A, et al. Islet Inflammation, Hemosiderosis, and Fibrosis in Intrauterine Growth-Restricted and High Fat-Fed Sprague-Dawley Rats. *Am. J. Pathol*. 2014;184(5):1446–1457.

21. Szostaczuk N, Priego T, Palou M, Palou A, Picó C. Oral leptin supplementation throughout lactation in rats prevents later metabolic alterations caused by gestational calorie restriction. *Int. J. Obes*. 2017;41(3):360–371.

22. Luo K, Chen P, Li S, et al. Effect of L-arginine supplementation on the hepatic phosphatidylinositol 3-kinase signaling pathway and gluconeogenic enzymes in early intrauterine growth-restricted rats. *Exp. Ther. Med*. 2017;14(3):2355–2360.

23. Halah MP, Marangon PB, Antunes-Rodrigues J, Elias LLK. Neonatal Nutritional Programming Impairs Adiponectin Effects On Energy Homeostasis In Adult Life Of Male Rats. *Am. J. Physiol.-Endocrinol. Metab*. 2018;

24. Crossland RF, Balasa A, Ramakrishnan R, et al. Chronic Maternal Low-Protein Diet in Mice Affects Anxiety, Night-Time Energy Expenditure and Sleep Patterns, but Not Circadian Rhythm in Male Offspring. *PLOS ONE*. 2017;12(1):e0170127.

Chapter 4 : Evidence of Increased Hypoxia Signalling in Fetal Liver from Maternal Nutrient Restriction in Mice

4.1   Introduction

Intrauterine growth restriction (IUGR) is a pregnancy condition where fetal growth is suboptimal, resulting in an infant born with a birth weight <10th percentile (1). Individuals born from pregnancies complicated by IUGR are at increased risk for peri- and post-natal complications, and as adults are at increased risk for metabolic disorders (2,3). Adverse intrauterine conditions may lead to adaptations to enhance fetal survival but contribute to aberrant metabolism as adults (2).

Hypoxia inducible factor (HIF) pathway is a cellular response to enhance survival in adverse conditions such as hypoxia and nutritional stress. Under normal physiological conditions, the α subunit (HIF-1α, HIF-2α, HIF-3α) is post-translationally hydroxylated and/or phosphorylated in the cytosol by regulators such as von Hippel–Lindau (VHL)/U3 ligase complex, factor inhibitor of hypoxia (FIH) and glycogen synthase kinase 3β (GSK-3β) (4–6). These post-translational modifications promote proteasomal degradation (4–6). During cellular stress, reduced hydroxylation and/or phosphorylation at stabilization sites inhibit recognition by the proteasome. Stabilization in the cytosol results in increased dimerization with the HIF-1β subunit. HIF dimers then translocate to the nucleus and transcriptionally regulate genes containing hypoxia responsive elements (HREs)(7). HRE-containing genes are involved in metabolism, cell cycle regulation and angiogenesis (5,7).

Changes in HIF signalling in placentas from growth restricted pregnancies (8) or kidney and liver of maternal nutrient restricted IUGR animal models have been documented (8–11). However, others fail to find differences in HIF signalling in these tissues (9,12). Previously we have shown that maternal nutrient restriction results in male offspring with reduced fetal and adult liver size and increased hepatic insulin sensitivity in adulthood (13). Here we aimed to investigate whether HIF signalling has a role in fetal liver adaptations after exposed to moderate calorie restriction *in utero*.

4.2   Methods

4.2.1 Animals

All animal procedures were approved by the Animal Use Subcommittee of the University Council on Animal Care at the University of Western Ontario and were described by Radford and Han, 2018(13). Briefly, mice were housed in 12-hour light and dark cycles. Virgin 8-week-old CD-1 female mice were bred, and the presence of a vaginal plug indicated E0.5. At E6.5, pregnant females received *ad libitum* standard chow (control, N=5) or maternal nutrient restriction (MNR, N=5) (70% total calories) (both groups receiving #F0173, Bio-Serv, Flemington, NJ). At E18.5 dams were euthanized with CO_2 narcosis and pups with cervical dislocation. Right liver lobes were removed from each pup, snap frozen in liquid nitrogen and stored at -80°C. Only male fetuses were identified with SRY PCR (forward primer - TGGACTGGTGACAARGCTA, reverse primer - TGGAAGTACAGGTGTGCACTCT) and used for further analysis.

4.2.2 RNA isolation

RNA for sequencing was isolated from 10 control and 10 MNR livers (2 mice per litter). Additional RNA from 8 control and 8 MNR littermates (1 or 2 mice per litter) were used as a validation cohort for real time PCR. Briefly, the frozen right liver lobe (30-50 mg for sequencing and 10-15 mg for real time PCR) was pulverised with a Bessman Tissue Pulveriser (Spectrum Laboratories, Rancho Dominguez, CA) then homogenized with a Brinkman homogenizer Polytron® 3000 for 50 seconds in 1mL or 500uL of ice cold trizol, respectively. The PureLink Mini RNA kit (Invitrogen, USA) with the on-column DNAseI treatment protocol was used to collect RNA from homogenate, as described by the manufacturer.

4.2.3 RNA sequencing

RNA/library QC and RNA sequencing was run at McGill University and Genome Quebec Innovation Centre, Quebec, CA. Libraries were generated with the NEBNext® Ultra™ Directional RNA Library Prep Kit for Illumina® (E7420S, New England BioLabs, Massachusetts, United States). Quality of RNA was verified on the Agilent Bioanalyzer (RIN > 7). Single-read 50bp sequencing was obtained from a HiSeq 2500

with 17-31M reads per sample (average depth of 23M). Reads were aligned to the mm9 transcriptome (14) with Bowtie2 (15) (90% alignment rate).

4.2.4 Real time PCR

Complementary DNA was generated with the SuperScript™ IV First-Strand Synthesis System (Invitrogen, USA). Taqman assays that covered multiple exons were purchased for select target genes including: Cyclin G2 (Ccng2) (4448892, Mm00432394_m1), B-cell Translocator Gene 2 (Btg2) (4453320, Mm00476162_m1), Lysine Demethylase 3A (Kdm3a) (4448892, Mm01182127_m1), FK506 Binding Protein (Fkbp5) (4448892, Mm00487406_m1), 6-phosphofructo-2-kinase/fructose-2,6-bisphosphatase-4 (Pfkbp3) (4448892, Mm00504650_m1), Hypoxia Inducible Factor 3α (Hif-3α) (Mm00469375_m1), von Hippel–Lindau (Vhl) (Mm00494137_m1), Hypoxia Inducible Factor 1α (Hif-1α) (Mm00468869_m1), and Hypoxia Inducible Factor 2α (Hif-2α) (Mm01236112_m1); and endogenous controls Glyceraldehyde-3-Phosphate Dehydrogenase (Gapdh) (4331182, Mm99999915_g1) and beta actin (4331182, Mm01205647_g1) (Invitrogen, USA). Reactions were run with TaqMan™ Fast Advanced Master Mix (Invitrogen, USA) on the ViiA™ 7 (Applied Biosystems, USA) according to the manufacturers protocol. Fold change was calculated using the delta delta CT method (ddCT).

4.2.5 Protein Isolations

Ten-Fifteen mg of tissue was homogenized with 1mL of ice cold 1x Cell Lysis buffer (9803S) from Cell Signaling (Danvers, MA, USA) with protease inhibitor cocktail 1, 2, and 3 (P1860, P5726, and P0044, Sigma-Aldrich, St. Louis, MO, USA) for 40 seconds with a Brinkman homogenizer Polytron® 3000. Lysates were sonicated (F550 Sonic Dismemberator, Fisher Scientific, Markham, ON Canada) and then shaken at 4°C for 2 hours. Cellular debris was removed from lysates by spinning at 12,000 x g for 10 minutes and the supernatant was collected for analysis. Protein concentrations were calculated with the Bio-Rad Protein Assay (Cat #500-0006, Bio-Rad Laboratories Inc., Des Plaines, IL) according to the manufacturer's protocol.

4.2.6 Western Blotting

Fifty μg of protein for HIF-2α blots and 25μg for all other blots were loaded and run on an 8% polyacrylamide gel. Protein was transferred to a PVDF membrane with the Transblot Turbo™ (Bio-rad Laboratories Inc., USA). Membranes were dipped in methanol and then blocked for an hour at room temperature in 5% milk in TBST. After rinsing 3 times (5 minutes each) in TBST, primary antibodies were incubated in 5% BSA in TBST overnight (**Table 4.2.1**). Blots were rinsed 3 times (5 minutes each) and incubated with secondary antibodies in 5% milk in TBST for 1 hour at room temperature (**Table 4.2.1**). Blots were images with the Clarity™ Western ECL Substrate (1705061, Bio-Rad Laboratories Inc., Des Plaines, IL) and band intensities were quantified using Imagelab software® version 5.1 BETA (Bio-Rad Laboratories Inc., Des Plaines, IL). Kdm3a was not assessed via western blot because we were not able to find an effective antibody for the mouse fetal liver samples. All sample lysates were run on three western blots to generate technical replicates for statistical comparisons. Only one representative blot is shown.

4.2.7 Statistical analysis

Samples that contributed more variation than expected to the each group were removed as outliers as described by *Gierliński et al*. with the median plus 2 times the interquartile range as the threshold (16). Differential expression was detected with a false discovery rate (FDR) < 0.1 and detection in 2 or more tools (EdgeR(17), DESeq2(18) and ALDex2(19)) using the default settings in R (version 3.4.3). Optimal number of clusters were generated with the gap statistic with the Cluster library (version 2.0.6) and PCA plots were plotted with ggplot2 (version 2.2.1) and ggrepel (version 0.8.0) in the R console (version 3.3.2 and 3.4.3). Gene ontology (GO) pathway enrichment was done on the Gene Ontology Tool (Panther)(20,21); and KEGG and NCI pathway enrichments were run on enrichR (22,23). For quantitative PCR (*q*PCR) and western blots unpaired t-tests were used to compare delta CT values or band intensities respectively on Graphpad Prism (version 5.2).

Table 4.2.1 Antibodies used for western blotting

Target	Company	Cat. No	Dilution
HIF-2α	Santa Cruz Biotechnology Inc.	sc-13596	1:250
HIF-3α	Santa Cruz Biotechnology Inc.	sc-390933	1:200
FKBP5	Santa Cruz Biotechnology Inc.	sc-271547	1:200
PFKFB3	Cell Signaling	13123S	1:1000
Mouse IGG	Bio-Rad Laboratories Inc.	170-6515	1: 10 000

4.3   Results

RNA sequencing data was assessed for sample outliers and gene distributions among remaining samples (16). One control and one MNR sample contributed more variance to their respective maternal nutrient groups than other samples within the group and were removed from further analysis (**Figure 4.3.1**). With remaining samples, two distributions of genes were formed along PC1 (**Figure 4.3.2**). The second distribution contained genes enriched in GO pathways in neural and epithelial cell development (**Supplementary Table 4.3.1**), since hepatocyte and hematopoietic populations are of primary interest in this study this second distribution of genes was removed from the analysis.

Overall gene expression was explored with PCA (principal component analysis) plots and cluster analysis. The optimal number of clusters with the gap statistic of the centered-log ratio and regularized-log ratio transformed data was 1. However, k-means clusters with k=2 resulted in clusters separating based on counts per sample (**Figure 4.3.2A and Supplementary Table 4.3.2**). The PCA plot of the top 500 variable genes from the centred-log ratio (**Figure 4.3.3A**) did not result in separation of samples based on maternal nutrition. Regularized-log ratio transformed data PCA of the top 500 variable genes indicates moderate separation of maternal nutrition along PC1. Although PC1 only explains 8% of the total variance in the samples (**Figure 4.3.3B**). These data suggest that overall gene expression was similar between control and MNR fetal livers.

Despite similar overall expression, 49 protein-coding genes were differentially expressed in MNR fetal livers relative to controls using a false discovery rate (FDR) cut-off of < 0.1 and consistency of two or more tools (**Supplementary Table 4.3.3**). GO enrichment

indicated negative regulation of transcription from RNA polymerase II promoter in response to hypoxia as the top pathway when ranked according to fold enrichment (Cited2 and Vhl) (**Figure 4.3.4A**). Hypoxia signalling was also the top pathway enrichment according to combined scores with KEGG (**Figure 4.3.4B**) and NCI (**Figure 4.3.4C**). Additional genes included in these enrichments are Pfkfb3 and Hif-3α. Investigation into gene functions of differentially expressed genes indicate further involvement in cellular response to hypoxia (**Figure 4.3.5 and Supplementary Table 4.3.4**).

Genes involved in hypoxic regulation of metabolism, cell cycle regulation and chronic hypoxia were selected to be validated by qPCR in a separate validation cohort (**Figure 4.3.6**). Pfkfb3 transcript was increased 1.8-fold ($p = 0.002$) in MNR relative to controls, similar to the fold change in the RNAseq data of 1.5 (FDR = 1.2x10-6). Fkbp5 and Kdm3a transcripts were also confirmed to be increased by 1.3 and 1.5-fold ($p = 0.03$ and 0.02) and similar to sequencing fold changes of 1.6 and 1.2, respectively (FDR = 0.006 and 0.04). Lastly, Hif-3α was significantly higher by 1.4-fold in the MNR livers in the validation cohort ($p = 0.01$), similar to the 1.3-fold increased initial MNR cohort (FDR = 0.009). Although not significant, Ccng2, which was 1.5-fold higher in the RNAseq data (FDR = 0.0001), was relatively higher in the MNR fetal livers by 1.4-fold ($p = 0.05$). Btg2 and Vhl were not significantly different in the validation cohort ($p = 0.1$ and 0.7). Hif-1α and Hif-2α transcripts were not significantly different in the initial MNR cohort, but Hif-1α was 1.3-fold decreased in the validation MNR group used for qPCR relative to controls ($p = 0.01$).

Protein levels for genes differentially expressed in the validation cohort, as well as HIF-2α, were determined by western blots (**Figure 4.3.7**). HIF-1α was not detected in the fetal liver (**Supplementary Figure S4.3.1**) but HIF-2α was increased 2.2-fold in MNR fetuses ($p = 0.002$). HIF-3α was also increased by 1.3-fold ($p = 0.03$) in MNR relative to controls (**Figure 4.3.7A and B**). FKBP5 and PFKFB3 protein levels were not

significantly different between maternal nutrient groups (1.6 1.3-fold change, $p = 0.09$ and 0.5, respectively) (**Figure 4.3.7C and D**).
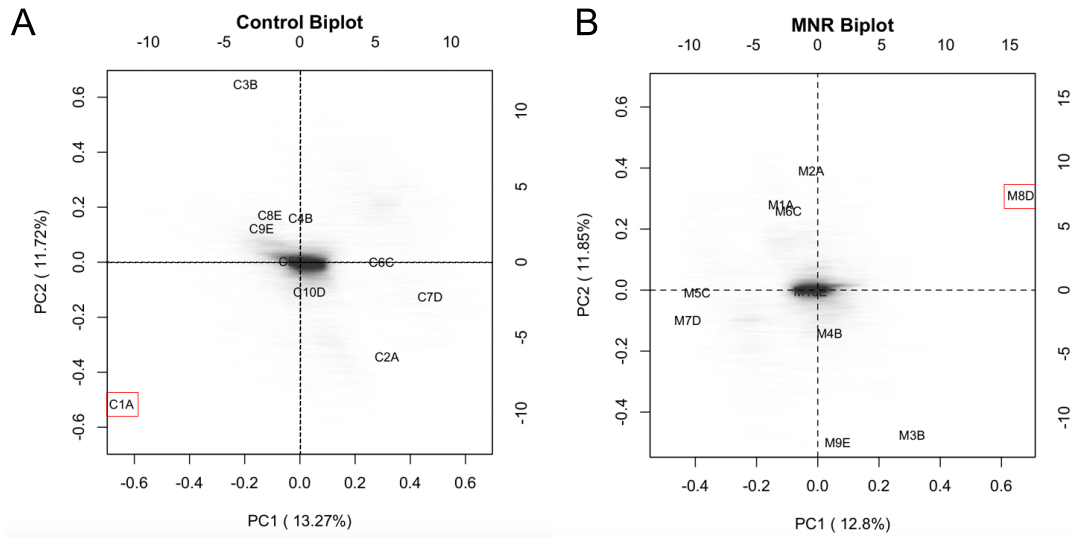
Figure 4.3.1 Biplots of E18.5 liver RNA sequencing data transformed with the centered-log ratio for controls (A) and MNR (B).

Group outliers are indicated by the red box. N=10 for both groups.
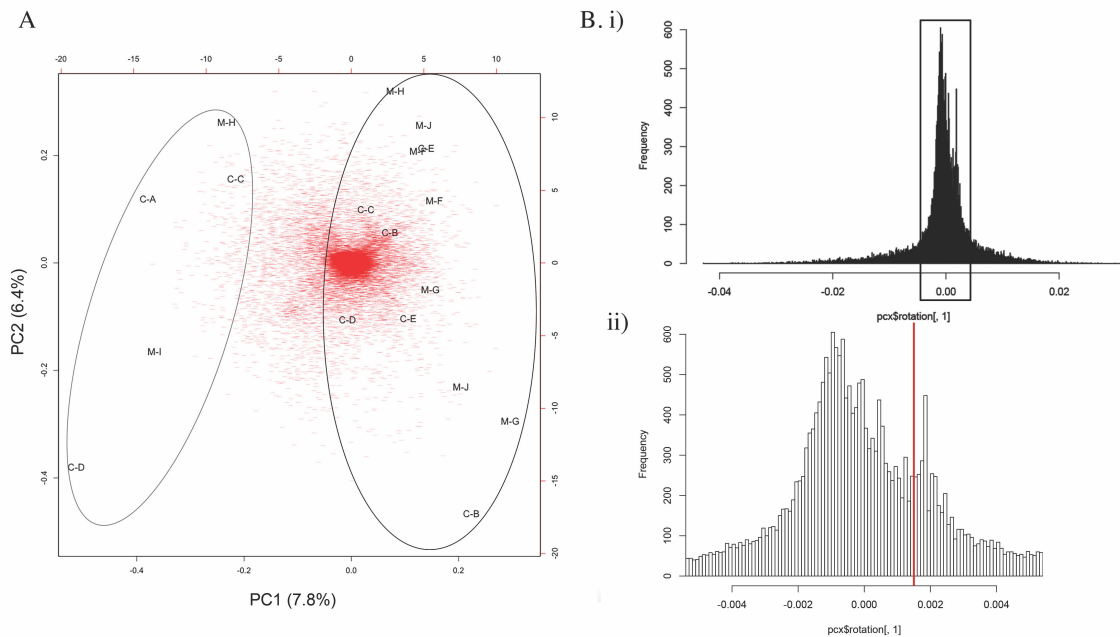
Figure 4.3.2 Distribution of genes in the center-log ratio transformed data.
Two overlapping distributions of genes contributing to PC1 are visible on the biplot,
which are not separating based on maternal nutrition or litters (Group-Litter, Group=
Control (C) or MNR (M) and Litters= A to J) (**A**). Two clusters are formed (k-means)
(cluster 1 = grey, cluster 2 = black). Histograms of all rotation values (**B i**) with a black
box indicating rotation values between -0.004 and 0.004. Distribution 1(left) and 2(right)
are separated by the red line (**B ii**) in a histogram only showing rotation values between -
0.004 and 0.004. Control N=9 and MNR N=9, 1-2 pups/litter.
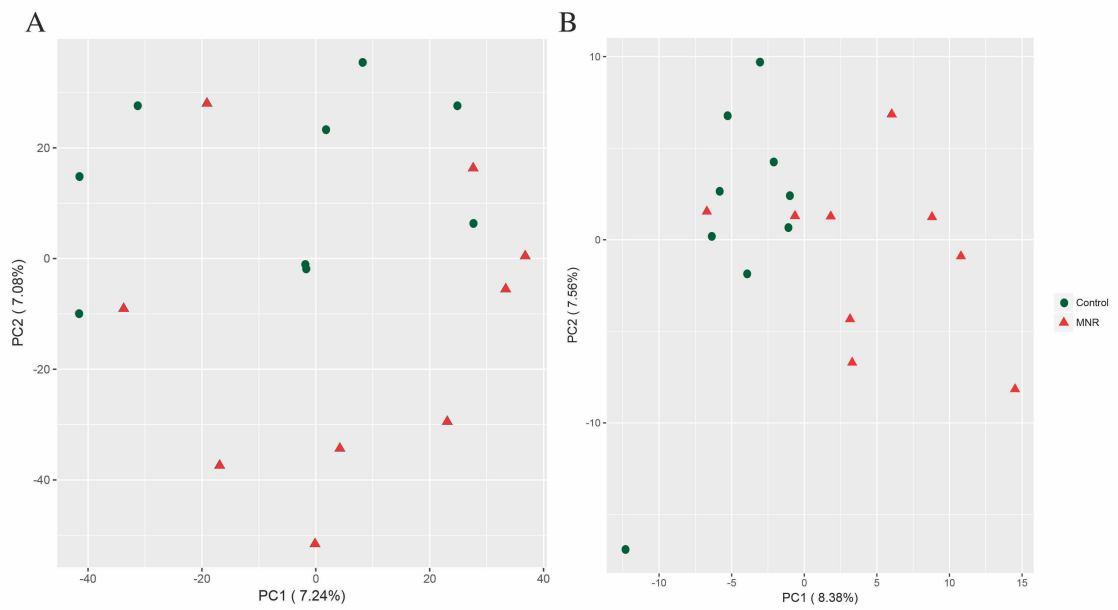
Figure 4.3.3 PCA of the top 500 variable genes.

Data was transformed with the centered-log ratio (A) and regularized log ratio (B).

Control N=9 and MNR N=9, 1-2 pups/litter.

A

	GO pathway	Fold Enrichment	FDR
1	negative regulation of transcription from RNA polymerase II promoter in response to hypoxia (GO:0061428)	> 100	3.78E-02
2	negative regulation of transcription from RNA polymerase II promoter in response to stress (GO:0097201)	> 100	1.73E-02
3	regulation of DNA-templated transcription in response to stress (GO:0043620)	32.45	2.03E-02
4	skeletal muscle cell differentiation (GO:0035914)	30.29	2.04E-02
5	muscle tissue development (GO:0060537)	8.29	4.07E-02
6	blood vessel morphogenesis (GO:0048514)	7.74	2.49E-02
7	blood vessel development (GO:0001568)	6.2	5.01E-02
8	response to hormone (GO:0009725)	6.11	2.87E-02
9	cellular response to stress (GO:0033554)	4.03	2.52E-02
10	positive regulation of RNA metabolic process (GO:0051254)	4.02	1.70E-02

B.

HIF-1 signaling pathway_Homo sapiens_hsa04066
Glycerophospholipid metabolism_Homo sapiens_hsa00564
cGMP-PKG signaling pathway_Homo sapiens_hsa04022
Other glycan degradation_Homo sapiens_hsa00511
Propanoate metabolism_Homo sapiens_hsa00640
Allograft rejection_Homo sapiens_hsa05330
Bladder cancer_Homo sapiens_hsa05219
Fructose and mannose metabolism_Homo sapiens_hsa00051
Graft-versus-host disease_Homo sapiens_hsa05332
Non-small cell lung cancer_Homo sapiens_hsa05223

C.

Hypoxic and oxygen homeostasis regulation of HIF-1-alpha_Homo sapiens_4c0f3584-6193-11e5-8ac5-06603eb7f303
HIF-2-alpha transcription factor network_Homo sapiens_37358832-6193-11e5-8ac5-06603eb7f303
HIF-1-alpha transcription factor network_Homo sapiens_20ef2b81-6193-11e5-8ac5-06603eb7f303
Regulation of Ras family activation_Homo sapiens_397d91c7-6195-11e5-8ac5-06603eb7f303
IL12 signaling mediated by STAT4_Homo sapiens_72cf19b8-6193-11e5-8ac5-06603eb7f303
Signaling events mediated by HDAC Class III_Homo sapiens_a7191c08-6195-11e5-8ac5-06603eb7f303
Noncanonical Wnt signaling pathway_Homo sapiens_7ff5fe76-6194-11e5-8ac5-06603eb7f303
Signaling events mediated by HDAC Class II_Homo sapiens_a1da5607-6195-11e5-8ac5-06603eb7f303
TCR signaling in naive CD8+ T cells_Homo sapiens_15a017bb-6196-11e5-8ac5-06603eb7f303
Notch-mediated HES/HEY network_Homo sapiens_8ee56389-6194-11e5-8ac5-06603eb7f303

Figure 4.3.4 Top 10 gene ontologies (A), KEGG (B), and NCI:Nature (C) gene pathway enrichments with protein-coding genes differentially expressed between control and MNR.

For B and C, significant pathways are in red and the bar size represents the combined scores.
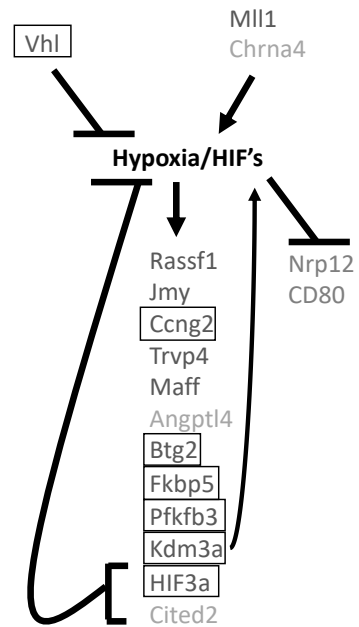
Figure 4.3.5 Genes differentially expressed in the RNA*seq* data (FDR <0.1 in 2 or more differential expression tools) in hypoxic inducible factor signalling.

Upregulated, down-regulated or no change. Boxes indicate genes selected for *q*PCR in a validation cohort, along with HIF-1α and HIF-2α.
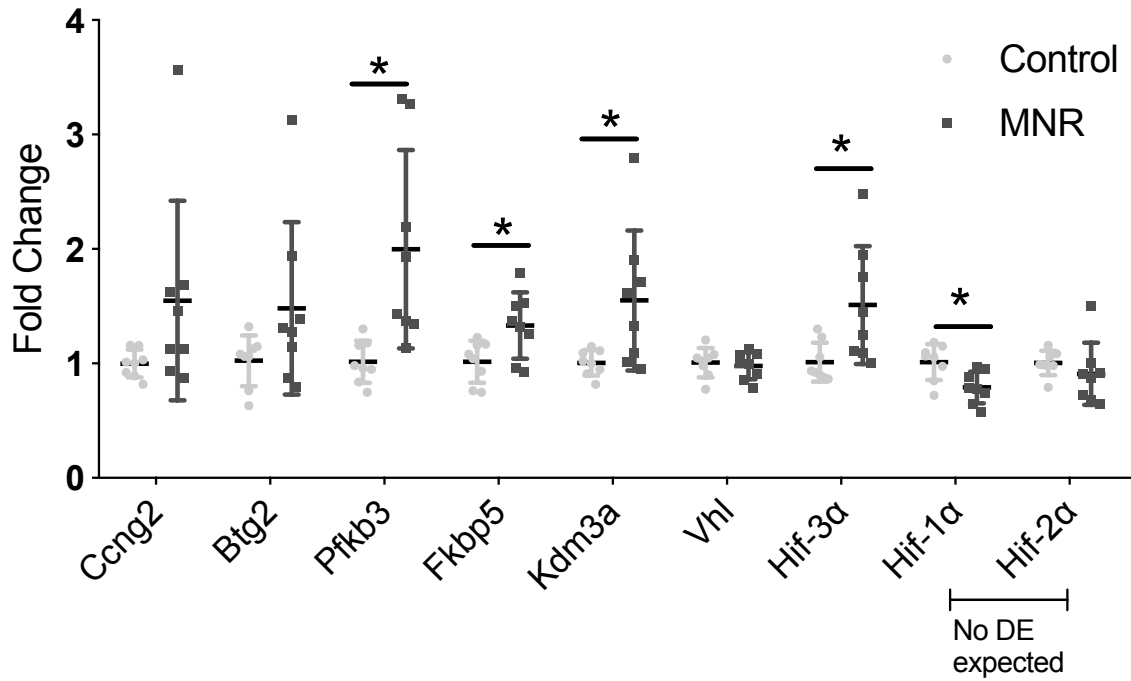
Figure 4.3.6. Relative fold change for genes involved in HIF signalling validated in an additional cohort with qPCR.

Data are plotted as mean $\pm$ SEM and asterisks represent $p < 0.05$ with an unpaired t-test. Control N=8 and MNR N=8, 1 or 2 pups/litter.
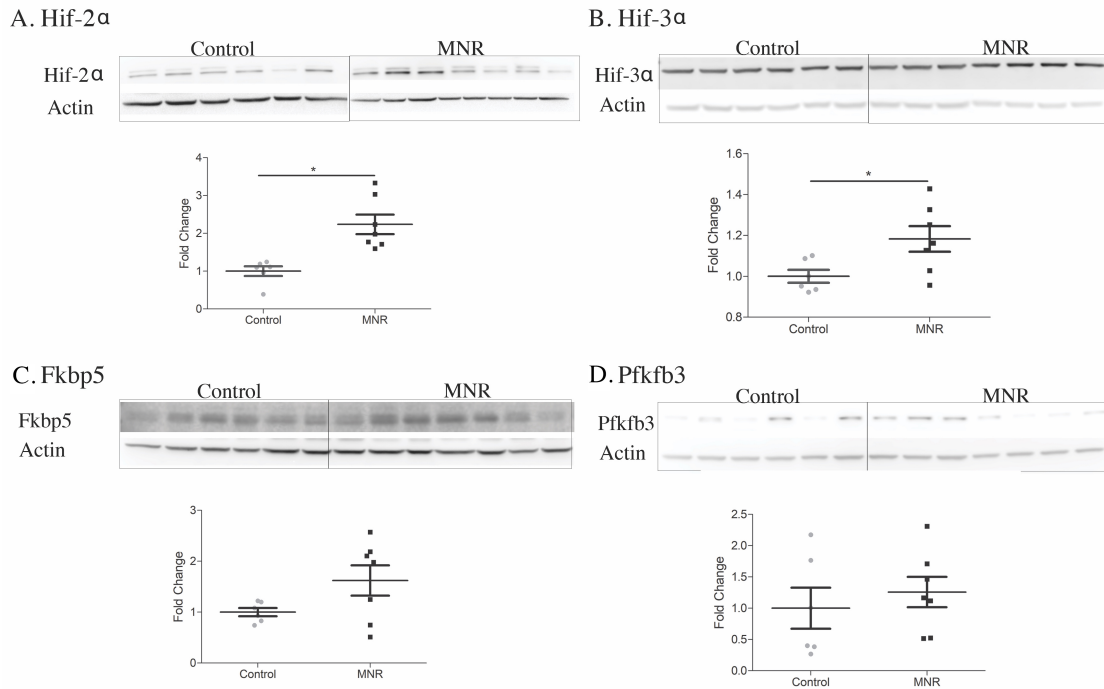
Figure 4.3.7 Western blots of proteins confirmed to be differentially expressed in the validation cohort.

HIF-2α (**A**) and HIF-3α (**B**) were significantly increased in MNR offspring by 2.2 and 1.3-fold ($p = 0.002$ and 0.03, respectively). FKBP5 (**C**) and PFKFB3 (**D**) were not significantly different in MNR relative to controls ($p = 0.09$ and 0.5, respectively). All blots were run in triplicates and representative blots are shown. Data are plotted as mean $\pm$ SEM and asterisks represent $p < 0.05$ with an unpaired t-test. Control N=6 and MNR N=7, 1 or 2 pups/litter.

4.4   Discussion

HIF-2α protein was increased in MNR offspring, but HIF-1α was not detected. Normal development in cells, such as endothelial cells, involve a switch from HIF-1α to HIF-2α as the primary HRE transcriptional regulator, similar to the transition observed with chronic hypoxia in cancer cells (24,25). During the liver bud maturation the HIF-1α transcript decline is associated with a shift in hepatoblast differentiation from biliary cells to hepatocytes (26). Although not known, it is conceivable that the developing liver shifts from HIF-1α to HIF-2α as well. In other tissues this switch is thought to occur in part because oxygen tension increases as organ perfusion during development becomes more efficient. FIH and PHDs less efficiently hydroxylate HIF-2α allowing it to stabilize and accumulate longer than HIF-1α (27,28). Additionally, differential expression of miRNAs can lead to decreased Hif-1α mRNA stability but not Hif-2α (29). HIF-1α and HIF-2α have both redundant and non-redundant gene targets that depend on cellular context and cell type (24,30). The presence of HIF-2α but not HIF-1α is likely due to the late-gestational sampling in this study and duration of hypoxia signalling.

Hif-3α mRNA and protein were higher in MNR compared to controls. Hif-3α mRNA is induced by HIF-1α during chronic hypoxia and transcriptionally down-regulates Hif-1α as a negative feedback mechanism (31,32). In mice Hif-3α has three isoforms, a full-length transcript and two variants, IPAS and NPAS. All three isoforms can inhibit the transcriptional activity of HIFs by binding with HIF-1β or HIF-1/2α, preventing dimerization and nuclear translocation (33). Some HIF-3α splice variants can also weakly induce canonical HIF-1α target genes (34). Consequently, increased HIF-3α protein could contribute to moderate differences between control and MNR HIF-induced transcription.

Fkbp5 was also increased at the transcript level and, although not significant, relatively increased at the protein level. FK506 Binding Protein (FKBP5) functions as co-chaperon

to HSP90 and as a scaffold protein. Subsequently, FKBP5 has diverse functions including reducing the affinity of glucocorticoid to the glucocorticoid receptor and promotion of adipocyte differentiation (35,36). As a chaperone FKBP5 also promotes the folding of PHLPP (a key phosphatase for AKT) resulting in reduced AKT phosphorylation (37). In adipose tissue chronic hypoxia results in increased FKBP5 (36) and in hepatocellular carcinoma cell lines sorafenib treatment resulted in HIF-2α-dependant induction of Fkbp5 transcription (38). FKBP5 has also been shown to regulate CDK5 interaction with DNMT1 and reduce DNA methylation activity (39). Most studies have been in neural cells or adipocytes, but this study suggests that FKBP5 may play a role cellular stress in the developing liver. An increase in FKBP5 could be induced by HIF-2α in MNR offspring, influencing metabolism, cell growth and/or DNA methylation.

Changes to hypoxia signalling in the liver could be indirect through placental adaptations. Decreased placental size could reduce oxygen and nutrient delivery, although the junctional zone is more impacted than the labyrinth zone (40). In guinea pigs, MNR results in increased hypoxyprobe-1 staining in both male and female liver and kidneys (10). However, no differences were detected in the placentas (10). Alternatively, MNR could increase HIF signalling in the developing liver through nutritional signalling and/or changes to fetal circulation. Further studies into the mechanism of HIF signalling need to be elucidated. However, increased HIF-induced transcripts support the concept that MNR results in increased hypoxia signalling in the fetal liver.

Maternal nutrient restriction resulted in fetal expression changes in hypoxia-inducible signalling pathways of E18.5 liver. Although expression changes were detected, the protein levels of genes induced by HIF transcription factors were not significantly different. Since tissue hypoxia declines during development (24, 26) it is possible that downstream changes were more evident earlier in liver development. Still, due to their importance in regulating multipotency, cell differentiation, and proliferation, HIF-induced transcription could result in differences in liver maturity and cell populations. Additionally, differential expression of epigenetic regulators such as Kdm3a and Fkbp5 may prime HRE-containing genes to respond differentially to aging or nutritional

abundance. Evidence of aberrant hypoxia signalling was evident in growth restricted mice, but the impact was moderate which may relate to the duration of nutrient restriction and the timing of analysis. Differentially expressed transcripts support the concept that hypoxia signaling may play a role in growth restriction in response to fetal undernutrition.

4.5   References

1.   Han VKM, Seferovic MD, Albion CD, Gupta MB (2012) Intrauterine Growth Restriction: Intervention Strategies. In: Buonocore G., Bracci R., Weindling M. (eds) Neonatology. Springer, Milano, p. 89-93.

2.   Hales CN, Barker DJP. Type 2 (non-insulin-dependent) diabetes mellitus: the thrifty phenotype hypothesis. *Int J Epidemiol*. 2013;42:1215–22.

3.   Oliveira D, Cezar J, Gomes RM, et al. Protein Restriction During the Last Third of Pregnancy Malprograms the Neuroendocrine Axes to Induce Metabolic Syndrome in Adult Male Rat Offspring. *Endocrinology*. 2016;157:1799–812.

4.   Bruick RK, McKnight SL. A Conserved Family of Prolyl-4-Hydroxylases That Modify HIF. *Scienc.e* 2001;294:1337–40.

5.   Brahimi-Horn C, Mazure N, Pouysségur J. Signalling via the hypoxia-inducible factor-1α requires multiple posttranslational modifications. *Cell Signal*. 2005;17:1–9.

6.   Mennerich D, Dimova EY, Kietzmann T. Direct phosphorylation events involved in HIF-α regulation: the role of GSK-3β. *Hypoxia Auckl NZ*. 2014;2:35–45.

7.   Slemc L, Kunej T. Transcription factor HIF1A: downstream targets, associated pathways, polymorphic hypoxia response element (HRE) sites, and initiative for standardization of reporting in scientific literature. *Tumour Biol J Int Soc Oncodevelopmental Biol Med*. 2016;37:14851–61.

8.   Paauw ND, Lely AT, Joles JA, et al. H3K27 acetylation and gene expression analysis reveals differences in placental chromatin activity in fetal growth restriction. *Clin Epigenetics*. 2018;10:85.

9.   Lewis RM, James LA, Zhang J, Byrne CD, Hales CN. Effects of maternal iron restriction in the rat on hypoxia-induced gene expression and fetal metabolite levels. *Br J Nutr*. 2001;85:193–201.

10. Elias AA, Maki Y, Matushewski B, Nygard K, Regnault TRH, Richardson BS. Maternal nutrient restriction in guinea pigs leads to fetal growth restriction with evidence for chronic hypoxia. *Pediatr Res*. 2017;82:141–7.

11. Robb KP, Cotechini T, Allaire C, Sperou A, Graham CH. Inflammation-induced fetal growth restriction in rats is associated with increased placental HIF-1α accumulation. *PloS One*. 2017;12:e0175805.

12. Rajakumar A, Jeyabalan A, Markovic N, Ness R, Gilmour C, Conrad KP. Placental HIF-1 alpha, HIF-2 alpha, membrane and soluble VEGF receptor-1 proteins are not increased in normotensive pregnancies complicated by late-onset intrauterine growth restriction. *Am J Physiol Regul Integr Comp Physiol*. 2007;293:R766-774.

13. Radford BN, Han VKM. Offspring from maternal nutrient restriction in mice show variations in adult glucose metabolism similar to human fetal growth 3 restriction. *J Dev Orig Health Dis*. 2018; DOI: 10.1017/S2040174418000983.

14. Karolchik D, Hinrichs AS, Furey TS, et al. The UCSC Table Browser data retrieval tool. *Nucleic Acids Res*. 2004;32:D493-496.

15. Langmead B, Salzberg SL. Fast gapped-read alignment with Bowtie 2. *Nat. Methods*. 2012;9:357-359.

16. Gierliński M, Cole C, Schofield P, et al. Statistical models for RNA-seq data derived from a two-condition 48-replicate experiment. *Bioinforma Oxf Engl*. 2015;31:3625–30.

17. Robinson MD, McCarthy DJ, Smyth GK. edgeR: a Bioconductor package for differential expression analysis of digital gene expression data. *Bioinforma Oxf Engl*. 2010;26:139–40.

18. Love MI, Huber W, Anders S. Moderated estimation of fold change and dispersion for RNA-seq data with DESeq2. *Genome Biol*. 2014;15:550.

19. Fernandes AD, Macklaim JM, Linn TG, Reid G, Gloor GB. ANOVA-like differential expression (ALDEx) analysis for mixed population RNA-Seq. *PloS One*. 2013;8:e67019.

20. Mi H, Thomas P. PANTHER Pathway: An Ontology-Based Pathway Database Coupled with Data Analysis Tools. *Methods Mol Biol*. 2009;563:123–40.

21. Mi H, Huang X, Muruganujan A, et al. PANTHER version 11: expanded annotation data from Gene Ontology and Reactome pathways, and data analysis tool enhancements. *Nucleic Acids Res*. 2017;45:D183–9.

22. Chen EY, Tan CM, Kou Y, et al. Enrichr: interactive and collaborative HTML5 gene list enrichment analysis tool. *BMC Bioinformatics*. 2013;14:128.

23. Kuleshov MV, Jones MR, Rouillard AD, et al. Enrichr: a comprehensive gene set enrichment analysis web server 2016 update. *Nucleic Acids Res*. 2016;44:W90-97.

24. Holmquist-Mengelbier L, Fredlund E, Löfstedt T, et al. Recruitment of HIF-1alpha and HIF-2alpha to common target genes is differentially regulated in neuroblastoma: HIF-2alpha promotes an aggressive phenotype. *Cancer Cell*. 2006;10:413–23.

25. Serocki M, Bartoszewska S, Janaszak-Jasiecka A, Ochocka RJ, Collawn JF, Bartoszewski R. miRNAs regulate the HIF switch during hypoxia: a novel therapeutic target. *Angiogenesis*. 2018;21:183–202.

26. Ayabe H, Anada T, Kamoya T, et al. Optimal Hypoxia Regulates Human iPSC-Derived Liver Bud Differentiation through Intercellular TGFB Signaling. *Stem Cell Rep*. 2018;11:306–16.

27. Berra E, Benizri E, Ginouvès A, Volmat V, Roux D, Pouysségur J. HIF prolyl-hydroxylase 2 is the key oxygen sensor setting low steady-state levels of HIF-1α in normoxia. *EMBO J*. 2003;22:4082–90.

28. Bracken CP, Fedele AO, Linke S, et al. Cell-specific regulation of hypoxia-inducible factor (HIF)-1alpha and HIF-2alpha stabilization and transactivation in a graded oxygen environment. *J Biol Chem*. 2006;281:22575–85.

29. Bruning U, Cerone L, Neufeld Z, et al. MicroRNA-155 promotes resolution of hypoxia-inducible factor 1alpha activity during prolonged hypoxia. *Mol Cell Biol*. 2011;31:4087–96.

30. Hu C-J, Wang L-Y, Chodosh LA, Keith B, Simon MC. Differential roles of hypoxia-inducible factor 1alpha (HIF-1alpha) and HIF-2alpha in hypoxic gene regulation. *Mol Cell Biol*. 2003;23:9361–74.

31. Tanaka T, Wiesener M, Bernhardt W, Eckardt K-U, Warnecke C. The human HIF (hypoxia-inducible factor)-3alpha gene is a HIF-1 target gene and may modulate hypoxic gene induction. *Biochem J*. 2009;424:143–51.

32. Ravenna L, Principessa L, Verdina A, Salvatori L, Russo MA, Petrangeli E. Distinct Phenotypes of Human Prostate Cancer Cells Associate with Different Adaptation to Hypoxia and Pro-Inflammatory Gene Expression. *PLoS ONE*. 2014;9;e96250.

33. Ravenna L, Salvatori L, Russo MA. HIF3α: the little we know. *FEBS J*. 2016;283:993–1003.

34. Zhang P, Yao Q, Lu L, Li Y, Chen P-J, Duan C. Hypoxia-inducible factor 3 is an oxygen-dependent transcription activator and regulates a distinct transcriptional response to hypoxia. *Cell Rep*. 2014;6:1110–21.

35. Antunica-Noguerol M, Budziñski ML, Druker J, et al. The activity of the glucocorticoid receptor is regulated by SUMO conjugation to FKBP51. *Cell Death Differ*. 2016;23:1579–91.

36. Zhang L, Qiu B, Wang T, et al. Loss of FKBP5 impedes adipocyte differentiation under both normoxia and hypoxic stress. *Biochem Biophys Res Commun*. 2017;485:761–7.

37. Luo K, Li Y, Yin Y, et al. USP49 negatively regulates tumorigenesis and chemoresistance through FKBP51-AKT signaling. *EMBO J*. 2017;36:1434–46.

38. Xu J, Zheng L, Chen J, et al. Increasing AR by HIF-2 inhibitor (PT-2385) overcomes the side-effects of sorafenib by suppressing hepatocellular carcinoma invasion via alteration of pSTAT3, pAKT and pERK signals. *Cell Death Dis*. 2017;8:e3095.

39. Gassen NC, Fries GR, Zannas AS, et al. Chaperoning epigenetics: FKBP51 decreases the activity of DNMT1 and mediates epigenetic effects of the antidepressant paroxetine. *Sci Signal*. 2015;8:ra119.

40. Gonzalez PN, Gasperowicz M, Barbeito-Andrés J, Klenin N, Cross JC, Hallgrímsson B. Chronic Protein Restriction in Mice Impacts Placental Function and Maternal Body Weight before Fetal Growth. *PLOS ONE*. 2016;11:e0152227.

Chapter 5 : Similar Gene Expression in Adult Liver, Adipose Tissue and Skeletal Muscle of Maternal Nutrient Restricted Offspring Susceptible or Resistant to Changes in Glucose Metabolism

The following chapter contains a manuscript prepared for submission in PLOSone

5.1 Introduction

Intrauterine Growth Restriction (IUGR) is a pregnancy condition where fetal growth is suboptimal, resulting in an infant born with a birthweight <10th percentile. The most common cause in developed countries is poor placental development (placental insufficiency) and in under-developed countries is maternal malnutrition (1). In both placental insufficiency and maternal malnutrition, the fetus is undernourished during development and the gestation at which it is impacted depends on the timing and type of pathology. In the short term, infants from IUGR pregnancies have higher morbidity and mortality rates in the perinatal and neonatal periods (2). As adults, offspring from IUGR pregnancies are also at increased risk for adult diseases such as cardiovascular disease, glucose intolerance and type 2 diabetes (3).

Initial studies demonstrating convincing evidence between pathologically small birth weights and long-term metabolic outcomes were in cohorts of the Dutch famine. Ravelli *et al* (1998), described an increased occurrence of glucose intolerance in these adults whose mothers experienced the Dutch famine during pregnancy (4). Further studies of this population, other IUGR populations and animal models have also demonstrated an influence of fetal environment on adult health (5–8). Such studies have led to the concept of 'Developmental Origins of Health and Disease' (DOHaD). In this concept, adversity during fetal and early life can lead to adaptations that may temporarily improve survival. However, these adaptations may not be beneficial to those individuals as an adult (9). One mechanism of fetal adaptation is through epigenetic changes such as DNA methylation, histone modifications, and differential miRNA expression, which result in altered gene expression that influence organ development or cell function in metabolically important tissues. The epigenetic marks can persist until later in life (adulthood) and may lead to altered gene expression and pathology.

The adaptations can be tissue-specific making animal models useful when studying long-term metabolic impacts of fetal undernutrition. Previous work in our laboratory has established a mouse model of IUGR using maternal nutrient restriction (MNR) (10). MNR male offspring from this model experienced growth restriction and had smaller liver-to-body weight ratios (10). At 6 months, 19% of the MNR offspring were glucose

intolerant and the remaining were not susceptible to glucose tolerance changes (10).
Despite the variation in glucose tolerance, most MNR had increased hepatic insulin
sensitivity (10). The aim of this study was to identify tissue-specific expression changes
that occur in response to fetal undernutrition in all MNR and/or in susceptible MNR
offspring. Liver, adipose tissue and skeletal muscle were the tissues of focus because
insulin sensitivity in these tissues precedes the development of type 2 diabetes (11).
Although at increased risk, not all individuals born from IUGR pregnancies will develop
metabolic disorders. Understanding the expression changes associated with susceptible
and resistant growth restricted populations to changes in glucose tolerance could help
identify IUGR populations in humans that will develop an altered glucose metabolism as
adults.

5.2   Methods

5.2.1 Animals

All animal care and procedures were approved by the Council on Animal Care at the
University of Western Ontario and as previously described (10). Briefly, pregnant CD-1
mice received *ad libitum* food or maternal nutrient restriction (MNR) (70% of *ad libitum*)
from E6.5 until birth. Only litters with 11-15 pups were studied and male to female ratios
did not vary between control and MNR litters (10). All pups were cross-fostered to an *ad
libitum*-fed mother at birth with litters culled or fostered to 13 pups per litter. Male
offspring were weaned onto a standard chow diet (Teklad LM-485 Mouse/Rat
Sterilizable Diet, Harlan Laboratories, USA). At 6 months, offspring were euthanized by
CO_2 necrosis (8 30 to 10 00 h) and right medial liver lobes, perigonadal fat pads, and
quadriceps femoris were snap frozen in liquid nitrogen. Frozen tissues were stored at -
80°C until further analysis.

5.2.2 RNA isolation

Fifty mg of liver (control N=8, intolerant MNR N=7, tolerant MNR N=8) and skeletal
muscle (control N=8, intolerant MNR N=9, tolerant MNR N=8) and 100 mg of adipose
tissue (control N=8, intolerant MNR N=9, tolerant MNR N=8) was pulverized and then
homogenized for 50 seconds in 1 mL of ice cold TRIzol (Invitrogen™, Carlsbad, CA,
USA). RNA was extracted from homogenate with RNA PureLink™ mini kit

(Invitrogen^TM, USA) according to the manufacturer's TRIzol and on-column DNAseI treatment protocol. RNA quality was verified (RIN ≥ 7) with an Agilent Bioanalyzer 2100 at McGill University and Génome Québec Innovation Centre (Montreal, QC, Canada) and the National Research Council Canada (NRC) (Saskatoon, SK, Canada).

5.2.3 RNA sequencing

Library preparation and quality control for the liver and skeletal muscle were done at the McGill University and Génome Québec Innovation Centre (Montreal, QC, Canada) with the Illumina TruSeq^TM mRNA Stranded library kit (Illumina). Single-reads sequencing was run on a HiSeq 2500 and the average read depth was 13 million per sample. Adipose RNA libraries and QC were prepared by the National Research Council Canada (NRC) (Saskatoon, SK, Canada) using the NEBNext® Ultra™ II Directional RNA Library Prep Kit for Illumina®. An average of 8 million paired reads per sample were obtained. Reads from all tissues were aligned to the mm9 transcriptome with Bowtie2 (12). Quality control of reads and removal of adapters or primer sequences were done with the Trim Galore (version 0.4.4) library.

5.2.4 Differential Gene Expression and Pathway Enrichment

Genes with no counts per samples were removed from count tables. Outlier detection, PCA plots and differential expression were done in the R console (version 3.3.2) (13) with Z Compositions (version 1.1.1) (14), CoDaSeq (version 0.99.1) (15,16) and ggplots2 (version 2.2.1) (17) libraries. Sample outliers in glucose tolerance groups with variation greater than the median plus 2 times the interquartile ratio were removed, as described by Gierliński et al. (**Supplementary Figure S5.2.1-5.2.3**) (18). The impaired fasting blood glucose (IFBG) group, which exhibited higher blood glucose than any controls (**Supplementary figure S5.2.4**), had a small sample size (N=4) and were not assessed for outliers. EdgeR (19), DESeq2 (20), and Aldex2 (21) tools were used in differential expression analysis and protein-coding genes were considered differentially expressed if there was consistency in two or more tools (FDR < 0.1, > 2-fold change). Gene ontology enrichment was done on the panther online tool (22,23), and NCI:Nature and KEGG enrichment was done on the EnrichR online tool (24,25).

5.3   Results

Gene expression of control and MNR offspring, as well as tolerant and intolerant MNR, were assessed in the right medial liver lobe, quadriceps femoris muscle and perigonadal adipose tissue at 6 months. PCA plots of expression data within each tissue suggest that samples do not cluster based on maternal nutrition or glucose tolerance in all three tissues (**Figure 5.3.1 and Supplementary Figure S5.3.1**). Sample-to-sample plots also demonstrate that samples do not separate based on maternal nutrition or glucose tolerance (**Figure 5.3.2**).

Although tissues showed similar overall gene expression, we examined pathway enrichment of genes differentially expressed between maternal nutrition and glucose tolerance groups (**Table 5.3.1-5.3.3 and Supplementary Table 5.3.1**). In the liver, 6 genes were differentially expressed in MNR offspring relative to controls (**Table 5.3.1 and Supplementary Table 5.3.1**). These genes include three heat shock protein chaperons (Hspab1, Hspa11) as well as FGF11 which are involved in MAPK signalling. Both heat shock proteins and Alas1 are also involved in the immune response to Epstein-Barr virus infections. Twenty four genes are differentially expressed in intolerant MNR relative to controls (**Table 5.3.1 and Supplementary Table 5.3.1**) including three heat shock proteins (Hspa1a, Hspa11, and Hsp1b) that are involved in cellular response to heat, unfolded proteins, immune response, MAPK pathway (Ntrk2, Fgf11), and longevity and estrogen signalling pathways (Adcy1). Pathway enrichment also shows differences in intolerant MNR in tyrosine receptor signalling (Dnaic1, Pdk4, Gdf15, Hspb1, and Ntrk2) and p53 effectors (Hspa1a, Fdf15). Although not indicated by pathways enrichment, differentially expressed genes associated with obesity, lipid metabolism and adipogenesis were increased (Vldlr, Adcy1, Ntrk2) or decreased (Cyp26b1) in intolerant MNR relative to controls (26,27). Despite differential expression of 7 genes in MNR with impaired fasting blood glucose, no pathways were enriched (**Table 5.3.1 and Supplementary Table 5.3.1**). Similar to intolerant MNR, genes involved in lipid and cholesterol metabolism were decreased (Cyp26b1, Mfsd2a, Cyp2b10)(28) in the impaired fasting blood glucose cohort. Only metallothionein 1 was differentially expressed between tolerant and intolerant MNR, and subsequently no pathways were enriched.

Minimal transcriptome changes were evident in 6-month quadriceps femoris muscle (**Table 5.3.2 and Supplementary Table 5.3.1**). Furthermore, no genes were differentially expressed between all MNR and controls. Only 3 genes in intolerant MNR and 4 genes in MNR exhibiting a higher fasting blood glucose and were differentially expressed compared to controls. Potassium voltage-gated channel, shaker-related, subfamily, member 6 (Kcna6) was differentially expressed between tolerant and intolerant MNR. No pathway enrichment was found in differentially expressed genes (**Table 5.3.2**).

In the adipose tissue differential gene expression analysis also revealed minimal differences between control and MNR offspring (**Table 5.3.3 and Supplementary Table 5.3.1**). Napsin A aspartic peptidase (Napsa) was differentially expressed between all MNR and controls. In the intolerant and impaired fasting blood glucose groups, 6 and 2 were differentially expressed between relative to controls, respectively. No genes were differentially expressed between tolerant and intolerant MNR. None of the genes differentially expressed in adipose tissue between maternal nutrition or glucose tolerance groups were significantly enriched in pathways (**Table 5.3.3**).
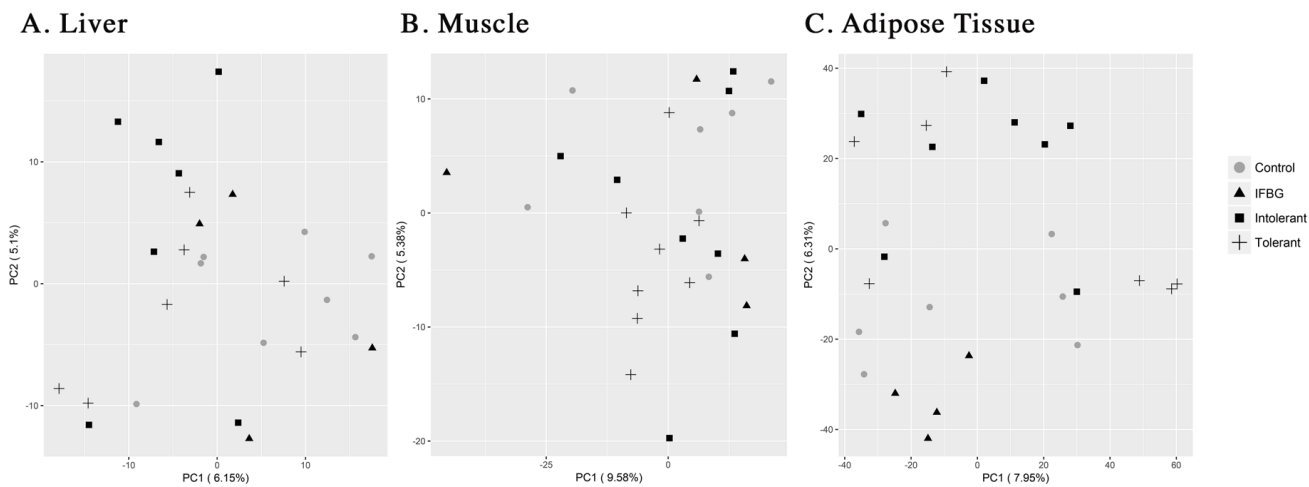
Figure 5.3.1 PCA plots of liver (A), skeletal muscle (B), and adipose tissue (C) demonstrate similar overall expression between control (grey) and MNR (black), and between glucose tolerance groups (symbols).
Plotted data was transformed with the centered log ratio and filtered for the top 500 variable genes.
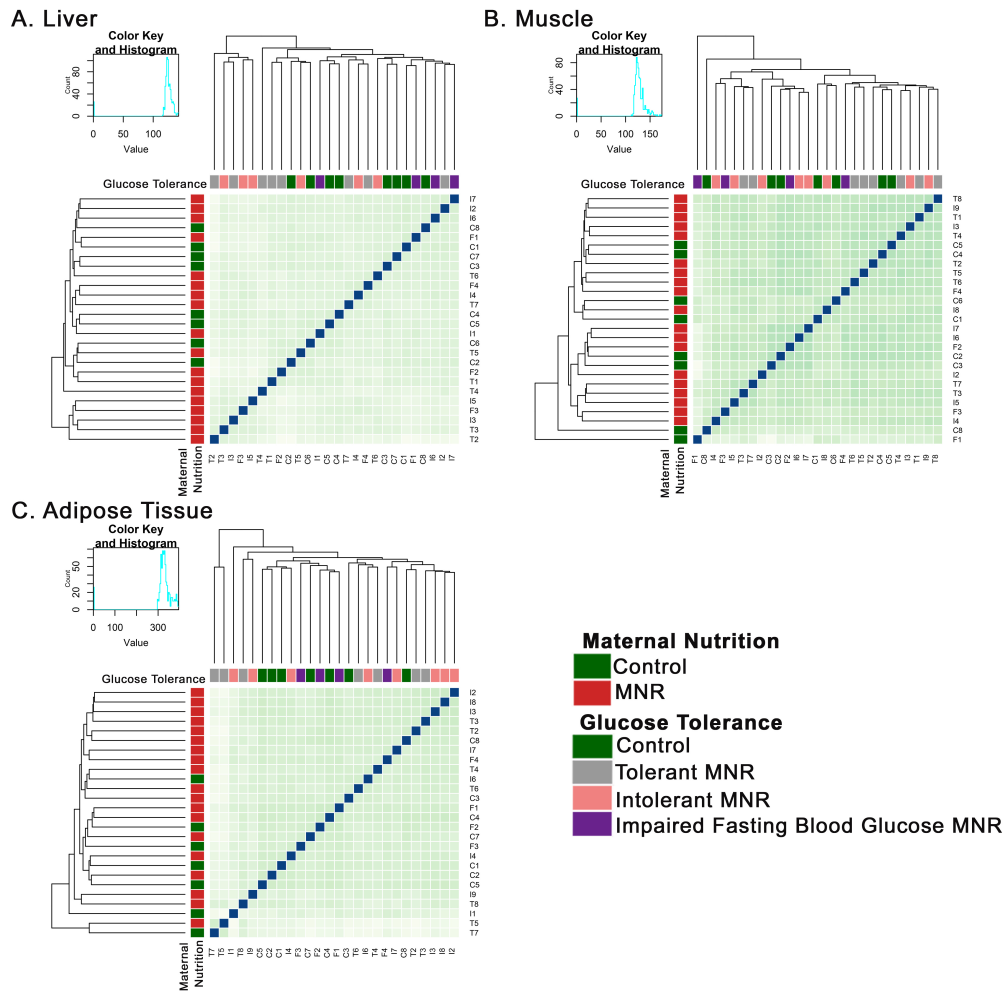
Figure 5.3.2 Sample-to-sample plots of RNA*seq* centered-log ratio transformed data from the liver (A), skeletal muscle (B), and adipose tissue (C).
Samples did not cluster based on maternal nutrition (Y-axis) or glucose tolerance (X-axis).

Table 5.3.1 Pathway enrichment of differentially expressed genes (FDR <0.1 in 2 > tools) in the liver of 6-month offspring.

Reference Group	Comparison Group	# Genes	GO Enrichment	KEGG Enrichment
Control	All MNR	6	NA	MAPK signalling pathway (20.24) (Hspb1, Hspa1l, Fgf11) Epstein-Barr virus infection (12.53) (Hspb1, Hspa1l, Alas1)
	Intolerant MNR	24	Protein refolding (4.49E-03), Chaperone cofactor-dependent protein refolding (1.04E-02), Cellular response to unfolded protein (4.14E-02), Cellular response to heat (4.07E-02) (Hspa1a, Hspa1l, Hspa1b) Transmembrane receptor protein tyrosine kinase signalling pathway (2.56E-02) (Dnaic1, Pdk4, Gdf15, Hspb1, Ntrk2)	MAPK signalling pathway (29.20) (Hspa1a, Hspa1l, Hspa1b, Ntrk2, Fgf11, Hspb1) Longevity regulating pathway (27.42), Estrogen signalling pathway (22.60) (Hspa1a, Hspa1l, Hspa1b, Adcy1) Antigen processing and presentation (14.94), Toxoplasmosis (13.94), Measles (12.40), Spliceosome (12.23), Influenza A (11.56), Legionellosis (18.25) (Hspa1a, Hspa1l, Hspa1b)
	MNR with Higher Fasting Blood Glucose	7	NA	NA
Tolerant MNR	Intolerant MNR	1	NA	NA

Note: Combined scores (KEGG and NCI:Nature) or FDR (GO) per pathway are indicated in brackets, followed by the genes included in the pathway.

Table 5.3.2 Pathway enrichment of differentially expressed genes (FDR < 0.1 in 2 > tools) in skeletal muscle of 6-month-old offspring.

Reference Group	Comparison Group	# Genes	GO Enrichment	KEGG Enrichment
Control	All MNR	0	NA	NA
	Intolerant MNR	3	NA	NA
	MNR with Higher Fasting Blood Glucose	4	NA	NA
Tolerant MNR	Intolerant MNR	1	NA	NA

Note: Combined scores (KEGG and NCI:Nature) or FDR (GO) per pathway are indicated in brackets, followed by the genes included in the pathway.

Table 5.3.3 Pathway enrichment of differentially expressed genes (FDR < 0.1 in 2 > tools) in adipose tissue of 6-month-old offspring.

Reference Group	Comparison Group	# Genes	GO Enrichment	KEGG Enrichment
Control	All MNR	1	NA	NA
	Intolerant MNR	6	NA	NA
	MNR with Higher Fasting Blood Glucose	3	NA	NA
Tolerant MNR	Intolerant MNR	0	NA	NA

Note: Combined scores (KEGG and NCI:Nature) or FDR (GO) per pathway are indicated in brackets, followed by the genes included in the pathway.

5.4   Discussion

In our mouse model of fetal growth restriction, the overall gene expression in 6-month-old liver, adipose and skeletal muscle was similar for offspring of maternal nutrition restriction and control pregnancies, and glucose tolerant and intolerant groups. Increased p-AKT to AKT ratios in response to insulin occurred in the liver of most MNR, but a cohort of MNR offspring were susceptible to impaired glucose tolerance with a higher under the curve (AUCs) during the glucose tolerance test than any controls (10). However, these changes are moderate and most evident after an insulin or glucose bolus (10). Subsequently, the gene expression changes may be detectable after during metabolic stress. Alternatively, impacts on transcription could be proportional to the extent of maternal nutrient restriction. For example, transcription of genes involved in regulation of epigenetics, circadian rhythms and lipid or glucose metabolism are altered at weaning in offspring from 50% MNR throughout or late gestation to weaning (29,30). These IUGR models are also in rats which have lower metabolic rates than mice (31). In humans, basal metabolic rate is negatively correlated to insulin resistance (32) and could suggest rats are more sensitive to disruptions in glucose homeostasis. Gene expression changes in tissues could also decrease with age. Even with 50% MNR in rats, a low number of genes and magnitude of effect are present in offspring at postnatal day 450 (30). It is also possible that gene expression changes occurred in tissues not assayed in this study. One study showed that transcriptional responses to maternal protein restriction was specific to each organ in the fetus (33).

Although transcription changes were limited in MNR offspring, liver had the most differentially expressed genes. Two heat shock proteins (HSPs) were decreased in all MNR and three in intolerant MNR. Small (Hspb2) and large (Hspa1a, Hsp1l, and Hspa1b) HSPs act as chaperons and are induced during cellular stress. Reduced HSP expression could indicate decreased cellular stress or a reduced response to similar stress in MNR compared to controls. For example, increased ER stress occurs in rat offspring from maternal protein restriction (34). Apart from the unfolded protein response, HSPs mediate protein-protein interactions and function in prevention of apoptosis in mitophagy

(35). Increased intracellular Hspa1a is associated with increased insulin sensitivity in skeletal muscle but extracellular Hspa1a may decrease insulin sensitivity (36–38). Depending on the cellular location, reduced Hspa1a expression in intolerant MNR could have anti-inflammatory or proinflammatory effects, reducing or promoting insulin sensitivity, respectively (36-38). HSPs also regulate cellular localization of transcription factors such as the androgen receptor (39) and this pathway was not enriched in the differentially expressed genes. Heat shock transcription factors (HSFs) regulate HSP transcription but also are not differentially expressed (40,41). HSF activity can be modulated via nuclear localization and post-translational modifications and were not examined in this study (40,41). While it cannot be excluded that stress response deviates in MNR and intolerant MNR through protein interaction with heat shock proteins, the underlying cause of cellular stress was not implicated with the gene expression data.

Despite changes in genes regulating lipid metabolism, no differences were observed in hepatic cholesterol or serum cholesterol and triglycerides in these adult MNR offspring on standard chow (10). Offspring of maternal protein restriction in rats are more sensitive to dietary-induced obesity and insulin resistance and have altered transcription of cytochrome p450 gene family members (42). Altered expression of lipid metabolism-related genes could indicate that MNR offspring are more sensitive to a high-caloric diet in adulthood. However, the absence of dyslipidemia in standard chow-fed offspring suggests genes regulating lipid metabolism are not likely the mechanism of glucose intolerance in this study.

Few genes were differentially expressed in muscle and adipose tissue between maternal nutrition or glucose tolerance groups. Differential gene expression in response to maternal nutrition or growth restriction in fat pads and skeletal muscles have been previously documented (43,44). It is possible that quadriceps femoris and perigonadal fat pads are less sensitive to maternal nutrition than subcutaneous fat and biceps femoris muscle that were used in previous studies (43,44). Maternal nutrient restriction may have also had a greater impact on the tissues if it was reduced more than 30%. Although in rats, even 50% MNR resulted in transcriptional changes in the fetal liver but not adipose

tissue and skeletal muscle, suggesting the muscle and adipose tissue could be more resistant to maternal diet (29). The absence of short and long-term impacts on gene expression in adipose and skeletal muscle may relate to developmental timing. In rodents and humans both of these tissues continue to develop into the postnatal period (45,46).

MNR offspring that had impaired glucose tolerance or higher fasting blood glucose levels also have similar gene expression in the liver, fat and muscle compared to controls. Similar expression suggests that fetal adaptations do not result transcriptome changes in metabolic genes that persist into adulthood, at least in liver, skeletal muscle and adipose tissue. Therefore, persistent gene expression changes are not likely the mechanism behind the altered adult metabolism in this model of IUGR. Maternal diet or fetal growth restriction can influence genomic stability, body mass composition, gut microbiome, and transcription in other tissues such as the pancreas in offspring which could mediate long term metabolism (47–50). Future studies are needed to identify alternate mechanisms mediating effects of reduced maternal nutrition on susceptibility to aberrant glucose metabolism in this model of growth restriction.

5.5 References

1. Han VKM, Seferovic MD, Albion CD, Gupta MB (2012) Intrauterine Growth Restriction: Intervention Strategies. In: Buonocore G., Bracci R., Weindling M. (eds) Neonatology. Springer, Milano, p. 89-93.

2. Garite TJ, Clark R, Thorp JA. Intrauterine growth restriction increases morbidity and mortality among premature neonates. *American Journal of Obstetrics and Gynecology.* 2004;191:481–7.

3. Morrison KM, Ramsingh L, Gunn E, et al. Cardiometabolic Health in Adults Born Premature With Extremely Low Birth Weight. *Pediatrics.* 2016;138:e20160515.

4. Ravelli AC, van der Meulen JH, Michels RP, et al. Glucose tolerance in adults after prenatal exposure to famine. *Lancet* 1998;351:173–7.

5. Hales CN, Barker DJP. Type 2 (non-insulin-dependent) diabetes mellitus: the thrifty phenotype hypothesis. *Int J Epidemiol.* 2013;42:1215–22.

6. Roseboom TJ, van der Meulen JH, Ravelli AC, et al. Blood pressure in adults after prenatal exposure to famine. *J Hypertens.* 1999;17:325–30.

7. Oliveira D, Cezar J, Gomes RM, et al. Protein Restriction During the Last Third of Pregnancy Malprograms the Neuroendocrine Axes to Induce Metabolic Syndrome in Adult Male Rat Offspring. *Endocrinology.* 2016;157:1799–812.

8. Chamson-Reig A, Thyssen SM, Hill DJ, Arany E. Exposure of the Pregnant Rat to Low Protein Diet Causes Impaired Glucose Homeostasis in the Young Adult Offspring by Different Mechanisms in Males and Females. *Exp Biol Med (Maywood).* 2009;234:1425–36.

9. Barker DJ. The fetal and infant origins of adult disease. *BMJ.* 1990;301:1111.

10. Radford BN, Han VKM. Offspring from maternal nutrient restriction in mice show variations in adult glucose metabolism similar to human fetal growth restriction. *J Dev Orig Health Dis.* 2018. doi: 10.1017/S2040174418000983.

11. Czech MP. Insulin action and resistance in obesity and type 2 diabetes. *Nat Med.* 2017;23:804–14.

12. Langmead B, Salzberg SL. Fast gapped-read alignment with Bowtie 2. *Nat. Methods.* 2012;9:357-359.

13. R Core Team (2013). R: A language and environment for statistical computing. R Foundation for Statistical Computing, Vienna, Austria. URL http://www.R-project.org/.

14. Palarea-Albaladejo J, Martín-Fernández JA. zCompositions — R package for multivariate imputation of left-censored data under a compositional approach. *Chemometrics and Intelligent Laboratory Systems.* 2015;143:85–96.

15. Gloor GB, Reid G. Compositional analysis: a valid approach to analyze microbiome high-throughput sequencing data. *Can J Microbiol.* 2016;62:692–703.

16. Gloor GB, Wu JR, Pawlowsky-Glahn V, Egozcue JJ. It's all relative: analyzing microbiome data as compositions. *Ann Epidemiol.* 2016;26:322–9.

17. Wickham H. ggplot2: Elegant Graphics for Data Analysis. New York: Springer-Verlag; 2016.

18. Gierliński M, Cole C, Schofield P, et al. Statistical models for RNA-seq data derived from a two-condition 48-replicate experiment. *Bioinformatics.* 2015;31:3625–30.

19. Robinson MD, McCarthy DJ, Smyth GK. edgeR: a Bioconductor package for differential expression analysis of digital gene expression data. *Bioinformatics.* 2010;26:139–40.

20. Love MI, Huber W, Anders S. Moderated estimation of fold change and dispersion for RNA-seq data with DESeq2. *Genome Biol.* 2014;15:550.

21. Fernandes AD, Macklaim JM, Linn TG, Reid G, Gloor GB. ANOVA-like differential expression (ALDEx) analysis for mixed population RNA-Seq. *PLoS ONE.* 2013;8:e67019.

22. Mi H, Thomas P. PANTHER Pathway: An Ontology-Based Pathway Database Coupled with Data Analysis Tools. *Methods Mol Biol.* 2009;563:123–40.

23. Mi H, Huang X, Muruganujan A, et al. PANTHER version 11: expanded annotation data from Gene Ontology and Reactome pathways, and data analysis tool enhancements. *Nucleic Acids Res*. 2017;45:D183–9.

24. Chen EY, Tan CM, Kou Y, et al. Enrichr: interactive and collaborative HTML5 gene list enrichment analysis tool. *BMC Bioinformatics.* 2013;14:128.

25. Kuleshov MV, Jones MR, Rouillard AD, et al. Enrichr: a comprehensive gene set enrichment analysis web server 2016 update. *Nucleic Acids Res.* 2016;44:W90-97.

26. Matsumoto M, Kondo K, Shiraki T, et al. Genomewide approaches for BACH1 target genes in mouse embryonic fibroblasts showed BACH1-Pparg pathway in adipogenesis. *Genes Cells.* 2016;21:553–67.

27. Stahel P, Sud SK, Lee SJ, et al. Phenotypic and genetic analysis of an adult cohort with extreme obesity. *Int J Obes (Lond).* 2018;

28. Tiwary S, Morales JE, Kwiatkowski SC, Lang FF, Rao G, McCarty JH. Metastatic Brain Tumors Disrupt the Blood-Brain Barrier and Alter Lipid Metabolism by Inhibiting Expression of the Endothelial Cell Fatty Acid Transporter Mfsd2a. *Sci Rep.* 2018;8:8267.

29. Nowacka-Woszuk J, Szczerbal I, Malinowska AM, Chmurzynska A. Transgenerational effects of prenatal restricted diet on gene expression and histone modifications in the rat. *PLoS ONE.* 2018;13:e0193464.

30.   Freije WA, Thamotharan S, Lee R, Shin B-C, Devaskar SU. The hepatic transcriptome of young suckling and aging intrauterine growth restricted male rats. *J Cell Biochem.* 2015;116:566–79.

31.   Perez VJ, Eatwell JC, Samorajski T. A metabolism chamber for measuring oxygen consumption in the laboratory rat and mouse. *Physiol Behav.* 1980;24:1185–9.

32.   Drabsch T, Holzapfel C, Stecher L, Petzold J, Skurk T, Hauner H. Associations Between C-Reactive Protein, Insulin Sensitivity, and Resting Metabolic Rate in Adults: A Mediator Analysis. *Front Endocrinol (Lausanne).* 2018;9:556.

33.   Vaiman D, Gascoin-Lachambre G, Boubred F, et al. The intensity of IUGR-induced transcriptome deregulations is inversely correlated with the onset of organ function in a rat model. *PLoS ONE.* 2011;6:e21222.

34.   Sohi G, Revesz A, Hardy DB. Nutritional mismatch in postnatal life of low birth weight rat offspring leads to increased phosphorylation of hepatic eukaryotic initiation factor 2 α in adulthood. *Metab Clin Exp.* 2013;62:1367–74.

35.   Mosser DD, Caron AW, Bourget L, et al. The chaperone function of hsp70 is required for protection against stress-induced apoptosis. *Mol Cell Biol.* 2000;20:7146–59.

36.   Gupte AA, Bomhoff GL, Morris JK, Gorres BK, Geiger PC. Lipoic acid increases heat shock protein expression and inhibits stress kinase activation to improve insulin signaling in skeletal muscle from high-fat-fed rats. *J Appl Physiol.* 2009;106:1425–34.

37.   Hulina-Tomašković A, Heijink IH, Jonker MR, Somborac-Bačura A, Grdić Rajković M, Rumora L. Pro-inflammatory effects of extracellular Hsp70 and cigarette smoke in primary airway epithelial cells from COPD patients. *Biochimie*. 2018;156:47–58.

38. Rodrigues-Krause J, Krause M, O'Hagan C, et al. Divergence of intracellular and extracellular HSP72 in type 2 diabetes: does fat matter? *Cell Stress Chaperones.* 2012;17:293–302.

39. Li J, Fu X, Cao S, et al. Membrane-associated androgen receptor (AR) potentiates its transcriptional activities by activating heat shock protein 27 (HSP27). *J Biol Chem.* 2018;293:12719–29.

40. Larson JS, Schuetz TJ, Kingston RE. Activation in vitro of sequence-specific DNA binding by a human regulatory factor. *Nature.* 1988;335:372–5.

41. Green M, Schuetz TJ, Sullivan EK, Kingston RE. A heat shock-responsive domain of human HSF1 that regulates transcription activation domain function. *Mol Cell Biol.* 1995;15:3354–62.

42. Sohi G, Marchand K, Revesz A, Arany E, Hardy DB. Maternal protein restriction elevates cholesterol in adult rat offspring due to repressive changes in histone modifications at the cholesterol 7alpha-hydroxylase promoter. *Mol Endocrinol.* 2011;25:785–98.

43. Soto SM, Blake AC, Wesolowski SR, et al. Myoblast replication is reduced in the IUGR fetus despite maintained proliferative capacity in vitro. *J Endocrinol.* 2017;232:475–91.

44. Peñagaricano F, Wang X, Rosa GJ, Radunz AE, Khatib H. Maternal nutrition induces gene expression changes in fetal muscle and adipose tissues in sheep. *BMC Genomics.* 2014;15:1034.

45. White RB, Biérinx A-S, Gnocchi VF, Zammit PS. Dynamics of muscle fibre growth during postnatal mouse development. *BMC Dev Biol.* 2010;10:21.

46. Holtrup B, Church CD, Berry R, et al. Puberty is an important developmental period for the establishment of adipose tissue mass and metabolic homeostasis. *Adipocyte.* 2017;6:224–33.

47.   Soderborg TK, Clark SE, Mulligan CE, et al. The gut microbiota in infants of obese mothers increases inflammation and susceptibility to NAFLD. *Nat Commun.* 2018;9:4462.

48.   Tarry-Adkins JL, Fernandez-Twinn DS, Chen JH, et al. Poor maternal nutrition and accelerated postnatal growth induces an accelerated aging phenotype and oxidative stress in skeletal muscle of male rats. *Dis Model Mech*. 2016;9:1221–9.

49.   Souza AP de, Pedroso AP, Watanabe RLH, et al. Gender-specific effects of intrauterine growth restriction on the adipose tissue of adult rats: a proteomic approach. *Proteome Science.* 2015;13:32.

50.   Deyssenroth MA, Peng S, Hao K, Lambertini L, Marsit CJ, Chen J. Whole-transcriptome analysis delineates the human placenta gene network and its associations with fetal growth. *BMC Genomics.* 2017;18:520.

Chapter 6 : Discussion

6.1 Summary and Prospective

6.1.1 MNR as a Model for Metabolic Changes Associated with IUGR

We demonstrated in this study that moderate maternal nutrient restriction during gestation in CD-1 mice resulted in fetal growth restriction and was associated with changes in glucose metabolism of adult male offspring. Reduced fetal and liver size was associated with increased hepatic transcription of genes in chronic hypoxia signalling. At 6-months, most male MNR offspring have increased hepatic insulin sensitivity and about 20% develop glucose intolerance. However, no changes in metabolically regulatory transcripts were detected in 6-month adipose tissue, skeletal muscle and right medial liver lobe. This suggested that in this model, fetal liver adaptations could be mediated by transcription changes, but long-term alterations in glucose metabolism are not induced by differential expression of metabolically regulatory genes in the liver, skeletal muscle and adipose tissue.

The model can be used to study adaptations in response to pathological IUGR resulting from fetal undernutrition in humans. Reduced nutrition is one adversity which is common in placental insufficiency and maternal malnutrition (1). Clinically, IUGR is defined as a pregnancy condition in which the estimated weight of the fetus is less than 10th percentile expected for gestational age and an infant born from these pregnancies is termed small for gestational age (SGA). However, infants can experience reduced nutrition, growth restriction and metabolic adaptations, and have a birth weight greater than 10th percentile. Clinically, these infants will not be identified as SGA, however, they are impacted similarly to those who are SGA from IUGR pregnancies. Since long-term human studies are challenging to conduct, we developed this model in mice to follow the offspring within a feasible time frame (6 months) to conduct tissue-specific gene expression and epigenetic studies. It was our expectation that the model of maternal nutrient restriction in mice would allow investigations into molecular mechanisms that underlie long-term morbidity in a number of tissues. In nutrient restriction models of IUGR, all offspring

experience reduced nutrition during fetal life. Therefore, the model provides an opportunity to investigate offspring that result in low birth weight as well as those who do not. Immediate and long-term adaptations in response to fetal undernutrition would be applicable to health outcomes of the newborns as well as in later life and include infants encompassed and missed by the current clinical definition of IUGR.

Individuals born low birth weight, often used as a proxy for fetal growth restriction (FGR) or intrauterine growth restriction (IUGR), are 1.4 times more likely to develop type 2 diabetes as adults (2). Although at greater risk, not all of these infants will develop type 2 diabetes. Results from this model indicate that maternal nutrient restricted offspring with similar genetic backgrounds, maternal nutrition, and postnatal diet develop variable glucose metabolism as adults. This model provides susceptible and non-susceptible IUGR populations, which can be used to understand fetal adaptations that may increase or decrease risk for adult glucose intolerance.

'Catch-up' growth, especially high growth rates in the first week of life in rodents (3,4) or infancy/early childhood in humans (5), is associated with a more aberrant adult metabolism; and prevention of early post-natal 'catch-up' is suggested to be metabolically protective (4). Due to the rapid period of 'catch-up' growth in mice, it is difficult to calculate growth rates between birth and day 3. While it is possible that variations in catch-up growth could contribute to differences in susceptibility, it is unlikely due to the short period of time in which it occurs.

Fetal implantation site may also contribute to degree of growth restriction in MNR offspring. The main blood supply to the uterus is located at the periphery and at the uterine horn (6). Fetuses implanted further away from the blood supply would have experienced greater fetal undernutrition than pups closer to the blood supply. In our study, no correlations between fetal weight at E18.5 and the site of implantation were found. Subsequently, birth weight could not be used to estimate distance from the blood supply but could contribute to variations within litters.

CD-1 mice used in this model are an outbred strain and contain more genetic variability relative to inbred strains. In humans, genetic polymorphisms such as a glycine to arginine transition at codon 972 of IRS-1 are associated with insulin resistance and type II diabetes (7). In mice, wild-type C57BL/6 develop diet-induced fatty liver but CD-1 do not (8). However, strains produced from inbreeding CD-1 are susceptible to glucose intolerance and obesity, indicating genes mediating adult metabolism exist in this population (9). Such genetic variation likely contributes adult glucose metabolism in response to fetal nutrition.

In both the fetal and the adult tissues studied, the liver was the most vulnerable to alterations in maternal nutrition. When protein is reduced in maternal diet, fetal liver weight is decreased relative to body weight (10). Small for gestational age infants also have reduced liver weight compared to appropriate for gestational age infants (11). In this model, both fetal and adult livers were reduced relative to body mass. Although not measured in fetal livers, adult MNR offspring had increased insulin sensitivity. Insulin signalling regulates pathways such as hepatic glucose output, glycogen synthesis and mitogenesis, influencing glucose metabolism and hepatic growth. Additionally, transcriptomic changes were most evident in the liver of adults relative to adipose tissue and skeletal muscle, especially among the MNR that were glucose intolerant. Maternal nutrient restriction in rats also resulted in hepatic transcriptional changes to epigenetic machinery with minimal changes in skeletal muscle and adipose tissue (12). In agreement with previous work, liver was sensitive to alterations in maternal nutrition, impacting liver size, gene expression and metabolism.

Increased insulin sensitivity developed in response to fetal hypoinsulinemia in SGA infants and growth restricted models and contribute to hypoglycemia early in life (13–15). Increased insulin sensitivity promotes tissues such as the skeletal muscle to take up and store glucose (14). This energy storage can cause rapid catch-up growth (13) which is associated visceral adiposity in humans (16). Both ectopic lipid accumulation and adiposity are risk factors for cardiometabolic disease (17). Unpublished work in our lab measured serum insulin during GTT and serum blood glucose in E18.5 fetuses, and have

demonstrated reduced insulin secretion and hypoglycemia also occur in the MNR fetus. While increased sensitivity continues at 6 months in most MNR, relatively higher serum insulin-to-glucagon ratios in intolerant MNR suggests that insulin resistance may have developed in the susceptible population.

6.1.2 Interaction between Maternal Nutrition and Postnatal Diet

It is well known that overnutrition and poor dietary quality can result in obesity, insulin resistance and glucose intolerance. Dietary and exercise intervention can be used to prevent glucose intolerant populations from becoming type II diabetics (18). The timing of obesity also influences risk for metabolic disorders. Obesity in children at puberty or later had a positive association with type II diabetes (19). However, children that were obese at age 7, but achieved and maintained a healthy body weight by puberty, had a similar risk as the population that was not obese (19). Postnatal diets can enhance or impair detrimental effects in offspring from maternal nutritional insults. Specifically, continued calorie restriction after birth can prevent aberrant metabolic outcomes, and overnutrition or poor dietary quality can exaggerate the maladaptive impacts of fetal undernutrition on adult metabolism (20). This is thought to occur because the fetus adapts to a nutrient restrictive environment, and when postnatal food is abundant adaptations promoting energy conservation rather than expenditure are no longer an advantage.

Contrary to other models of growth restriction demonstrating increased susceptibility to diet-induced obesity and metabolic disorders, a HFHS post-weaning diet did not result in a difference between control and MNR offspring in the metabolic parameters measured. Often these diets are high-fat rather than high-fat high-sugar (3). HFD and growth restriction in rats impaired beta cell survival independently (21). When HFD and growth restriction were combined, islet damage was not cumulatively worse, suggesting that growth restriction and calorie dense diets could converge on similar mechanisms (21). Additionally, although some controversy exists on whether high-sugar or high-fat diets are more detrimental, most studies agree that excess calories is one of the main factors contributing to metabolic health. In this study, mice on the HFHS diet ate less food (in grams) and resulted in a similar calorie intake as standard chow-fed offspring. Similar to

our study, male, but not female, rat offspring from maternal protein restriction on a HFD ate less (in grams), resulting in an isocaloric diet (22). While this dietary challenge did not vary based on maternal nutrition, all offspring developed and a reduced glucose tolerance and increased body weights. These data indicate an importance in dietary quality in determining adult metabolism. It is possible that a high-fat diet or high caloric diet would have different impacts on control and MNR adult glucose metabolism. However, isocaloric high-fat high-sugar post-weaning diet did not increase MNR susceptibility to metabolic disorders relative to controls.

6.1.3 Gene Expression Changes in Offspring Associated with Maternal Nutrition and Adult Glucose Metabolism

In this study, gene expression was analyzed by three common differential expression tools, DESeq2, EdgeR and Aldex2, that perform well in synthetic and real RNA*seq* data sets (23,24). Genes were considered differentially expressed if they were detected by two or more tools. This approach was taken because no 'gold standard' for differential gene expression exists. In all three tools, counts are normalized or transformed to control for differences in library size and composition. Following normalization or transformation, the counts were fitted to a model and statistical comparisons between groups and multiple testing corrections were done. However, each program uses different approaches for these steps (**Table 6.1.1**). Quin et al. (2018), recently compared the precision (minimizing false positives) and recall (true positives) between all three software (24). The authors found Aldex2 had high precision but low recall for studies with < 10 samples, and that EdgeR and DESeq2 have more sensitivity for this range of replicates (24). Although their study used the Wilcox Rank test in Aldex2 which would have lower power than the Welch's test used in this study for few replicates (25). Still, with 7-9 replicates per group few differentially expressed genes were detected by Aldex2 likely due to the limited statistical power of the non-parametric test. Focusing on genes that were differentially expressed in multiple tools may address the reproducibility issues found with RNA sequencing studies, and was the approach taken in this study.

To identify genes associated with fetal adaptations and adult metabolism, the transcriptome of liver, skeletal muscle and adipose tissue in adult mice and fetal liver

were analyzed. Genes that were differentially expressed, particularly those changed in both the fetus and the adult, could be mediate fetal adaptations and maladaptive changes that influence adult glucose metabolism. Because changes in glucose metabolism were only detected in standard chow-fed adult offspring, adult expression was only examined on this diet.

In the liver of MNR fetuses, differentially expressed genes were involved in overlapping regulation of various transcription factors (**Figure 6.1.1**). However, hypoxia-induced signalling was the primary pathway with changes up- and down-stream of the transcription factors. Additionally, with moderate fold change in transcription and significant enrichment with multiple pathway enrichment tools, we focused on the cumulative change in HIF signalling.

Growth restriction caused by reduced maternal nutrition and maternal hypoxia result in similar fetal and placental adaptations. Increased placental size, more efficient vasculature, and no changes in placental hypoxia, suggest that both hypoxic and nutrient restricted placentas are able to compensate (29–31). Despite placental adaptations, hypoxia and MNR cause fetal circulation to redistribute oxygenated blood from the umbilical cord away from the liver and to the brain (32,33). In growth restricted humans, blood flow from the umbilical cord is reduced to both liver lobes, but the reduction is greater to the right and is the portion of the liver examined in this study (34). Additionally, glucose deprivation in colon cancer cell lines can induce hypoxia signalling (35,36), suggesting fetal nutrient availability may also be modulating HIF signalling in MNR offspring. Increased HIF-2α and HIF-3α transcripts and protein, and increased transcription of HRE-containing genes in this study support evidence of hypoxia signalling in MNR fetal liver. Further studies need to be done to understand whether redistribution of fetal circulation and/or nutritional regulation cause the induction of hypoxia-inducible signaling in response to maternal nutrition. Regardless of the mechanism, maternal hypoxia and MNR could induced the HIF pathway in the right lobes of the liver and contribute to similar adaptations in offspring.

Hypoxia signalling is involved in the regulation of metabolism, pluripotency and differentiation of progenitor cell populations and angiogenesis (37,38), which are important pathways tightly regulated in tissue development. Increased HIF-2α and HIF-3α are associated with chronic hypoxia and the switch from HIF-1α to HIF-2α occurs in developing tissue when vascularity and oxygen tension increase (39,40). Tissue sampling late in gestation, when the HIF-1α to HIF-2α switch may have occurred, likely contribute to the detection of HIF-2α but not HIF-1α. Additionally, the prolonged exposure of the fetus to nutrient restriction in this model could result in chronic hypoxia signalling and mediate an increase in HIF-2α and HIF-3α protein.

HIF-1α transcriptional targets were initially thought to be involved in promoting glycolytic metabolism and HIF-2α targets in fatty acid oxidation and matrix remodeling. (41,42). Both HIF-1α and HIF-2α regulate angiogenesis(42). Gene expression in neuroblastoma cells exposed to acute hypoxia and to chronic or moderate hypoxia were similar suggesting that the number of HIF redundant targets may be less than initially cited, and that conflicting evidence might be confounded by the temporal regulation of HIF-1α or HIF-2α (39). Additionally, Kdm3a, Ccng2, Hif-3α and Pfkfb3 were induced with both HIF-2α and HIF-1α overexpression in human umbilical vein endothelial cells (42). Subsequently, hypoxia inducible genes were not sorted based on HIF-1α or HIF-2α targets in the literature.

HIF-dependent hypoxia inducible transcripts increased in MNR were involved in metabolic (PFKFB3, FKBP5) and direct (KDM3a) or indirect (FKBP5) epigenetic responses. Enhanced expression of 6-phosphofructo-2-kinase/fructose-2,6-biphosphatase 3 (PFKFB3) promotes glycolysis and could influence hepatic glycogen (43). FKBP5 is associated with insulin resistance through inhibition of glucocorticoid signalling and as a co-chaperone to the Akt phosphatse, PHLPP(44,45). Both glucocorticoids and insulin promote glycogen deposition in the liver (46). While transcript levels were increased, protein changes were not significant suggesting these adaptations were not sufficient in preventing glycogen depletion during MNR fetal hypoglycemia. Near birth fetal metabolism in the liver shifts from glycolytic to gluconeogenic which may also indicate a

delay in this shift in MNR male offspring (47). Reduced liver size, increased hypoxia signaling, as well an increased marker of proliferation and reduced glycogen identified in this model, suggests that MNR have immature livers at E18.5.

Differential expression of genes involved in the regulation of epigenetic machinery provide a mechanism for long-term impacts of fetal undernutrition. In neural cells, FKFBP5 increase is negatively associated with global methylation by competitively inhibiting FKBP52 recruitment and reducing DNTM1 efficiency (48). KDM3a is a histone methyl transferase which removes mono and di-methylation at histone 3 lysine 9, typically associated with heterochromatin, especially at HRE-containing genes(49). Increased transcription of both modifiers could suggest epigenetic changes are influencing fetal transcription at HRE and non-HRE-containing genes and require further studies.

Although increased transcription of genes induced by HIFs were detected, the increase was moderate and not significantly reflected at the protein level. HIF-3α has been shown to weakly induce some HRE-containing genes, but most functional evidence suggests a role in repression of HIF-1/2α-dependent transcription (50,51). Increased HIF-3α might be repressing the transcriptional activity of HIF-2α and the magnitude of hypoxia response in MNR offspring. In MNR in guinea pigs, increased hepatic EPO protein were only significantly different in females suggesting that female fetuses may adapt with increased erythropoiesis (30). Although females were not examined in this study, it is possible that the hypoxic response in males is more moderate and could be mediated through HIF-3α.

Hypoxic gene expression changes were not detectable in MNR adult livers. In fact, few transcriptional changes were detected in liver, skeletal muscle and adipose tissue. Maternal nutrient restriction in rats resulted in alterations in fetal epigenetic machinery but histone acetylation changes did not persist to 4 weeks (12). Additionally, the number of genes impacted was reduced over time, despite metabolic changes becoming more evident with age (52). However, if fetal undernutrition during pregnancy established differences in cell populations and/or differences in how the cells are functioning,

changes in gene expression would be expected. Consequently, although these adaptations may occur, they do not persist and are not likely the mechanism underlying changes in glucose metabolism in this model.

It should be noted most changes in glucose metabolism were only detected in stress conditions, such as glucose tolerance and insulin challenge tests. Fetal hepatic changes were detected when the stress of nutrient restriction was still evident and altered HIF signaling might be evident in MNR offspring during a glucose or insulin challenge. In chronic myeloid leukemia patients, VHL loss-of-function mutations result in changes to methylation at HRE-promoters but do not result in increased HIF signaling until a 'second hit' occurs (53). The differential priming of HRE-genes in these individuals increase anti-apoptotic and angiogenic responses in the tumor (53). While differences in VHL were not confirmed in the validation cohort, KDM3a and FKBP5 were increased. It cannot be excluded that the transcription during stressed conditions could vary in HIF or other stress response pathways in tissues of MNR adult offspring.

Intrauterine fetal adaptations to moderate nutrition restriction could also be independent of changes in cell populations or persistent epigenetic changes. Evidence of altered gut microbiome and reduced genomic stability have been observed in response to different maternal diets (54,55). Protein function and stability can also be regulated by genetic polymorphisms and miRNAs. Lastly, tissues not yet examined in this model could have influenced fetal adaptations and modulated susceptibility in the MNR population.

Table 6.1.1 Comparison of tools used for differential expression

Tool	Normalization/ Transformation	Statistical analysis	Model of Count Means	Multiple comparisons adjustments	Outlier Detection	Reference
DESeq2	• Normalize with a scaling factor • Median of ratios to the geometric mean	Empirical Bayes estimation of dispersion and log fold change for the Wald test (parametric)	Negative binomial	Benjamini-Hochberg correction	Cooks Distance (>99th percentile) for ≥ 7 samples	(26)
EdgeR	• Normalized with a scaling factor • Weighted mean of ratios in a pairwise comparison of each sample and a reference sample	Empirical Bayes estimation of dispersion and an adapted Fisher's exact test (parametric)	Negative binomial	Benjamini-Hochberg correction	None	(27)
Aldex2	• Transformed by the centered log ratio (clr)	Empirical Bayes to estimate Monte Carlo Dirichlet instances and Welch's test (non-parametric)	Poisson distribution	Benjamini-Hochberg correction	None	(25,28)
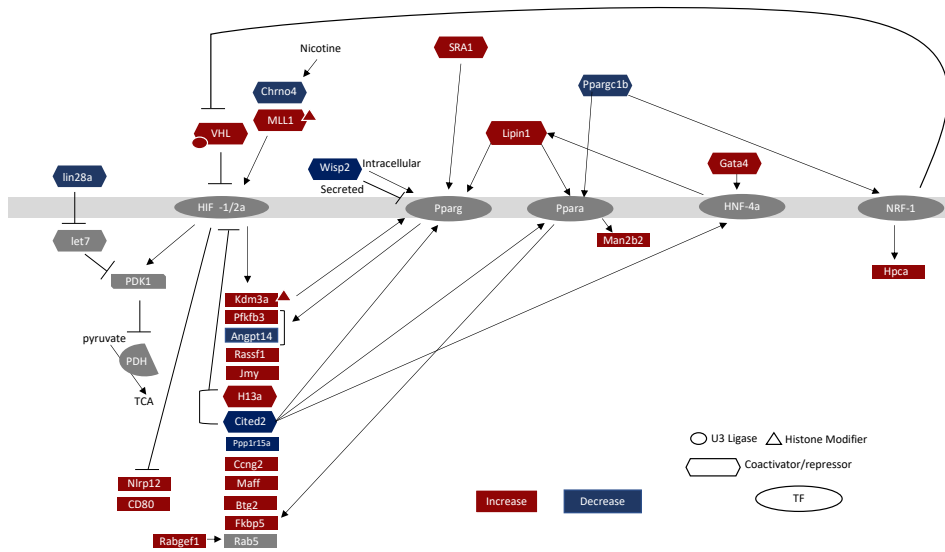
Figure 6.1.1 Genes differentially expressed up- and down-stream of transcription factors in fetal hepatic liver.

Differential expression was detected upstream from many transcription factors (indicated by the grey bar) important in tissue development and metabolism. However, genes involved in hypoxia-inducible factor signalling were differentially regulated up- and downstream from HIF transcription factors.

6.2   Limitations and Future Studies

This the first in-depth use of maternal nutrient restriction post-implantation to birth in CD-1 mice to study the association between reduced fetal nutrition and long-term metabolic outcomes. While metabolic and expression changes identified in this study provide insight for understanding the relationship between maternal nutrition and fetal adaptations, there are also associated limitations that can be addressed with further studies.

6.2.1 Further Characterization of Metabolic and Expression Outcomes in MNR Offspring

Increased PAI-1 and resistin in MNR serum could indicate increased fat mass or meta-inflammation. However, mRNA of PAI-1 and resistin were not different in MNR adipose tissue compared to controls. Transcripts in inflammatory pathways were also similar in control and MNR adipose tissue, suggesting increased fat mass rather than adipocyte meta-inflammation in MNR offspring. Reduced lean mass been associated with other models of MNR and can contribute to decreased glucose tolerance (56). In animal studies, the 'gold method' is via chemical carcass analysis which is terminal and requires the entire carcass (57). Micro-CT imaging is accessible to our lab, can be done on live specimens, distinguishes between subcutaneous and visceral adipose tissue, and provide accurate estimate of body mass composition in mice (58,59). Utilizing this technology in adult offspring would determine whether body mass composition is different in MNR offspring and allow metabolic and expression analysis in the same mouse.

Insulin sensitivity was only measured in a portion of the cohort due to technical limitations in the hepatic portal vein insulin challenge. The most accurate and sensitive method for tissue-specific and whole-body insulin sensitivity is hyperinsulinemic euglycemic clamp studies. While this method can be performed on a large sample number, it is technically challenging, requires expensive equipment, and is difficult to analyze. If the equipment or expertise were available, this technique could be used. Alternatively, injection of insulin or saline and collecting tissues could be done in all animal of a cohort after 6-month glucose tolerance testing. Similar to the gene expression analysis in this study, tolerant, intolerant and average controls could be used to detect pAKT to AKT ratios. While the sample size per group would not increase with this

design, tissue-specific insulin sensitivity could be quantified for intolerant MNR relative to control and tolerant MNR populations.

During the insulin challenge test or hyperinsulinemic euglycemic clamp study, liver, adipose tissue and skeletal muscle could also be collected for gene expression analysis. Studies in humans show that hyperglycemia and hyperinsulinemia initiate gene expression changes in many tissues (60,61). Additionally, insulin-induced gene expression in the skeletal muscle and adipose tissues during hyperinsulinemic clamp studies were blunted in type 2 diabetics compared to controls, despite having similar basal expression (60). To our knowledge, gene expression in adult offspring from growth restricted models have not been examined after a glucose or insulin bolus. This would assess whether adaptations are present in MNR offspring in metabolic 'stress' conditions.

6.2.2 Influence of Reduced Nutrition in Gestation and Throughout Lactation of Skeletal Muscle and Adipose Tissue

In addition to examining changes in gene expression during hyperinsulinemia, extending nutrient restriction until weaning could also influence long term impacts. With the current model, skeletal muscle and adipose tissue had few differentially expressed genes. In mice the number of muscle fibers is determined around day 7 and the number of myonuclei by day 21 (62). Establishment of white adipose tissue occurs in two phases, the first from birth to two weeks of life and the second in puberty (around weaning) (63). Although hyperplasia and hypertrophy of white adipose tissue continue throughout life, the rate of increase is steady through adulthood (63). The offspring in this study were fostered to *ad libitum*-fed mothers, receiving *ad libitum* for the postnatal developmental periods. Extension of nutrient restriction throughout lactation would provide further insight into the effects of reduced nutrition on development of these tissues. However, it may also modify 'catch-up' growth and adult metabolism (64). Extending nutrient restriction to weaning would assess the interaction between MNR and nutrition during lactation and could increase impacts on skeletal muscle and adipose tissue.

6.2.3 Mechanism of Fetal Hepatic Hypoxia in Adaptations to Growth Restriction

The concept of hypoxia signalling in growth restricted infants is relatively new. Dynamic changes to hypoxic signalling suggest that the impact at different developmental stages could vary (37,65). Temporal analysis of hepatic HIF-1α, HIF-2α, and HIF-3α mRNA and protein during liver development in control and MNR offspring is needed. This study would determine if a switch from HIF-1α to HIF-2α occurs in the liver and whether the peak expression or stabilization vary between control and MNR. RNA*seq* at peak expression could provide insight into the changes mediated by altered HIF signalling in the MNR offspring.

In addition to understanding the timing of HIF signalling, further experiments need to determine how increased hepatic hypoxia influences fetal adaptations to nutrient restriction. Knocking down and overexpressing fetal hepatic HIF-2α and HIF-3α, and HIF-1α if MNR influences protein levels earlier in gestation, during MNR would clarify whether increased HIF signalling is an advantage for fetal survival. Recombinant adeno-associated virus (rAAV) injected into the amniotic sac with miRNA or expression vectors under the control of the alpha fetoprotein promoter would allow for such liver-specific fetal gene manipulation (66,67). Since differentially expressed genes in the fetus did not persistent into adult life, temporal knock down or overexpression is preferable. These studies would gain insight into the role of HIFs in liver development and fetal survival during undernutrition. It would also determine whether these adaptations mediate long term metabolic outcomes of the MNR offspring.

6.3   Overall Conclusions and Significance

This study investigated fetal and adult adaptations in liver, adipose tissue and skeletal muscle of maternal nutrient restricted male offspring in mice on a post-weaning standard chow or a HFHS diet (**Figure 6.3.2**). Offspring from MNR pregnancies experienced fetal growth restriction and changes to adult glucose tolerance or insulin signalling. In the fetus, reductions in maternal calories disproportionately impacted the liver and might be mediated through increased hypoxia signalling. Differences in hypoxia-inducible transcripts did not persist to 6 months. As adults, minimal changes in gene expression in

all three tissues were detected. However, the liver of MNR offspring was smaller with increased insulin sensitivity. As adults, MNR was associated with increased serum peptide markers that suggest changes to body mass composition. Despite the changes in standard chow-fed offspring, no differences between MNR and controls on an isocaloric post-weaning HFHS diet were detected. While liver weight, insulin sensitivity and potentially body mass composition are influenced by MNR, post-weaning diet overcame maternal nutrient effects.

To our knowledge this is the first study of growth restriction where susceptible and non-susceptible populations are examined in addition to changes occurring in all offspring. Despite having susceptible and non-susceptible adult populations in standard chow-fed offspring, metabolic and gene expression changes were only moderately impacted. Gene expression during metabolic stress could provide insight into variability in the MNR offspring. Additionally, serum peptide markers suggest body mass composition and appetite could be influencing susceptibility. Despite fetal liver adaptations and adult metabolic changes gene expression changes in metabolically regulatory genes were not differentially expressed.

Understanding tissue-specific adaptations from reduced fetal nutrition and how they mediate adult glucose intolerance will provide insight into the increased risk for type 2 diabetes in human growth restricted populations. Type 2 diabetes has significant complications and causes a substantial financial burden on the medical system (68). Early identification and prevention can reduce cost and improve patient quality of life. Identifying such adaptations will aid in recognizing, preventing and/or treating aberrant glucose metabolism in these individuals. Additionally, this study supports the notion that fetal nutrition is important in establishing adult liver metabolism which could impact chronic diseases beyond metabolic disorders.
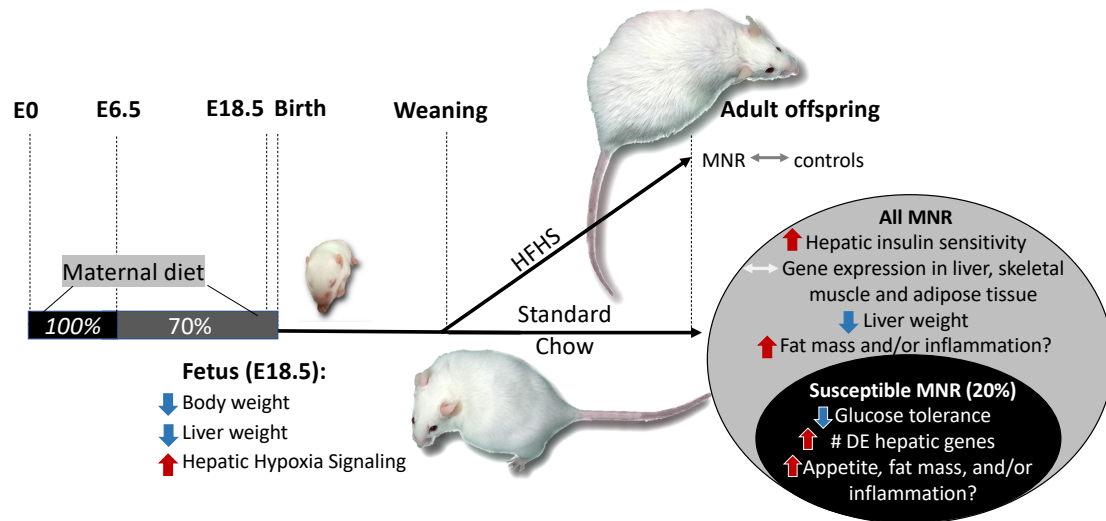
Figure 6.3.1 Metabolic and expression changes in the male fetal and adult offspring from maternal nutrient restriction.

In the fetus, body and liver weight is reduced (chapter 2) and transcripts in HIF signalling were induced (chapter 4). On standard chow, MNR offspring had increased hepatic insulin sensitivity, reduced liver weight and increased serum markers for adiposity relative to controls (chapter 2). 20% of the MNR offspring were susceptible to glucose intolerance (chapter 2) and had increased differentially expressed (DE) genes (chapter 5). Post-weaning HFHS diet did not differentially impact MNR and control offspring in the parameters measured in this study (chapter 3).

6.4   References

1.   Han VKM, Seferovic MD, Albion CD, Gupta MB (2012) Intrauterine Growth
Restriction: Intervention Strategies. In: Buonocore G., Bracci R., Weindling M.
(eds) Neonatology. Springer, Milano, p. 89-93.

2.   Zhao H, Song A, Zhang Y, Zhen Y, Song G, Ma H. The association between birth
weight and the risk of type 2 diabetes mellitus: a systematic review and meta-
analysis. *Endocr J*. 2018;65:923–33.

3.   Xiao D, Kou H, Zhang L, Guo Y, Wang H. Prenatal Food Restriction with
Postweaning High-fat Diet Alters Glucose Metabolic Function in Adult Rat
Offspring. *Archives of Medical Research*. 2017;48:35–45.

4.   Jimenez-Chillaron JC, Hernandez-Valencia M, Lightner A, et al. Reductions in
caloric intake and early postnatal growth prevent glucose intolerance and obesity
associated with low birthweight. *Diabetologia*. 2006;49:1974–84.

5.   Veening MA, Weissenbruch V, M M, Waal D de, A H. Glucose Tolerance,
Insulin Sensitivity, and Insulin Secretion in Children Born Small for Gestational
Age. *J Clin Endocrinol Metab*. 2002;87:4657–61.

6.   Raz T, Avni R, Addadi Y, et al. The hemodynamic basis for positional- and inter-
fetal dependent effects in dual arterial supply of mouse pregnancies. *PLoS ONE*.
2012;7:e52273.

7.   Yousef AA, Behiry EG, Allah WMA, et al. IRS-1 genetic polymorphism
(r.2963G>A) in type 2 diabetes mellitus patients associated with insulin
resistance. *Appl Clin Genet*. 2018;11:99–106.

8.   Fengler VHI, Macheiner T, Kessler SM, et al. Susceptibility of Different Mouse
Wild Type Strains to Develop Diet-Induced NAFLD/AFLD-Associated Liver
Disease. *PLOS ONE*. 2016;11:e0155163.

9.   Mathews CE, Bagley R, Leiter EH. ALS/Lt: a new type 2 diabetes mouse model associated with low free radical scavenging potential. *Diabetes*. 2004;53 Suppl 1:S125-129.

10.   Liu X, Qi Y, Tian B, et al. Maternal protein restriction induces alterations in hepatic tumor necrosis factor-α/CYP7A1 signaling and disorders regulation of cholesterol metabolism in the adult rat offspring. *J Clin Biochem Nutr*. 2014;55:40–7.

11.   Man J, Hutchinson JC, Ashworth M, Jeffrey I, Heazell AE, Sebire NJ. Organ weights and ratios for postmortem identification of fetal growth restriction: utility and confounding factors. *Ultrasound Obstet Gynecol*. 2016;48:585–90.

12.   Nowacka-Woszuk J, Szczerbal I, Malinowska AM, Chmurzynska A. Transgenerational effects of prenatal restricted diet on gene expression and histone modifications in the rat. *PLoS ONE*. 2018;13:e0193464.

13.   Mericq V, Ong KK, Bazaes R, et al. Longitudinal changes in insulin sensitivity and secretion from birth to age three years in small- and appropriate-for-gestational-age children. *Diabetologia*. 2005;48:2609–14.

14.   Limesand SW, Rozance PJ, Smith D, Hay WW. Increased insulin sensitivity and maintenance of glucose utilization rates in fetal sheep with placental insufficiency and intrauterine growth restriction. *Am J Physiol Endocrinol Metab*. 2007;293:E1716-1725.

15.   Camacho LE, Chen X, Hay WW, Limesand SW. Enhanced insulin secretion and insulin sensitivity in young lambs with placental insufficiency-induced intrauterine growth restriction. *Am J Physiol Regul Integr Comp Physiol*. 2017;313:R101–9.

16.   Sebastiani G, García-Beltran C, Pie S, et al. The sequence of prenatal growth restraint and postnatal catch-up growth: normal heart but thicker intima-media and more pre-peritoneal fat in late infancy. *Pediatr Obes*. 2018;

17. Lee JJ, Pedley A, Hoffmann U, Massaro JM, Levy D, Long MT. Visceral and Intrahepatic Fat Are Associated with Cardiometabolic Risk Factors Above Other Ectopic Fat Depots: The Framingham Heart Study. *Am J Med*. 2018;131:684-692.e12.

18. Sylvetsky AC, Edelstein SL, Walford G, et al. A High-Carbohydrate, High-Fiber, Low-Fat Diet Results in Weight Loss among Adults at High Risk of Type 2 *Diabetes*. *J Nutr*. 2017;147:2060–6.

19. Can B, Can B. Change in Overweight from Childhood to Early Adulthood and Risk of Type 2 Diabetes. *N Engl J Med*. 2018;378:2537.

20. Bieswal F, Ahn M-T, Reusens B, et al. The Importance of Catch-up Growth after Early Malnutrition for the Programming of Obesity in Male Rat. *Obesity*. 2006;14:1330–43.

21. Delghingaro-Augusto V, Madad L, Chandra A, Simeonovic CJ, Dahlstrom JE, Nolan CJ. Islet Inflammation, Hemosiderosis, and Fibrosis in Intrauterine Growth-Restricted and High Fat-Fed Sprague-Dawley Rats. *Am J Pathol*. 2014;184:1446–57.

22. Bellinger L, Lilley C, Langley-Evans SC. Prenatal exposure to a maternal low-protein diet programmes a preference for high-fat foods in the young adult rat. *Br J Nutr*. 2004;92:513–20.

23. Dillies M-A, Rau A, Aubert J, et al. A comprehensive evaluation of normalization methods for Illumina high-throughput RNA sequencing data analysis. *Brief Bioinformatics*. 2013;14:671–83.

24. Quinn TP, Crowley TM, Richardson MF. Benchmarking differential expression analysis tools for RNA-Seq: normalization-based vs. log-ratio transformation-based methods. *BMC Bioinformatics*. 2018;19:274.

25. Fernandes AD, Reid JN, Macklaim JM, McMurrough TA, Edgell DR, Gloor GB. Unifying the analysis of high-throughput sequencing datasets: characterizing RNA-seq, 16S rRNA gene sequencing and selective growth experiments by compositional data analysis. *Microbiome*. 2014;2:15.

26. Love MI, Huber W, Anders S. Moderated estimation of fold change and dispersion for RNA-seq data with DESeq2. *Genome Biol*. 2014;15:550.

27. Robinson MD, McCarthy DJ, Smyth GK. edgeR: a Bioconductor package for differential expression analysis of digital gene expression data. *Bioinformatics*. 2010;26:139–40.

28. Fernandes AD, Macklaim JM, Linn TG, Reid G, Gloor GB. ANOVA-like differential expression (ALDEx) analysis for mixed population RNA-Seq. *PLoS ONE*. 2013;8:e67019.

29. Gonzalez PN, Gasperowicz M, Barbeito-Andrés J, Klenin N, Cross JC, Hallgrímsson B. Chronic Protein Restriction in Mice Impacts Placental Function and Maternal Body Weight before Fetal Growth. *PLOS ONE*. 2016;11:e0152227.

30. Elias AA, Maki Y, Matushewski B, Nygard K, Regnault TRH, Richardson BS. Maternal nutrient restriction in guinea pigs leads to fetal growth restriction with evidence for chronic hypoxia. *Pediatric Research*. 2017;82:141–7.

31. Cahill LS, Rennie MY, Hoggarth J, et al. Feto- and utero-placental vascular adaptations to chronic maternal hypoxia in the mouse. *J Physiol (Lond)*. 2018;596:3285–97.

32. López-Tello J, Barbero A, González-Bulnes A, et al. Characterization of early changes in fetoplacental hemodynamics in a diet-induced rabbit model of IUGR. *J Dev Orig Health Dis*. 2015;6:454–61.

33. Allison BJ, Brain KL, Niu Y, et al. Fetal in vivo continuous cardiovascular function during chronic hypoxia. *J Physiol (Lond)*. 2016;594:1247–64.

34.   Kessler J, Rasmussen S, Godfrey K, Hanson M, Kiserud T. Fetal growth restriction is associated with prioritization of umbilical blood flow to the left hepatic lobe at the expense of the right lobe. *Pediatr Res*. 2009;66:113–7.

35.   Kwon SJ, Lee YJ. Effect of low glutamine/glucose on hypoxia-induced elevation of hypoxia-inducible factor-1alpha in human pancreatic cancer MiaPaCa-2 and human prostatic cancer DU-145 cells. *Clin Cancer Res*. 2005;11:4694–700.

36.   Nishimoto A, Kugimiya N, Hosoyama T, Enoki T, Li T-S, Hamano K. HIF-1α activation under glucose deprivation plays a central role in the acquisition of anti-apoptosis in human colon cancer cells. *Int J Oncol*. 2014;44:2077–84.

37.   Guimarães-Camboa N, Stowe J, Aneas I, et al. HIF1α Represses Cell Stress Pathways to Allow Proliferation of Hypoxic Fetal Cardiomyocytes. *Dev Cell*. 2015;33:507–21.

38.   Slemc L, Kunej T. Transcription factor HIF1A: downstream targets, associated pathways, polymorphic hypoxia response element (HRE) sites, and initiative for standardization of reporting in scientific literature. *Tumour Biol*. 2016;37:14851–61.

39.   Holmquist-Mengelbier L, Fredlund E, Löfstedt T, et al. Recruitment of HIF-1alpha and HIF-2alpha to common target genes is differentially regulated in neuroblastoma: HIF-2alpha promotes an aggressive phenotype. *Cancer Cell*. 2006;10:413–23.

40.   Serocki M, Bartoszewska S, Janaszak-Jasiecka A, Ochocka RJ, Collawn JF, Bartoszewski R. miRNAs regulate the HIF switch during hypoxia: a novel therapeutic target. *Angiogenesis*. 2018;21:183–202.

41.   Rankin EB, Rha J, Selak MA, et al. Hypoxia-inducible factor 2 regulates hepatic lipid metabolism. *Mol Cell Biol*. 2009;29:4527–38.

42. Downes NL, Laham-Karam N, Kaikkonen MU, Ylä-Herttuala S. Differential but Complementary HIF1α and HIF2α Transcriptional Regulation. *Mol Ther*. 2018;26:1735–45.

43. Calvo MN, Bartrons R, Castaño E, Perales JC, Navarro-Sabaté A, Manzano A. PFKFB3 gene silencing decreases glycolysis, induces cell-cycle delay and inhibits anchorage-independent growth in HeLa cells. *FEBS Lett*. 2006;580:3308–14.

44. Antunica-Noguerol M, Budziñski ML, Druker J, et al. The activity of the glucocorticoid receptor is regulated by SUMO conjugation to FKBP51. *Cell Death Differ*. 2016;23:1579–91.

45. Luo K, Li Y, Yin Y, et al. USP49 negatively regulates tumorigenesis and chemoresistance through FKBP51-AKT signaling. *EMBO J* 2017;36:1434–46.

46. Eisen HJ, Goldfine ID, Glinsmann WH. Regulation of hepatic glycogen synthesis during fetal development: roles of hydrocortisone, insulin, and insulin receptors. *Proc Natl Acad Sci USA*. 1973;70:3454–7.

47. Sadava D, Frykman P, Harris E, Majerus D, Mustard J, Bernard B. Development of enzymes of glycolysis and gluconeogenesis in human fetal liver. *Biol Neonate*. 1992;62:89–95.

48. Gassen NC, Fries GR, Zannas AS, et al. Chaperoning epigenetics: FKBP51 decreases the activity of DNMT1 and mediates epigenetic effects of the antidepressant paroxetine. *Sci Signal*. 2015;8:ra119.

49. Krieg AJ, Rankin EB, Chan D, Razorenova O, Fernandez S, Giaccia AJ. Regulation of the histone demethylase JMJD1A by hypoxia-inducible factor 1 alpha enhances hypoxic gene expression and tumor growth. *Mol Cell Biol*. 2010;30:344–53.

50. Zhang P, Yao Q, Lu L, Li Y, Chen P-J, Duan C. Hypoxia-inducible factor 3 is an oxygen-dependent transcription activator and regulates a distinct transcriptional response to hypoxia. *Cell Rep*. 2014;6:1110–21.

51. Ravenna L, Salvatori L, Russo MA. HIF3α: the little we know. *FEBS J*. 2016;283:993–1003.

52. Freije WA, Thamotharan S, Lee R, Shin B-C, Devaskar SU. The hepatic transcriptome of young suckling and aging intrauterine growth restricted male rats. *J Cell Biochem*. 2015;116:566–79.

53. Robinson CM, Lefebvre F, Poon BP, et al. Consequences of VHL Loss on Global DNA Methylome. *Sci Rep*. 2018;8:3313. DOI: 10.1038/s41598-018-21524-5.

54. Tarry-Adkins JL, Fernandez-Twinn DS, Chen JH, et al. Poor maternal nutrition and accelerated postnatal growth induces an accelerated aging phenotype and oxidative stress in skeletal muscle of male rats. *Dis Model Mech*. 2016;9:1221–9.

55. Soderborg TK, Clark SE, Mulligan CE, et al. The gut microbiota in infants of obese mothers increases inflammation and susceptibility to NAFLD. *Nat Commun*. 2018;9:4462.

56. Souza AP de, Pedroso AP, Watanabe RLH, et al. Gender-specific effects of intrauterine growth restriction on the adipose tissue of adult rats: a proteomic approach. *Proteome Science*. 2015;13:32.

57. Leshner AI, Litwin VA, Squibb RL. A simple method for carcass analysis. *Physiol Behav*. 1972;9:281–2.

58. Luu YK, Lublinsky S, Ozcivici E, et al. In vivo quantification of subcutaneous and visceral adiposity by micro-computed tomography in a small animal model. *Med Eng Phys*. 2009;31:34–41.

59. Beaucage KL, Pollmann SI, Sims SM, Dixon SJ, Holdsworth DW. Quantitative in vivo micro-computed tomography for assessment of age-dependent changes in murine whole-body composition. *Bone Rep*. 2016;5:70–80.

60. Ducluzeau PH, Perretti N, Laville M, et al. Regulation by insulin of gene expression in human skeletal muscle and adipose tissue. Evidence for specific defects in type 2 diabetes. *Diabetes*. 2001;50:1134–42.

61. Choi HJ, Yun HS, Kang HJ, et al. Human transcriptome analysis of acute responses to glucose ingestion reveals the role of leukocytes in hyperglycemia-induced inflammation. *Physiol Genomics*. 2012;44:1179–87.

62. White RB, Biérinx A-S, Gnocchi VF, Zammit PS. Dynamics of muscle fibre growth during postnatal mouse development. *BMC Dev Biol*. 2010;10:21.

63. Holtrup B, Church CD, Berry R, et al. Puberty is an important developmental period for the establishment of adipose tissue mass and metabolic homeostasis. *Adipocyte*. 2017;6:224–33.

64. Abuzgaia AM, Hardy DB, Arany E. Regulation of postnatal pancreatic Pdx1 and downstream target genes after gestational exposure to protein restriction in rats. Reproduction 2015;149:293–303.

65. Ayabe H, Anada T, Kamoya T, et al. Optimal Hypoxia Regulates Human iPSC-Derived Liver Bud Differentiation through Intercellular TGFB Signaling. *Stem Cell Reports*. 2018;11:306–16.

66. Schneider H, Adebakin S, Themis M, et al. Therapeutic plasma concentrations of human factor IX in mice after gene delivery into the amniotic cavity: a model for the prenatal treatment of haemophilia B. *J Gene Med*. 1999;1:424–32.

67. Giering JC, Grimm D, Storm TA, Kay MA. Expression of shRNA from a tissue-specific pol II promoter is an effective and safe RNAi therapeutic. *Mol Ther*. 2008;16:1630–6.

68.	Rosella LC, Lebenbaum M, Fitzpatrick T, et al. Impact of diabetes on healthcare costs in a population-based cohort: a cost analysis. *Diabet Med*. 2016;33:395-403.

Appendix 1

Chapter 2 Supplementary Figures
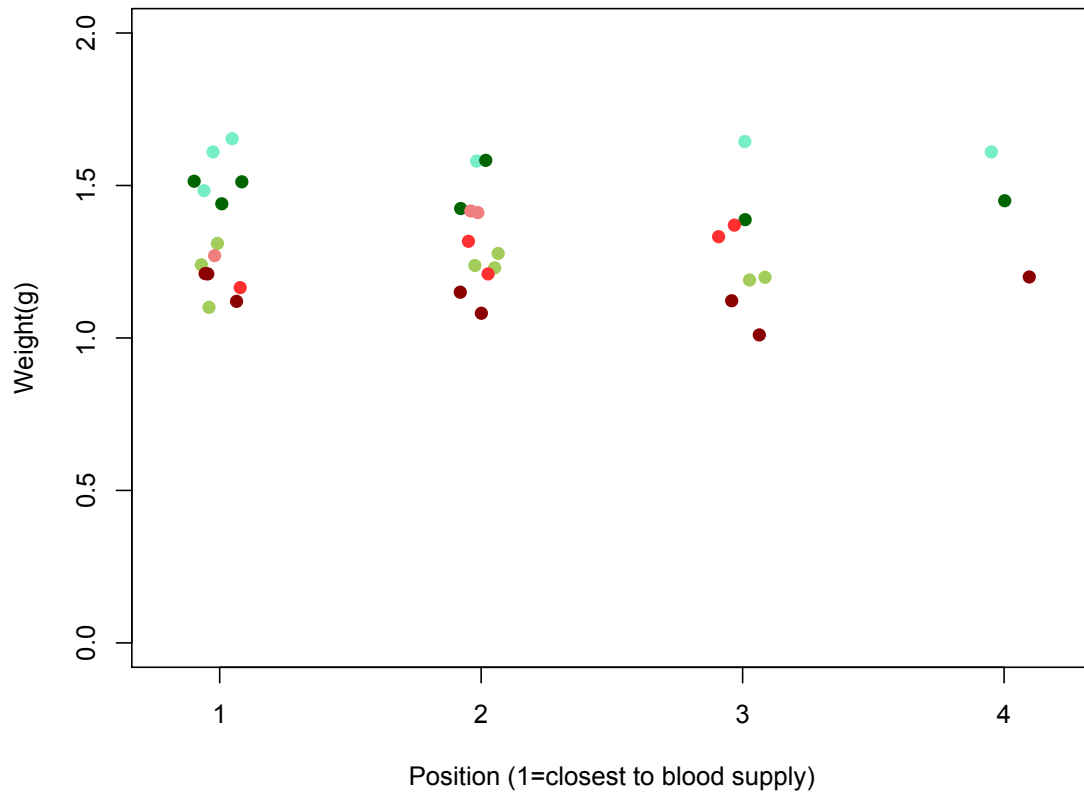
Supplementary Figure S2.3.1. Fetal weight relative to distance from the uterine blood supply. Pups at position 1 are closest to the ovaries or cervix in the uterine horn. Control (green) and MNR (red) litters are represented by different shades. Weight did not significantly differ between according to position ($p = 0.4$).
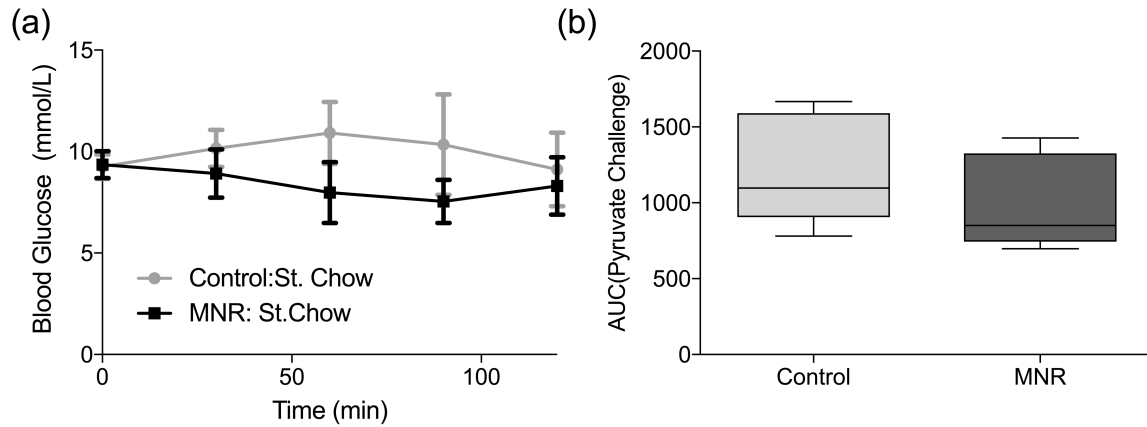
Supplementary Figure S2.3.2 Pyruvate challenge tests in male MNR and control offspring at 6 month of age. (*a*) There were no significant differences in blood glucose from 0 to 120 min (*p* = 0.4). (*b*) Similar total AUC between control and MNR indicate no differences in hepatic glucose output (*p* = 0.3). Control N=5, MNR N=5 (1 pup/litter). Data are mean ± SEM (*a*). Asterisk represents a *p* < 0.05 with a repeated measures ANOVA (*a*) or unpaired *t*-test (b).

Supplementary Table 2.2.1. Litter sizes and sex ratios for litters included in pre- and postnatal studies.

Study Type	Maternal Nutrition	Fraction of Males	Litter Size
Fetal	Control	0.42	14
	Control	0.57	14
	Control	0.62	13
	Average	0.54 +/- 0.06	13.7 +/- 0.3
	MNR	0.57	14
	MNR	0.5	12
	MNR	0.27	11
	Average	0.45 +/- 0.09	12.33 +/- 0.8
Postnatal	Control	0.46	15
	Control	0.67	12
	Control	0.79	14
	Control	0.54	13
	Control	0.54	13
	Average	0.6 +/-0.06	13.4 +/- 0.5
	MNR	0.55	11
	MNR	0.45	11
	MNR	0.38	13
	MNR	0.46	13
	MNR	0.69	13
	MNR	0.62	13
	MNR	0.5	12
	MNR	0.3	13
	MNR	0.38	13
	MNR	0.75	12
	Average	0.51 +/- 0.46	12.4 +/- 0.3

Note: No significant differences between control and MNR were observed with an unpaired *t*-test. Mean is expressed as +/- SEM.

Appendix 2

Chapter 4 Supplementary Figures
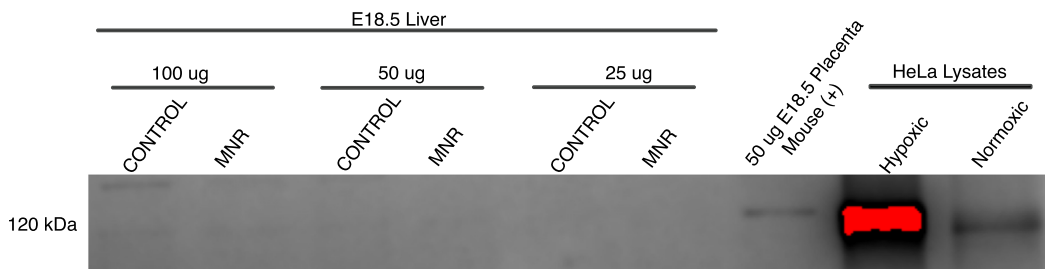
Supplementary Figure S4.3.3 HIF-1α protein in mouse fetal (E18.5) liver and placenta, and normoxic and hypoxic HeLa cells.

HIF-1α was detected in the placenta and HeLa cells but was not detected in the liver.

Supplementary Table 4.3.1 Top 50 pathways arranged by fold change (FC) of genes in distribution 2 on principle component 1 enriched in GO pathways (FDR < 0.05).

	GO pathway	FC	FDR
1	regulation of response to nutrient levels (GO:0032107)	3.59	1.93E-02
2	regulation of response to extracellular stimulus (GO:0032104)	3.59	1.92E-02
3	zymogen activation (GO:0031638)	2.59	2.77E-02
4	hippocampus development (GO:0021766)	2.29	3.29E-02
5	limbic system development (GO:0021761)	2.22	1.28E-02
6	homophilic cell adhesion via plasma membrane adhesion molecules (GO:0007156)	2.14	1.43E-02
7	cell-cell adhesion via plasma-membrane adhesion molecules (GO:0098742)	1.94	6.25E-03
8	potassium ion transmembrane transport (GO:0071805)	1.93	2.45E-02
9	cellular potassium ion transport (GO:0071804)	1.93	2.44E-02
10	positive regulation of epithelial cell proliferation (GO:0050679)	1.88	4.85E-03
11	visual perception (GO:0007601)	1.88	3.13E-02
12	sensory perception of light stimulus (GO:0050953)	1.87	3.41E-02
13	regulation of blood pressure (GO:0008217)	1.73	3.39E-02
14	second-messenger-mediated signaling (GO:0019932)	1.63	1.70E-02
15	regulation of epithelial cell proliferation (GO:0050678)	1.62	6.38E-03
16	regulation of anatomical structure size (GO:0090066)	1.58	3.58E-04
17	positive regulation of response to external stimulus (GO:0032103)	1.57	4.93E-02
18	positive regulation of cellular component biogenesis (GO:0044089)	1.56	1.40E-03
19	inorganic cation transmembrane transport (GO:0098662)	1.55	1.24E-02
20	response to growth factor (GO:0070848)	1.55	1.21E-02
21	cellular response to growth factor stimulus (GO:0071363)	1.53	2.13E-02
22	cell-cell adhesion (GO:0098609)	1.53	2.83E-02
23	cation transmembrane transport (GO:0098655)	1.53	1.22E-02
24	axon development (GO:0061564)	1.53	3.97E-02
25	regulation of cellular component size (GO:0032535)	1.53	1.97E-02
26	inorganic ion transmembrane transport (GO:0098660)	1.53	1.20E-02
27	forebrain development (GO:0030900)	1.52	3.26E-02
28	metal ion transport (GO:0030001)	1.52	3.57E-03
29	negative regulation of cell development (GO:0010721)	1.51	3.95E-02
30	regulation of ion transmembrane transport (GO:0034765)	1.5	1.33E-02
31	positive regulation of nervous system development (GO:0051962)	1.5	1.79E-03
32	regulation of ion transport (GO:0043269)	1.49	5.61E-04
33	positive regulation of neuron differentiation (GO:0045666)	1.49	2.09E-02
34	regulation of metal ion transport (GO:0010959)	1.48	4.88E-02
35	regulation of neuron differentiation (GO:0045664)	1.46	9.11E-04
36	positive regulation of cell proliferation (GO:0008284)	1.46	6.76E-05
37	muscle structure development (GO:0061061)	1.46	2.83E-02
38	positive regulation of MAPK cascade (GO:0043410)	1.46	1.49E-02
39	regulation of nervous system development (GO:0051960)	1.46	4.91E-05
40	calcium ion homeostasis (GO:0055074)	1.45	4.34E-02
41	negative regulation of cell proliferation (GO:0008285)	1.44	4.43E-03
42	regulation of cellular component biogenesis (GO:0044087)	1.44	3.31E-04
43	negative regulation of cell differentiation (GO:0045596)	1.44	2.67E-03
44	divalent inorganic cation homeostasis (GO:0072507)	1.44	4.91E-02
45	regulation of cell cycle process (GO:0010564)	1.44	1.46E-02
46	regulation of cell cycle (GO:0051726)	1.43	3.07E-04
47	cell proliferation (GO:0008283)	1.43	1.65E-02
48	regulation of MAPK cascade (GO:0043408)	1.43	3.32E-03
49	regulation of cell proliferation (GO:0042127)	1.43	1.39E-07
50	positive regulation of secretion (GO:0051047)	1.43	3.87E-02

Supplementary Table 4.3.2 Counts and cluster membership per sample (k-means clustering, K=2)

Condition	Cluster	Counts
MNR	2	74305030
Control	2	75865086
Control	2	80360976
MNR	2	80920037
Control	2	81553460
MNR	2	83508564
Control	2	83775128
MNR	2	84106928
MNR	2	84462329
MNR	2	85525474
Control	2	86281726
MNR	2	87068555
Control	1	92585570
MNR	1	98375605
Control	1	99626219
Control	1	105476459
MNR	1	105755590

Supplementary Table 4.3.3 49 protein-coding genes differentially expressed in MNR E18.5 liver relative to controls (FDR < 0.1 in 2 or more tools).

	Gene Symbol	Gene Name	DESeq2		EdgeR		Aldex2	
			FC	FDR	FC	FDR	FC	FDR
1	Lin28a	lin-28 homolog A (C. elegans)	-1.92	0.00	-6.03	0.00	NA	NA
2	Rnf169	ring finger protein 169	-1.78	0.00	-9.51	0.00	NA	NA
3	Chrna4	cholinergic receptor, nicotinic, alpha polypeptide 4	-1.61	0.00	-2.28	0.01	NA	NA
4	Angptl4	angiopoietin-like 4	-1.59	0.00	-2.49	0.01	NA	NA
5	Cited2	Cbp/p300-interacting transactivator, with Glu/Asp-rich carboxy-terminal domain, 2	-1.52	0.00	-1.74	0.03	NA	NA
6	Ppargc1b	peroxisome proliferative activated receptor, gamma, coactivator 1 beta	-1.50	0.02	-2.47	0.07	NA	NA
7	Echdc1	enoyl Coenzyme A hydratase domain containing 1	-1.46	0.00	-1.49	0.00	NA	NA
8	Kbtbd8	kelch repeat and BTB (POZ) domain containing 8	-1.37	0.01	-1.45	0.07	NA	NA
9	Atp2b2	ATPase, Ca++ transporting, plasma membrane 2	-1.31	0.00	-1.36	0.01	NA	NA
10	Cars	cysteinyl-tRNA synthetase	-1.29	0.03	-1.34	0.08	NA	NA
11	Wisp2	WNT1 inducible signalling pathway protein 2	-1.28	0.03	-1353.64	0.00	NA	NA
12	Mll1	myeloid/lymphoid or mixed-lineage leukemia 1	1.15	0.00	1.15	0.10	NA	NA
13	Ppp1r15a	protein phosphatase 1, regulatory (inhibitor) subunit 15A	1.17	0.06	1.18	0.09	NA	NA
14	Capn10	calpain 10	1.19	0.00	1.19	0.08	NA	NA
15	Man2b2	mannosidase 2, alpha B2	1.19	0.00	1.19	0.08	NA	NA
16	Syne1	synaptic nuclear envelope 1	1.19	0.00	1.20	0.00	NA	NA
17	Rassf1	Ras association (RalGDS/AF-6) domain family member 1	1.22	0.01	1.23	0.05	NA	NA
18	Coro7	coronin 7	1.22	0.00	1.22	0.08	NA	NA
19	Kdm3a	lysine (K)-specific demethylase 3A	1.22	0.00	1.23	0.08	NA	NA
20	Chd7	chromodomain helicase DNA binding protein 7	1.23	0.01	1.24	0.03	NA	NA
21	Mycbp2	MYC binding protein 2	1.23	0.00	1.23	0.00	NA	NA
22	Crls1	cardiolipin synthase 1	1.23	0.00	1.24	0.08	NA	NA
23	Cep170	centrosomal protein 170	1.26	0.00	1.27	0.06	NA	NA

24	Maff	v-maf musculoaponeurotic fibrosarcoma oncogene family, protein F (avian)	1.26	0.02	1.28	0.10	NA	NA
25	Stard5	StAR-related lipid transfer (START) domain containing 5	1.28	0.00	1.29	0.02	NA	NA
26	Rabgef1	RAB guanine nucleotide exchange factor (GEF) 1	1.28	0.00	1.29	0.00	NA	NA
27	Hif3a	hypoxia inducible factor 3, alpha subunit	1.29	0.01	1.32	0.03	NA	NA
28	Pex26	peroxisomal biogenesis factor 26	1.31	0.01	1.35	0.10	NA	NA
29	Vhl	von Hippel-Lindau tumor suppressor	1.32	0.03	1.39	0.10	NA	NA
30	Inpp4a	inositol polyphosphate-4-phosphatase, type I	1.33	0.00	1.36	0.00	NA	NA
31	Lpin1	lipin 1	1.35	0.02	1.44	0.09	NA	NA
32	Kif21a	kinesin family member 21A	1.36	0.00	1.40	0.02	NA	NA
33	Hpca	hippocalcin	1.37	0.01	1.44	0.03	NA	NA
34	Fam126b	family with sequence similarity 126, member B	1.37	0.01	1.46	0.04	NA	NA
35	Nlrp12	NLR family, pyrin domain containing 12	1.40	0.00	1.50	0.03	NA	NA
36	Sra1	steroid receptor RNA activator 1	1.42	0.00	1.52	0.02	NA	NA
37	Cd80	CD80 antigen	1.45	0.02	1.69	0.08	NA	NA
38	Gata4	GATA binding protein 4	1.45	0.01	1.63	0.03	NA	NA
39	Jmy	junction-mediating and regulatory protein	1.47	0.00	1.52	0.00	NA	NA
40	Trpv4	transient receptor potential cation channel, subfamily V, member 4	1.48	0.01	1.70	0.03	NA	NA
41	Ccng2	cyclin G2	1.50	0.00	1.62	0.00	NA	NA
42	Cobll1	Cobl-like 1	1.51	0.00	1.57	0.00	NA	NA
43	Pfkfb3	6-phosphofructo-2-kinase/fructose-2,6-biphosphatase 3	1.53	0.00	1.61	0.00	NA	NA
44	Tiparp	TCDD-inducible poly(ADP-ribose) polymerase	1.53	0.00	1.71	0.01	NA	NA
45	Fkbp5	FK506 binding protein 5	1.56	0.00	1.82	0.01	NA	NA
46	Josd1	Josephin domain containing 1	1.64	0.00	NA	NA	2.03	0.10
47	Btg2	B cell translocation gene 2, anti-proliferative	1.64	0.00	NA	NA	2.16	0.06
48	Tubb2a	tubulin, beta 2A class IIA	1.69	0.00	2.35	0.01	NA	NA
49	Fbxo31	F-box protein 31	1.75	0.00	NA	NA	1.98	0.08

Note: Fold change (FC) discussed was taken from the DESeq2 analysis which was the most conservative. False discovery rate (FDR) was calculated with a Benjamini-Hochberg correction.

Supplementary Table 4.3.4 Function of hypoxia-inducible genes differentially expressed in MNR offspring.

| Gene Symbol	Role in HIF signalling	Functions	References
Vhl	Negative regulator of Hif-1a and Hif-2a	U3 ubiquitin ligase complex	(1)
Mll1	Transcriptional co-activator at HRE-containing genes	H3K4 Histone demethyltransferase	(2)
Chrna4	Neuronal acetylcholine receptors promote accumulation and stability of Hif-1a	Nicotine receptor	(3)
Rassf1	Upregulated with hypoxia and HIF1/2a expression	Tumor suppressor	(4,5)
Jmy	Hypoxia-induced HRE-containing gene	Actin polymerization	(6)
Nrp12	Transcriptionally downregulated by HIF-1a	Receptor, ligands include VEGF	(7)
CD80	Reduction on myeloid cells in response to hypoxia	Stimulates T-cell innate immunity	(8)
Ccng2	Hypoxia-induced HRE-containing gene	Negative cell cycle regulation/regulation of the cytoskeleton	(9,10)
Maff	Hypoxia-induced HRE-containing gene	Transcriptional regulator	(5,11)
Angptl4	Hypoxia-induced HRE-containing gene	Secreted protein involved in angiogenesis and is a negative regulator of lipoprotein lipase	(12–14)
Btg2	Hypoxia-induced Hif-1a dependent transcription	Negative cell cycle regulation	(15)
Fkbp5	Hypoxia-induced gene potentially via HIF-2a inhibition of AR, and as a KDM3a target	Co-chaperon and scaffold protein	(5,16,17)
Pfkfb3	Hypoxia-induced HRE-containing gene	Phosphatase and diphosphatase to fructose-2,6-bisphosphotate	(5,18)
Kdm3a	Hypoxia-induced HRE-containing gene and is recruited to promoters of HRE-containing genes	H3K9 histone demethylase	(5,14)
Hif-3a	Induced by HIF-1a and a negative regulator of HIF-induced transcription	Transcriptional regulator	(19,20)
Ppp1r15a	Hypoxia-induced HRE-containing gene	Unfolded protein response reducing protein synthesis	(5,21)
Cited2	Prevents CBP/P300 binding inhibiting HIF-1a transactivation	Transcriptional regulator	(22)

Appendix 2 References

1.   Wang J, Lu Z, Xu Z, et al. Reduction of hepatic fibrosis by overexpression of von Hippel–Lindau protein in experimental models of chronic liver disease. Scientific Reports 2017;7:41038.

2.   Bhan A, Deb P, Shihabeddin N, Ansari KI, Brotto M, Mandal SS. Histone methylase MLL1 coordinates with HIF and regulate lncRNA HOTAIR expression under hypoxia. Gene 2017;629:16–28.

3.   Singh SP, Chand HS, Gundavarapu S, et al. HIF-1α Plays a Critical Role in the Gestational Sidestream Smoke-Induced Bronchopulmonary Dysplasia in Mice. PLoS ONE 2015;10:e0137757.

4.   Wang V, Davis DA, Haque M, Huang LE, Yarchoan R. Differential gene up-regulation by hypoxia-inducible factor-1alpha and hypoxia-inducible factor-2alpha in HEK293T cells. Cancer Res 2005;65:3299–306.

5.   Krieg AJ, Rankin EB, Chan D, Razorenova O, Fernandez S, Giaccia AJ. Regulation of the histone demethylase JMJD1A by hypoxia-inducible factor 1 alpha enhances hypoxic gene expression and tumor growth. Mol Cell Biol 2010;30:344–53.

6.   Coutts AS, Pires IM, Weston L, et al. Hypoxia-driven cell motility reflects the interplay between JMY and HIF-1α. Oncogene 2011;30:4835–42.

7.   Coma S, Shimizu A, Klagsbrun M. Hypoxia induces tumor and endothelial cell migration in a semaphorin 3F- and VEGF-dependent manner via transcriptional repression of their common receptor neuropilin 2. Cell Adh Migr 2011;5:266–75.

8.   Lahat N, Rahat MA, Ballan M, Weiss-Cerem L, Engelmayer M, Bitterman H. Hypoxia reduces CD80 expression on monocytes but enhances their LPS-stimulated TNF-alpha secretion. J Leukoc Biol 2003;74:197–205.

9.   Cui DW, Cheng YJ, Jing SW, Sun GG. Effect of cyclin G2 on proliferative ability of prostate cancer PC-3 cell. Tumour Biol 2014;35:3017–24.

10.   Cui DW, Cheng YJ, Jing SW, Sun GG. Effect of cyclin G2 on proliferative ability of prostate cancer PC-3 cell. Tumor Biol 2014;35:3017–24.

11.   Ortiz-Barahona A, Villar D, Pescador N, Amigo J, del Peso L. Genome-wide identification of hypoxia-inducible factor binding sites and target genes by a probabilistic model integrating transcription-profiling data and in silico binding site prediction. Nucleic Acids Res 2010;38:2332–45.

12.   Inoue T, Kohro T, Tanaka T, et al. Cross-enhancement of ANGPTL4 transcription by HIF1 alpha and PPAR beta/delta is the result of the conformational proximity of two response elements. Genome Biol 2014;15:R63.

13.   Dijk W, Ruppert PMM, Oost LJ, Kersten S. Angiopoietin-like 4 promotes the intracellular cleavage of lipoprotein lipase by PCSK3/furin in adipocytes. J Biol Chem 2018;293:14134–45.

14.   Downes NL, Laham-Karam N, Kaikkonen MU, Ylä-Herttuala S. Differential but Complementary HIF1α and HIF2α Transcriptional Regulation. Mol Ther 2018;26:1735–45.

15.   Chung L-C, Tsui K-H, Feng T-H, Lee S-L, Chang P-L, Juang H-H. l-Mimosine blocks cell proliferation via upregulation of B-cell translocation gene 2 and N-myc downstream regulated gene 1 in prostate carcinoma cells. American Journal of Physiology-Cell Physiology 2011;302:C676–85.

16.   Xu J, Zheng L, Chen J, et al. Increasing AR by HIF-2 inhibitor (PT-2385) overcomes the side-effects of sorafenib by suppressing hepatocellular carcinoma invasion via alteration of pSTAT3, pAKT and pERK signals. Cell Death and Disease 2017;8:e3095.

17.   Zhang L, Qiu B, Wang T, et al. Loss of FKBP5 impedes adipocyte differentiation under both normoxia and hypoxic stress. Biochemical and Biophysical Research Communications 2017;485:761–7.

18.   Minchenko A, Leshchinsky I, Opentanova I, et al. Hypoxia-inducible factor-1-mediated expression of the 6-phosphofructo-2-kinase/fructose-2,6-bisphosphatase-3 (PFKFB3) gene. Its possible role in the Warburg effect. J Biol Chem 2002;277:6183–7.

19.   Tanaka T, Wiesener M, Bernhardt W, Eckardt K-U, Warnecke C. The human HIF (hypoxia-inducible factor)-3alpha gene is a HIF-1 target gene and may modulate hypoxic gene induction. Biochem J 2009;424:143–51.

20.   Ravenna L, Principessa L, Verdina A, Salvatori L, Russo MA, Petrangeli E. Distinct Phenotypes of Human Prostate Cancer Cells Associate with Different Adaptation to Hypoxia and Pro-Inflammatory Gene Expression. PLoS One [Internet] 2014 [cited 2018 Sep 11];9. Available from: https://www.ncbi.nlm.nih.gov/pmc/articles/PMC4011733/

21.   Guimarães-Camboa N, Stowe J, Aneas I, et al. HIF1α Represses Cell Stress Pathways to Allow Proliferation of Hypoxic Fetal Cardiomyocytes. Dev Cell 2015;33:507–21.

22.   Freedman SJ, Sun Z-YJ, Kung AL, France DS, Wagner G, Eck MJ. Structural basis for negative regulation of hypoxia-inducible factor-1alpha by CITED2. Nat Struct Biol 2003;10:504–12.

Appendix 3

Chapter 5 Supplementary Figures
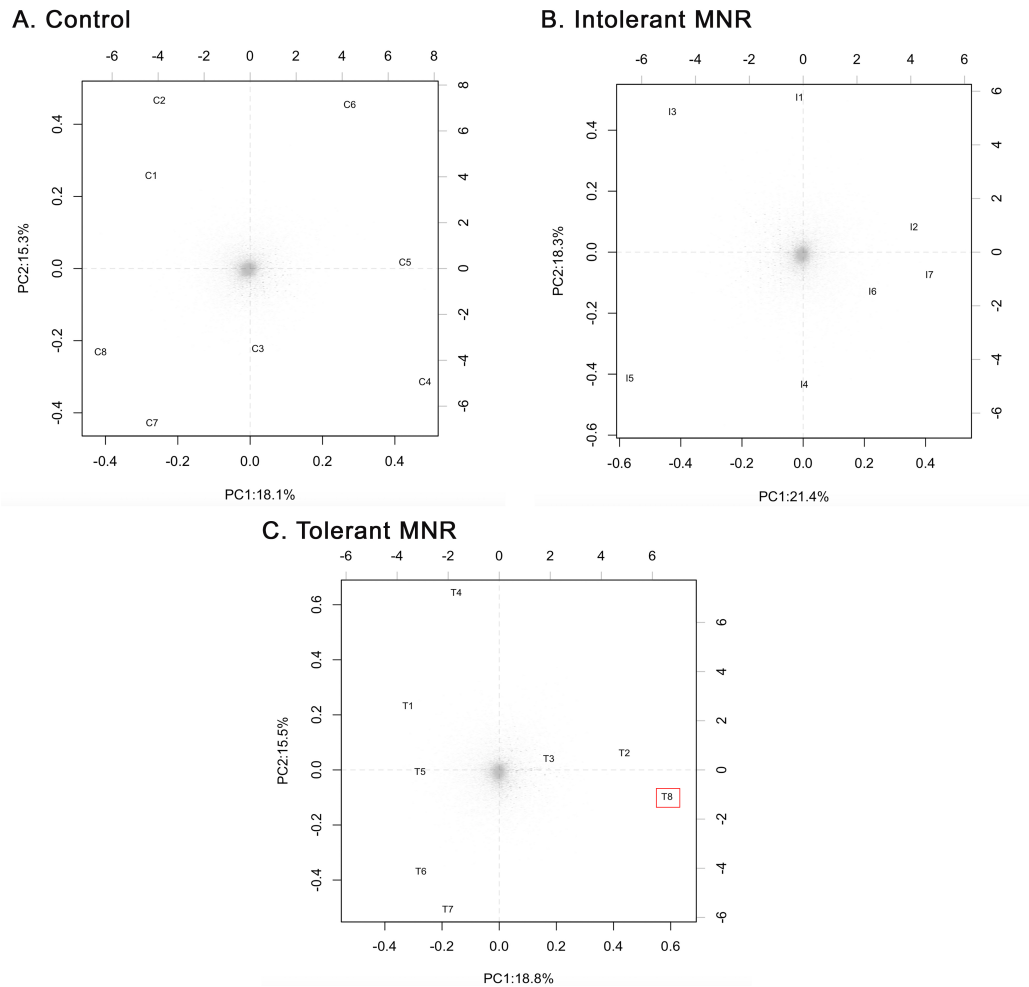
Supplementary Figure S5.2.1 Biplots of controls (A), intolerant MNR (B) and tolerant MNR (C) in liver RNA*seq* data.

One sample in the tolerant MNR (red box) contributed more variation to the group than any other samples and was removed from further analysis.
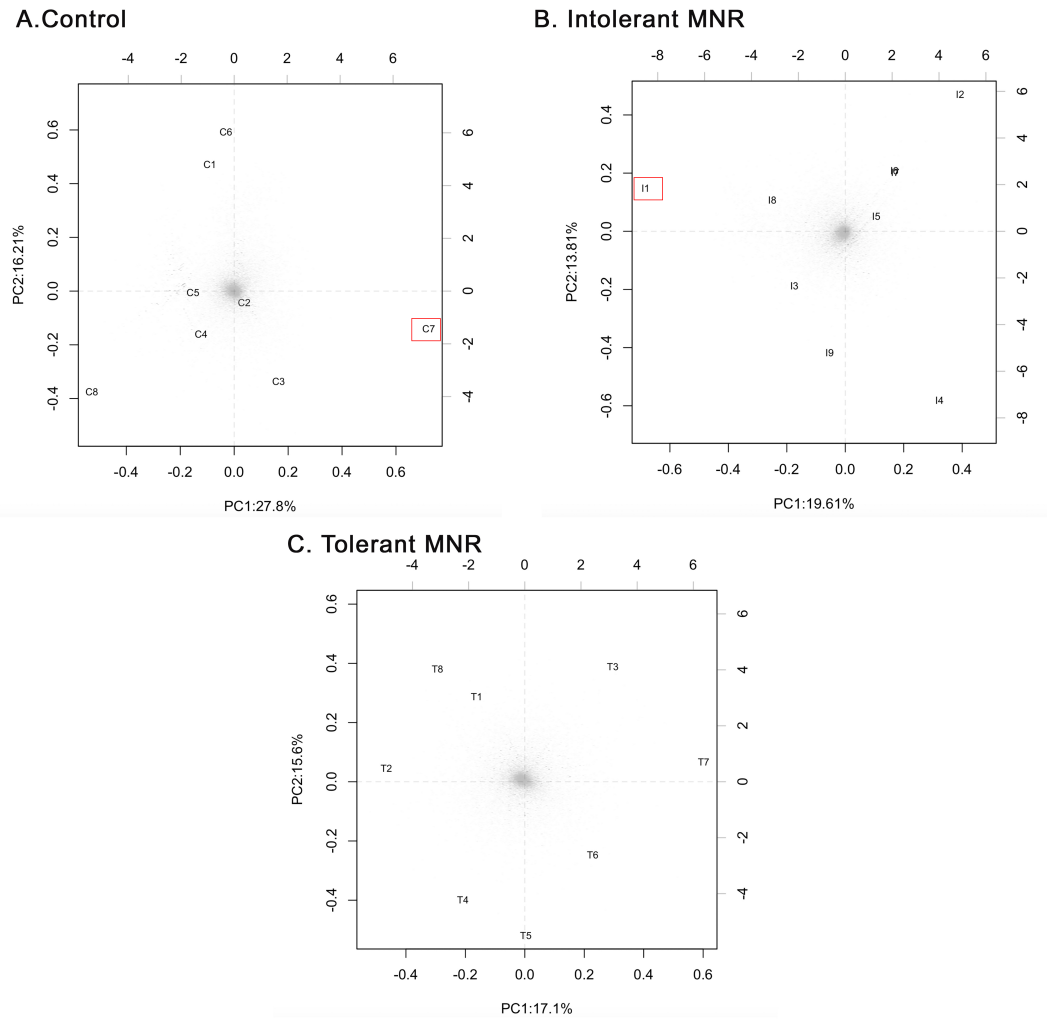
Supplementary Figure S5.2.2 Biplots of controls (A), intolerant MNR (B) and tolerant MNR (C) muscle RNA sequencing data.

One control and one intolerant MNR (red box) contributed more variation to the group than any other samples with the group. Outliers were removed from further analysis.
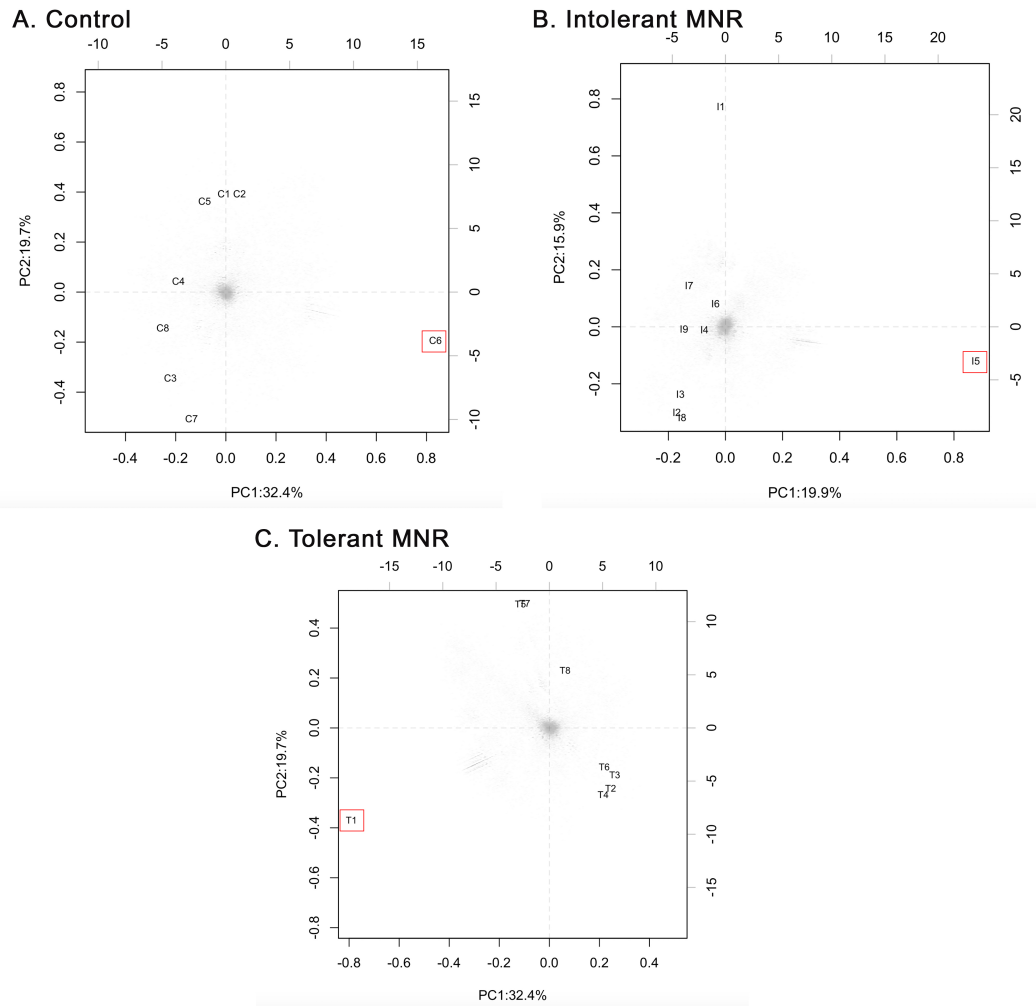
Supplementary Figure S5.2.3 Biplots of sequenced RNA from adipose tissue of controls (A), intolerant MNR (B) and tolerant MNR (C).
One sample from each group (red box) contributed more variation to the group than any other samples with the group and were removed from further analysis.
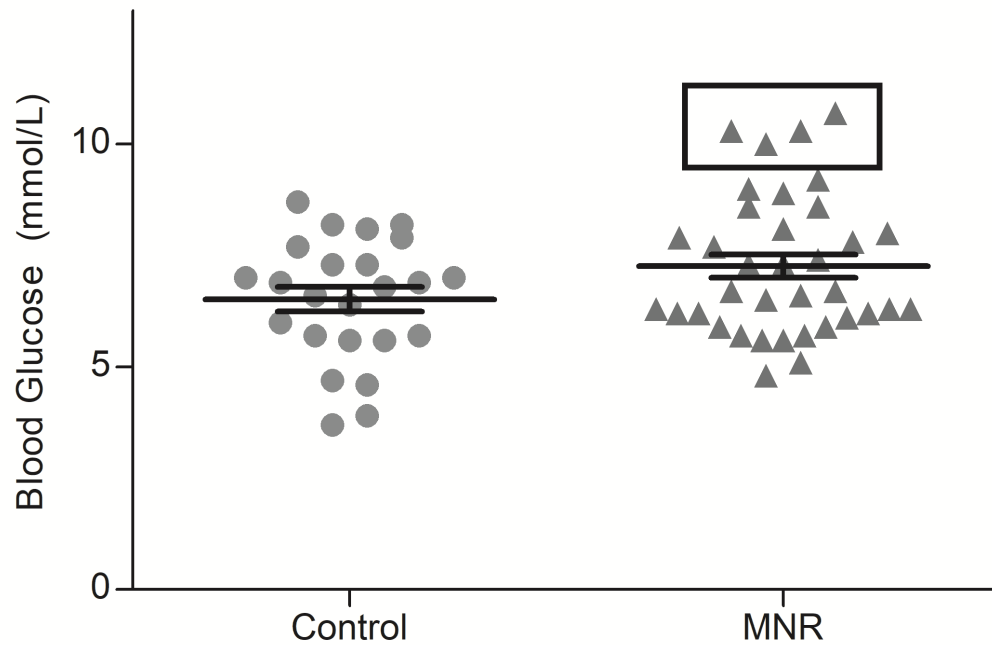
Supplementary Figure S5.2.4 Fasting blood glucose of 6-month-old control and MNR offspring.

Fasting blood glucose was similar for control (6.5 ± 0.3 mmol/L) and MNR (7.3 ± 0.3 mmol/L) offspring ($p = 0.2$), however, 4 MNR had a higher fasting blood glucose than any controls (as indicate by the box). Data are expressed as mean ± SEM and compared with a Mann-Whitney test.
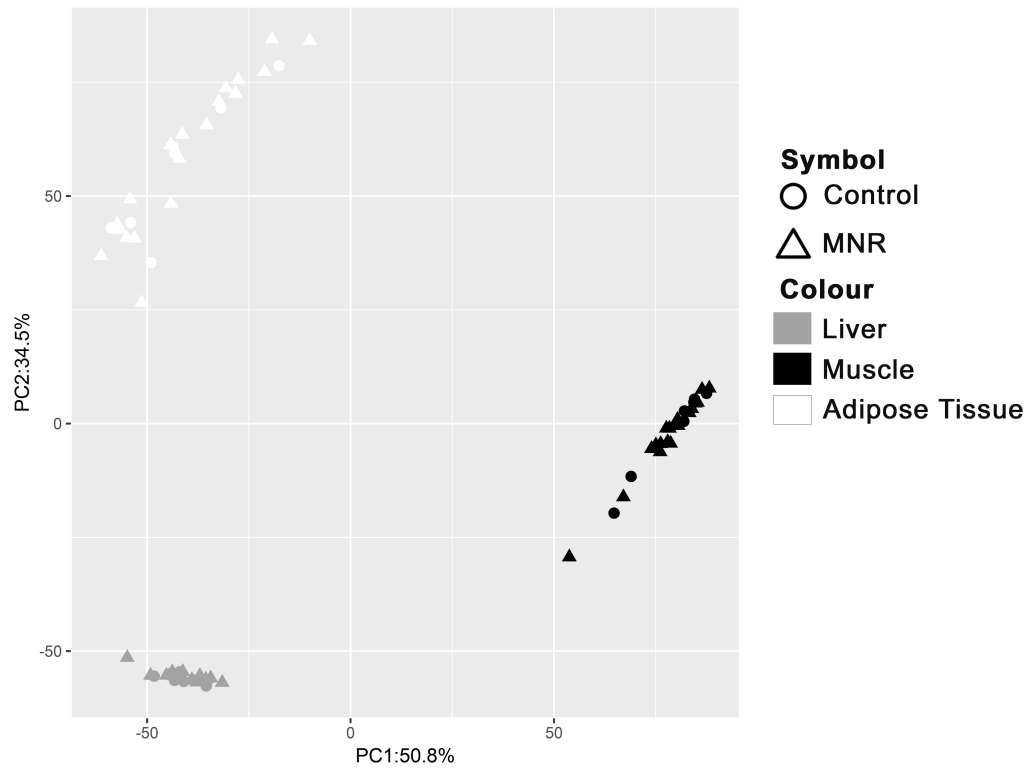
Supplementary Figure S5.3.1 PCA of top 500 variable genes in RNA*seq* data of the liver, adipose tissue, and skeletal muscle of 6-month-old MNR offspring. Samples clustered based on tissue (colour) but not maternal nutrition (symbol).

Supplementary Table 5.3.1 Differentially expressed genes (0.1 >FDR, Fold change [FC] ≥ 2, 2 or more tools) in liver, skeletal muscle and adipose tissue of 6-month-old offspring.

Tissue	Reference	Comparison Group	Gene ID	Gene Name	Ave. FC	Ave. FDR	Tools
Liver	Control	MNR	Alas1	aminolevulinic acid synthase 1 [Source:MGI Symbol;Acc:MGI:87989]	-2.69	0.045	DESeq2. EdgeR. Aldex2
			Hspa1l	heat shock protein 1-like [Source:MGI Symbol;Acc:MGI:96231]	-2.43	0.027	DESeq2. EdgeR. Aldex2
			Hspb1	heat shock protein 1 [Source:MGI Symbol;Acc:MGI:96240]	-2.14	0.085	DESeq2. EdgeR. Aldex2
			Fgf11	fibroblast growth factor 11 [Source:MGI Symbol;Acc:MGI:109167]	-2.06	0.062	DESeq2. EdgeR. Aldex2
			Rfx4	regulatory factor X, 4 (influences HLA class II expression) [Source:MGI Symbol;Acc:MGI:1918387]	2.21	0.049	DESeq2. EdgeR
			Trem2	triggering receptor expressed on myeloid cells 2 [Source:MGI Symbol;Acc:MGI:1913150]	2.22	0.004	DESeq2. EdgeR
	Control	Intolerant MNR	Hspa1a	heat shock protein 1A [Source:MGI Symbol;Acc:MGI:96244]	-3.54	0.002	DESeq2. EdgeR
			Hspa1l	heat shock protein 1-like [Source:MGI Symbol;Acc:MGI:96231]	-3.36	0.001	DESeq2. EdgeR
			Alas1	aminolevulinic acid synthase 1 [Source:MGI Symbol;Acc:MGI:87989]	-3.25	0.011	DESeq2. EdgeR
			Hspa1b	heat shock protein 1B [Source:MGI Symbol;Acc:MGI:99517]	-3.14	0.004	DESeq2. EdgeR
			Dnaic1	dynein, axonemal, intermediate chain 1 [Source:MGI Symbol;Acc:MGI:1916172]	-2.94	0.059	DESeq2. EdgeR
			Hspb1	heat shock protein 1 [Source:MGI Symbol;Acc:MGI:96240]	-2.63	0.022	DESeq2. EdgeR
			Eif4ebp3	eukaryotic translation initiation factor 4E binding protein 3 [Source:MGI Symbol;Acc:MGI:1270847]	-2.45	0.006	DESeq2. EdgeR
			Saa1	serum amyloid A 1 [Source:MGI Symbol;Acc:MGI:98221]	-2.44	0.047	DESeq2. EdgeR
			Grem2	gremlin 2 homolog, cysteine knot superfamily (Xenopus laevis) [Source:MGI Symbol;Acc:MGI:1344367]	-2.37	0.047	DESeq2. EdgeR
			Pcp4l1	Purkinje cell protein 4-like 1 [Source:MGI	-2.19	0.000	DESeq2. EdgeR

				Symbol;Acc:MGI:1913675]			
			Tbc1d30	TBC1 domain family, member 30 [Source:MGI Symbol;Acc:MGI:1921944]	-2.09	0.001	DESeq2. EdgeR
			Cyp26b1	cytochrome P450, family 26, subfamily b, polypeptide 1 [Source:MGI Symbol;Acc:MGI:2176159]	-2.07	0.056	DESeq2. EdgeR
			Fgf11	fibroblast growth factor 11 [Source:MGI Symbol;Acc:MGI:109167]	-2.04	0.089	DESeq2. EdgeR
			Ank3	ankyrin 3, epithelial [Source:MGI Symbol;Acc:MGI:88026]	2.03	0.001	DESeq2. EdgeR
			Gdf15	growth differentiation factor 15 [Source:MGI Symbol;Acc:MGI:1346047]	2.03	0.065	DESeq2. EdgeR
			Trem2	triggering receptor expressed on myeloid cells 2 [Source:MGI Symbol;Acc:MGI:1913150]	2.04	0.008	DESeq2. EdgeR
			Gngt1	guanine nucleotide binding protein (G protein), gamma transducing activity polypeptide 1 [Source:MGI Symbol;Acc:MGI:109165]	2.06	0.062	DESeq2. EdgeR
			Vldlr	very low density lipoprotein receptor [Source:MGI Symbol;Acc:MGI:98935]	2.13	0.056	DESeq2. EdgeR
			Rfx4	regulatory factor X, 4 (influences HLA class II expression) [Source:MGI Symbol;Acc:MGI:1918387]	2.20	0.012	DESeq2. EdgeR
			Raet1d	retinoic acid early transcript delta [Source:MGI Symbol;Acc:MGI:1861032]	2.38	0.050	DESeq2. EdgeR
			Pdk4	pyruvate dehydrogenase kinase, isoenzyme 4 [Source:MGI Symbol;Acc:MGI:1351481]	2.65	0.001	DESeq2. EdgeR
			Adcy1	adenylate cyclase 1 [Source:MGI Symbol;Acc:MGI:99677]	4.10	0.039	DESeq2. EdgeR
			Ntrk2	neurotrophic tyrosine kinase, receptor, type 2 [Source:MGI Symbol;Acc:MGI:97384]	4.90	0.000	DESeq2. EdgeR
			Cyp2b9	cytochrome P450, family 2, subfamily b, polypeptide 9 [Source:MGI Symbol;Acc:MGI:88600]	7.03	0.063	DESeq2. EdgeR
	Control	Impaired fasting blood glucose	ccl21c	C-C motif chemokine 21c [Source:UniProtKB/Swiss-Prot;Acc:P86793]	-6.32	0.022	DESeq2. EdgeR
			Cyp26b1	cytochrome P450, family 26, subfamily b, polypeptide 1 [Source:MGI Symbol;Acc:MGI:2176159]	-5.16	0.000	DESeq2. EdgeR
			Mfsd2a	major facilitator superfamily domain containing 2A [Source:MGI Symbol;Acc:MGI:1923824]	-4.74	0.004	DESeq2. EdgeR

			Cyp2b10	cytochrome P450, family 2, subfamily b, polypeptide 10 [Source:MGI Symbol;Acc:MGI:88598]	-2.93	0.001	DESeq2. EdgeR
			Serpina12	serine (or cysteine) peptidase inhibitor, clade A (alpha-1 antiproteinase, antitrypsin), member 12 [Source:MGI Symbol;Acc:MGI:1915304]	-2.19	0.015	DESeq2. EdgeR
			Adarb2	adenosine deaminase, RNA-specific, B2 [Source:MGI Symbol;Acc:MGI:2151118]	2.29	0.016	DESeq2. EdgeR
			Epha5	Eph receptor A5 [Source:MGI Symbol;Acc:MGI:99654]	2.62	0.065	DESeq2. EdgeR
	Tolerant MNR	Intolerant MNR	mt1	metallothionein 1	2.47	0.057	DESeq2. EdgeR
Muscle	Control	MNR	NA	NA	NA	NA	NA
	Control	Intolerant MNR	Gdpd3	glycerophosphodiester phosphodiesterase domain containing 3 [Source:MGI Symbol;Acc:MGI:1915866]	-5.78	0.071	DESeq2. EdgeR
			Il1f9	interleukin 1 family, member 9 [Source:MGI Symbol;Acc:MGI:2449929]	-3.59	0.013	DESeq2. EdgeR
			Cyp1b1	cytochrome P450, family 1, subfamily b, polypeptide 1 [Source:MGI Symbol;Acc:MGI:88590]	-2.34	0.028	DESeq2. EdgeR
	Control	Impaired fasting blood glucose	Nr4a3	nuclear receptor subfamily 4, group A, member 3 [Source:MGI Symbol;Acc:MGI:1352457]	-4.54	0.050	DESeq2. EdgeR
			Slc25a25	solute carrier family 25 (mitochondrial carrier, phosphate carrier), member 25 [Source:MGI Symbol;Acc:MGI:1915913]	-2.81	0.040	DESeq2. EdgeR
			Irs2	insulin receptor substrate 2 [Source:MGI Symbol;Acc:MGI:109334]	-2.80	0.025	DESeq2. EdgeR
			Panx1	pannexin 1 [Source:MGI Symbol;Acc:MGI:1860055]	2.08	0.014	DESeq2. EdgeR
	Tolerant MNR	Intolerant MNR	Kcna6	potassium voltage-gated channel, shaker-related, subfamily, member 6 [Source:MGI Symbol;Acc:MGI:96663]	2.31	0.061	DESeq2. EdgeR
Adipose tissue	Control	MNR	Napsa	napsin A aspartic peptidase [Source:MGI Symbol;Acc:MGI:109365]	-172.97	0.012	DESeq2. EdgeR
	Control	Intolerant MNR	Cox8a	cytochrome c oxidase, subunit VIIIa [Source:MGI Symbol;Acc:MGI:105959]	2.30	0.038	DESeq2. EdgeR
			Zcchc24	zinc finger, CCHC domain containing 24 [Source:MGI Symbol;Acc:MGI:1919168]	2.35	0.067	DESeq2. EdgeR
			Inpp5d	inositol polyphosphate-5-phosphatase D [Source:MGI Symbol;Acc:MGI:107357]	2.70	0.032	DESeq2. EdgeR
			Vwa1	von Willebrand factor A	2.84	0.079	DESeq2.

				domain containing 1 [Source:MGI Symbol;Acc:MGI:2179729]			EdgeR
			Timp4	tissue inhibitor of metalloproteinase 4 [Source:MGI Symbol;Acc:MGI:109125]	3.43	0.020	DESeq2. EdgeR
			Gcnt1	glucosaminyl (N-acetyl) transferase 1, core 2 [Source:MGI Symbol;Acc:MGI:95676]	3.56	0.052	DESeq2. EdgeR
			Xlr3b	X-linked lymphocyte-regulated 3B	-2.09	0.019	DESeq2. EdgeR
			Lrriq3	leucine-rich repeats and IQ motif containing 3	-2.02	0.032	DESeq2. EdgeR
			Napsa	napsin A aspartic peptidase [Source:MGI Symbol;Acc:MGI:109365]	1.96	0.001	DESeq2. EdgeR
			NA	NA	NA	NA	NA

Note: Fold change (FC) and false discovery rate (FDR) are expressed as an average between to the differential expression tools.

Appendix 4

Copyrights chapter 2

Dear Bethany Radford,

Radford, B., & Han, V. (n.d.). Offspring from maternal nutrient restriction in mice show variations in adult glucose metabolism similar to human fetal growth restriction. *Journal of Developmental Origins of Health and Disease,* 1-10 © Cambridge University Press and the International Society for Developmental Origins of Health and Disease 2018

Thank you for your request to reproduce the above material in your forthcoming thesis, for non-commercial publication. Cambridge University Press are pleased to grant non-exclusive permission, free of charge, for this specific one time use, on the understanding you have checked that we do not acknowledge any other source for the material. This permission does not include the use of copyright material owned by any party other than the authors. Consent to use any such material must be sought by you from the copyright owner concerned.

Please ensure full acknowledgement appears in your work.

Should you wish to publish your work commercially in the future, please reapply to the appropriate Cambridge University Press office, depending on where your forthcoming work will be published. Further information can be found on our website at the following link:

http://www.cambridge.org/about-us/rights-permissions/permissions/

Kind regards,

Permissions Sales Team
Cambridge University Press
University Printing House
Shaftesbury Road
Cambridge CB2 8BS, UK

http://www.cambridge.org/about-us/rights-permissions/permissions/

Appendix 5

Animal Ethics Approval

Western

AUP Number: 2017-033
PI Name: Han, Victor
AUP Title: Insulin-like Growth Factors And Igf Binding Proteins In The Fetus And Newborn From Dietary Restricted Mothers
Approval Date: 05/23/2017

Official Notice of Animal Use Subcommittee (AUS) Approval: Your new Animal Use Protocol (AUP) entitled "Insulin-like Growth Factors And Igf Binding Proteins In The Fetus And Newborn From Dietary Restricted Mothers" has been APPROVED by the Animal Use Subcommittee of the University Council on Animal Care. This approval, although valid for four years, and is subject to annual Protocol Renewal.2017-033::1

1. This AUP number must be indicated when ordering animals for this project.
2. Animals for other projects may not be ordered under this AUP number.
3. Purchases of animals other than through this system must be cleared through the ACVS office. Health certificates will be required.

The holder of this Animal Use Protocol is responsible to ensure that all associated safety components (biosafety, radiation safety, general laboratory safety) comply with institutional safety standards and have received all necessary approvals. Please consult directly with your institutional safety officers.

Submitted by: Copeman, Laura
on behalf of the Animal Use Subcommittee
University Council on Animal Care

Curriculum Vitae

Name:	Bethany Radord
Post-secondary Education and Degrees:	University of Western Ontario London, Ontario, Canada 2006-2011 HBsc in Biochemistry
	The University of Western Ontario London, Ontario, Canada 2013-2019 Ph.D. in Biochemistry
Honours and Awards:	Western Research Scholarship 2014-2018
	Schulich Graduate scholarship 2014-2018
	1rst Place, Poster Presentation Canadian Nation Perinatal Research Meeting 2018
	Epigenetics Program Travel Award London Health Sciences Center 2018
	Children's Health Research Institute Travel Award London Health Sciences Center 2017
	1rst Place, Poster Presentation Pediatrics Research Day 2016
Related Work Experience	Clinical Research Associate London Health Sciences Center 2016-2017
	Exam Proctor The University of Western Ontario 2013-2015
	Research Associate London Health Sciences Center February 2013-August 2013

Laboratory Technician
Advanced Mineral Mining Technologies
2011-2012

Research Internship
Agri-Foods and Agriculture Canada
2009-2010

Publications:

Radford, B. and Han, V. Offspring from Maternal Nutrient Restriction in Mice Show Variations in Adult Glucose Metabolism Similar to Human Fetal Growth Restriction. J Dev Orig Health Dis. 2018. DOI: 10.1017/S2040174418000983.

Radford, B., Gros, R. and Han, V. High-fat high-sugar diet impairs glucose tolerance independent of fetal growth restriction caused by poor maternal nutrition in mice. Submitted for consideration in J Dev Orig Health Dis.

Radford B., and Han, V. Evidence of Increased Hypoxia Signalling in Fetal Liver from Maternal Nutrient Restriction in Mice. Manuscript in preparation.

Radford B., and Han V. Similar gene expression in liver, adipose tissue and skeletal muscle in maternal nutrient restricted offspring susceptible and resistant to changes in glucose metabolism. Manuscript in preparation.